An investigation of the kynurenine pathway in experimental arthritis

by

Łukasz Kołodziej

A Thesis Submitted To Imperial College London

For the degree of Doctor of Philosophy

Imperial College London

September 2011

Abstract

The kynurenine pathway is a catabolic biochemical pathway responsible for degradation of tryptophan, an essential amino acid. As a consequence, biologically active molecules, kynurenines, are produced. These chemical entities can influence immune responses. Previously, it has been shown that pharmacological inhibition of the initial step on the pathway increases the severity of collagen-induced arthritis (CIA), an animal model of rheumatoid arthritis. In contrast, treatment with kynurenine, a major by product of tryptophan degradation, effectively ameliorated the disease. This project was based around the hypothesis that tryptophan metabolism via the kynurenine pathway represents an endogenous regulatory mechanism that is activated in response to inflammation. To test this hypothesis, I carried out a comprehensive analysis of the kynurenine pathway in the immune system in CIA as well as in the liver or kidneys, organs in which kynurenine pathway is the most active under normal conditions.

In this study, the endogenous activity of the kynurenine pathway in the immune system (lymph nodes and spleen), inflamed paws, liver, and kidneys was monitored during the induction phase of CIA (day 14 after immunisation) and during the period of disease resolution (day 10 after disease onset). In addition, the concentration of tryptophan, kynurenine and its selected catabolites anthranilic acid (AA) and 3-hydroxyanthranilic acid (3-HAA) was determined in the sera. All results were compared with naive tissues.Increased expression of all enzymes along the kynurenine pathway was observed locally in draining lymph nodes during the pre-arthritic phase of arthritis and this was accompanied by reduced levels of tryptophan. In contrast, during the resolution phase of arthritis not only was there decreased tryptophan concentration, but also there was an accumulation of the downstream tryptophan metabolites, kynurenine, AA, and 3-HAA in lymph nodes. In addition, the accumulation of kynurenine and its downstream metabolites observed during the resolution

of arthritis was accompanied by reduced expression of enzymes involved in kynurenine catabolism (kynureninase, kynurenine 3-monooxygenase, and 3-hydroxyanthranilate 3,4 dioxygenase) towards the levels found in naïve mice. These findings provide for the first time evidence of an association between resolution of arthritis and the local accumulation of kynurenines in lymph nodes. However, in the paws and spleens of mice with CIA, there was no evidence of activation of the kynurenine pathway. Surprisingly, however, kynurenine catabolism was increased in the kidneys and liver during CIA which may explain why in sera from mice with CIA, the tryptophan concentration was not changed, whereas levels of kynurenine, AA, and 3-HAA actually decreased, despite the increased levels found in lymph nodes at the same time points.

Based on these findings I assessed the potential therapeutic effect of exogenous administration of AA and 3-HAA in mice with established CIA and in order to facilitate this study I established a novel method of assessment of bone integrity based on 3-dimensional imaging using micro-computed tomography. Using *in vivo* observations, micro-computed tomography and histological sectioning with hematoxylin and eosin staining, I showed that neither AA nor 3-HAA treatment was effective in established CIA. However, treatment with etanercept, a potent inhibitor of TNF, profoundly reduced the severity of bone and cartilage damage. I also confirmed previous findings that tranilast, a derivative of 3-HAA which exhibits kynurenine-like activity and has a longer half-life than naturally occurring tryptophan metabolite, was effective in established CIA. Thus, taken together, activation of the kynurenine pathway in the lymph nodes may constitute a fine tuning mechanism involved in resolution of inflammation. However, exogenous administration of naturally occurring kynurenines is unlikely to be an effective therapeutic strategy to reduce inflammation in arthritis, possibly because of their rapid clearance from the circulation.

Acknowledgments

I am deeply grateful to my parents and my friends: Anna Woskowicz, Tomasz Wicinski, Marta and Michal Rysz, Iwona and Marek Majkowscy who encouraged me to finish writing up this thesis. In addition, I would like to express my great attitude towards my academic supervisors (Dr Ewa Paleolog and Richard O Williams), Dr Robert Visse who helped me to establish HPLC, and Dr Richard Abel, who taught me micro-computed tomography in the Natural History Museum in London. I would like to also thank Professor Ido Kema from the Department of Laboratory Medicine, University Medical Centre, University of Groningen, the Netherlands, who has kindly helped me to measure the concentration of tryptophan and kynurenine in the lymph nodes, spleens, and paws. Finally, without help from David Essex and his colleagues from the Department of Histopathology in Charing Cross Hospital I would not have been able to use immunohistochemistry in this project.

Table of contents

Abstract 2
Acknowledgments 4
Table of contents 5
List of Figures 9
List of Tables 11
Common Abbreviations of Enzymes and Genes on the Kynurenine Pathway 13
Common Abbreviations Used Throughout This Thesis 14

Chapter 1. Introduction 16

1.1 General overview 17
1.2. Metabolism 18
1.2.1. Regulatory mechanisms in metabolism 19
1.2.1.1. The amount of an enzyme 20
1.2.1.2. Regulation of the catalytic activity of enzyme 22
1.2.2. Metabolism of amino acids 23
1.2.3. The kynurenine pathway 23
1.2.3.1. Enzymes involved in the kynurenine pathway 24
1.2.3.2. The kynurenine pathway in physiology 29
1.2.3.3. Physiological consequences of tryptophan starvation 33
1.2.3.4. Cellular and molecular consequences of activation of the kynurenine pathway 34
1.2.3.4.1. Cumulative effects of kynurenines and tryptophan starvation on the immune cell 39
1.2.3.5. Regulation of the kynurenine pathway 40
1.2.3.5.1. The amount of enzymes on involved in the kynurenine pathway 40
1.2.3.6. Regulation of catalytic activities of enzymes on the kynurenine pathway 43
1.2.3.7. The kynurenine pathway in the experimental medicine 45
1.3. Arthritic diseases 47
1.3.1. Joints and arthritic diseases 47
1.3.2. Rheumatoid arthritis 47
1.3.2.1. Pharmacotherapy of RA 49

1.3.3. Animal models of RA 53
1.3.3.1. Collagen induced arthritis 55
1.3.3.1.1. Induction and pathogenesis of CIA 55
1.3.3.1.2. A comparison between CIA and RA 56
1.4. Imaging methods in RA and CIA 56
1.4.1. Overview of the existing imaging modalities 56
1.4.2. Micro-computed tomography in clinical medicine of RA 58
1.5. Objectives and an outline of the thesis 61
Chapter 2. Methods 65
2.1. Experimental animals 66
2.1.1. Genotyping of Ido1 KO mice 66
2.2. Collagen-induced arthritis 68
2.2.1. Extraction of type II collagen 68
2.2.2. Induction of arthritis 69
2.2.3. Assessment of arthritis 70
2.3. Tissue collection and processing 70
2.3.1. Serum 70
2.3.2. Tissues 71
2.3.3. Collection of hind paws for ex vivo imaging and histological assessment 71
2.4. Micro-computed tomography 71
2.4.1. Recording of movies and preparation of figures 71
2.4.2. BoneJ 72
2.5. Histological assessment of inflamed paws with CIA 73
2.5.1.1. Assessment of joint damage using histological scores 73
2.5.1.2. Assessment of cartilage damage in CIA using Mankin scale 75
2.6. Therapy of mice with kynurenines and etanercept 77
2.7. Biochemical analysis of collected tissues 78
2.7.1. Isolation of mRNAand real-time PCR 78
2.7.2. Tissue homogenisation and metabolite extraction 80
2.7.3. Development of the quantitative HPLC 81

2.7.4. Determination of kynurenine concentration 83
2.7.5. Immunohistochemistry 83
2.7.5.1. Tissue collection and processing 84
2.7.5.2. De-paraffinizing and hydrating of tissue sections 84
2.7.5.3. Retrieving antigen epitopes 85
2.7.5.4. Staining 85
2.7.5.5. Dehydration and mounting of tissue sections 87
2.7.5.6. Limitations of the immunohistochemistry 89
2.8. Statistical analysis and data presentation 89

Chapter 3. Systemic changes in levels of tryptophan and its metabolites during arthritis 90

3.1 INTRODUCTION 91
3.2. RESULTS 93
3.2.1. Changes in the concentration of tryptophan and kynurenines in sera from mice with CIA 93
3.2.3. The involvement of the liver in tryptophan metabolism via the kynurenine pathway during CIA 95
3.2.4. The involvement of the kidneys in tryptophan catabolism via the kynurenine pathway during CIA 101
3.3. DISCUSSION 109

Chapter 4. Comparative study of tryptophan catabolism via the kynurenine pathway in the secondary lymphoid organs and inflamed paws during arthritis 112

4.1 INTRODUCTION 113
4.2. RESULTS 115
4.2.1. Tryptophan catabolism in the inguinal lymph nodes 115
4.2.1.1. Accumulation of AA and 3-HAA in iLN of mice with established CIA 119
4.2.2 Tryptophan catabolism in the spleen during CIA 122
4.2.3 Tryptophan catabolism in the inflamed paws during CIA 127

4.3. DISCUSSION 132

Chapter 5. Evaluation of the therapeutic potential of kynurenine catabolites in collagen induced arthritis 136

5.1. INTRODUCTION 137

5.2. RESULTS 140

5.2.1 Multiple bone deformities can be observed in CIA and their severity can be assessed semi-quantitatively 140

5.2.2. Bone pathology is associated with a decrease in the mean cortical thickness of the metatarsal bone 146

5.2.3 The formation of novel pathological features of bone destruction are driven in a TNF- dependent manner 147

5.2.4 Neither treatment with AA nor with 3-HAA could reduce severity of CIA 151

5.3. DISCUSSION 158

Chapter 6. General discussion and future directions 162

Chapter 7. Bibliography 170

Supplement 1. People who helped me to accomplish this thesis.. 171

List of Figures

Figure 1 Schematic representation of the kynurenine pathway 24

Figure2 Various types of imaging modalities applied in clinical and preclinical medicine of RA 57

Figure 3 Schematic representations of bone erosions and their origin in two types of inflammatory arthritis. 60

Figure 4 Genotyping of Ido1 KO mice 67

Figure 5 Application of μCT and boneJ in CIA 72

Figure 6 Sagittal cross sections of PIP joint stained with H&E 74

Figure 7 Representative pictures of cartilage assigned with Mankin's grades (based onMankin *et al.* 1971; Pritzker *et al.* 2006) 77

Figure 8 Representative pictures of chromatograms with 3-HAA, AA, and tryptophan 82

Figure 9 Unchanged kynurenine to tryptophan ratio in the livers of mice with CIA..... 97

Figure 10 Catabolism of kynurenine in the livers taken from mice with CIA 99

Figure 11 Increased levels of tryptophan in the kidneys from mice with established CIA 103

Figure 12 Increased levels of 3-HAA inthe kidneys of mice with CIA 107

Figure 13 Increased initiation of tryptophan metabolism via the kynurenine pathway in lymph nodes of mice with CIA 116

Figure 14 Catabolism of kynurenine in lymph nodes of mice with CIA 121

Figure 15 mRNA expression for initial enzymes on the kynurnine pathway was unchanged in spleens of mice with CIA 124

Figure 16 Expression of genes encoding KMO, KYNU, and HAAO in spleens of mice with CIA..... 126

Figure 17 Tryptophan and kynurenine concentrations and IDO expression in paws of mice with CIA 128

Figure 18 Concentration of AA and expression of kynureninase in paws of mice with CIA..... 129

Figure 19 HAAO could not be detected in the paws of naive mice or mice with established CIA 131

Figure 20 Multiple lesions are observed in the bones in CIA as visualised by μCT 141

Figure 21 Scoring of bone and joint pathology in CIA by μCT 143

Figure 22 Treatment of CIA mice with etanercept reduced bone pathology 148

Figure 23 Treatment of mice with established CIA with 3-HAA was not effective.....151

Figure 24 Treatment with 3-HAA did not reduce histological severity or prevent cartilage damage 154

Figure 25 Treatment of established CIA with AA was not effective.....156

Figure 26 Summery of the experimental results showing changes in the concentration of tryptophan, kynurenine, and her metabolites in various organs with CIA 165

List of Tables

Table 1 Comparison of the selected biophysical and kinetic parameters of recombinant forms of human and mouse IDO1 enzyme 25

Table 2 Comparison of the selected biophysical and kinetic parameters of recombinant forms of murine IDO1 and IDO2 27

Table 3 Therapeutic applications of the kynurenines in animals 46

Table 4 Quantitative comparison of bone erosions observed in two types of inflammatory arthritis 61

Table 5 Oligonucleotide sequences used for Ido1 KO mice genotyping 67

Table 6 Description of histological grades assigned to the arthritic PIP joints 74

Table 7 Semi-quantitative assessment of cartilage damage using Mankin's scale 76

Table 8 Settings applied for RNA reverse transcription 78

Table 9 TaqMan probes with their reference numbers bought from Applied Biosystems Company 79

Table 10 Primary antibodies used for detection of the kynurenine pathway enzymes in iLN, inflamed paws, and small intestine 84

Table11 Primary antibodies used for detection of the kynurenine pathway enzymes in iLN, inflamed paws, and small intestine 86

Table 12 Establishment of immunocytochemical reactions using antibodies against selected enzymes on the kynurenine pathway. 88

Table 13 The concentration of tryptophan was not changed whereas the concentration of kynurenines was decreased in sera from mice with CIA 94

Table 14 The concentration of kynurenine was decreased in sera from arthritic *Ido1*-/- mice but not from WT mice 95

Table 15 In the spleen during CIA the concentration of tryptophan and kynurenine was not changed 123

Table 16 In the spleen during CIA the concentration of AA and 3-HAA was not changed 125

Table 17 Semi-quantitative scoring system for assessment of bone pathology in the hind paws of mice with CIA 145

Table 18 Decrease in the mean cortical thickness of the 3rd metatarsal bone is negatively correlated with increasing severity of bone and joint damage 146

Table 19 Summary of results showing changes in the expression of mRNA for subsequent genes on the kynurenine pathway in the several types of organs during CIA ..... **Error! Bookmark not defined.**

Common Abbreviations of Enzymes and Genes on the Kynurenine Pathway[1]

Enzyme	**Protein abbreviation***	**Gene abbreviation***
arylformamidase	AFM	*Afm*
3-hydroxyanthranilate 3,4, dioxygenase hypoxanthine	HAAO	*Haao*
phosphoribosyltransferase 1	HPRT	*Hprt1*
indoleamine 2,3 dioxygenase 1	IDO1	*Ido1*
indoleamine 2,3 dioxygenase 2	IDO2	*Ido2*
kynureninase	KYNU	*Kynu*
kynurenine 3- monooxygenase	KMO	*Kmo*
tryptophan 2,3 dioxygenase	TDO	*Tdo2*

[1]These abbrevations have been used in the review article published by the author of this thesis and his academic superviors ("Kynurenine metabolism in health and disease" Amino acids, DOI:10.1007/s00726-010-0787-9)

Common Abbreviations Used Throughout This Thesis

Abbreviation	Full name
AA	Anthranilic acid
AhR	Aryl hydrocarbon receptor
bp	Base pair
CD	Cluster of designation
CFA	Complete Freund's adjuvant
CIA	Collagen-induced arthritis
DC	Dendritic cells
EAE	Experimental autoimmune encephalomyelitis
EC	Enzyme Commission number
GTP	Guanosine-5'-triphosphate
GCN2	General control nonrepressed kinase 2
3-HAA	3-hydroxyanthranilic acid
3-HK	3-hydroxykynurenine
HPLC	High pressure liquid chromatography
IC_{50}	half maximal inhibitory concentration
IFN-γ	Interferon gamma
Il-	Interleukin
kDa	Kilo Dalton
KA	Kynurenic acid
KO	Knock out
LPS	Lipopolysaccharides
1-MT	1-methyl tryptophan

MRI	Magnetic resonance imaging
NADPH	Nicotinamide adenine dinucleotide phosphate
NF_KB	nuclear factor kappa-light-chain-enhancer of activated B cells
PBL	Peripheral blood lymphocytes
PCR	Polymerase chain reaction
PET	Positron emission tomography
PHA	Phytohaemagglutinin
PIP	Proximal interphalangeal
PLP	Pyridoxal phosphate
PsA	Psoriatic arthritis
PWN	Pokeweed mitogen
RA	Rheumatoid arthritis
RANKL	Receptor activator of nuclear factor kappa-B ligand
SLE	Systemic Lupus erythemamatosis
Th cells	T helper cells
TNF	Tumour necrosis factor
Treg cells	Regulatory T cells
WT	Wild type
μCT	Microscopic computer tomography
QA	Quinolinic acid
XaA	Xanthurenic acid

Chapter 1

INTRODUCTION

1.1 General overview

Rheumatoid arthritis (RA) is thought to be driven by exagerated immune responses towards self-antigens (Zwerina et al. 2006). As a result joints became inflamed, bone erosions form together with cartilage damage. Thus, many patients with RA become disabled and may die prematurely (Taylor). Therefore, not surprisingly, the aim of therapy in RA is a reduction of inflammation. In line with this, it was of interest to study endogenous mechanisms involved in dampening immune and inflammatory responses (Smolen and Steiner 2003).

The kynurenine pathway was chosen amongst other metabolic pathways because this is the major route of tryptophan catabolism (Knox and Mehler 1950). Tryptophan is an essential amino acid (Willcock 1906) which serves as a precursor for biosynthesis of other vital small molecules like: serotonin (neurotransmitter) and melatonin (a hormone involved in a circadian rhythm) as well as for protein synthesis (Kolodziej et al. 2010). Thus, the activity of the kynurenine pathway regulates tryptophan availability for all these processes. In addition, it is known that the major by-products of tryptophan catabolism via the kynurenine pathway, kynurenine and 3-hydroxyanthranilic acid (3-HAA), exhibit anti-inflammatory properties (Munn et al. 1999). In fact, previously, it has been shown that inhibition of tryptophan catabolism exacerbated symptoms of arthritis in the animal models of RA whereas exogenous administration of kynyrenine reduced pathology (Criado et al. 2009). Therefore, the aim of my thesis was to conduct a thorough analysis of the kynurenine pathway in collagen-induced arthritis (CIA), an animal model of RA. To accomplish the task, I applied several types of experimental techniques, ranging from analysis of mRNA expression, histochemistry, and quantification of metabolites in tissues to micro-computed tomography (μCT) for assessment of the anti-arthritic potential of 3-HAA.

1.2. Metabolism

The word “metabolism” is derived from Greek language (μεταβολισμός) and means “to throw out”. In the scientific literature “metabolism” describes “a series of linked chemical reactions that begins with a particular molecule and converts it into some other molecule or molecules in a carefully defined fashion” (Stryer 1995). In the cell, there are many such defined pathways. Nonetheless, metabolic pathways can be grouped into two broad classes: anabolic and catabolic reactions. Anabolism refers to the synthesis of molecules from its precursors, whereas catabolism refers to the breakdown of molecules and subsequent production of free energy (Stryer 1995). Such energy is required for:

1) Mechanical work (e.g. cell movement and/or contraction of muscles)

2) Active transport of molecules and ions through cell membranes

3) The synthesis of macromolecules and other biomolecules from simple precursors

Continuous production of free energy is essential to maintain cells and organisms alive (Stryer 1995). Carbohydrates (e.g. glucose) are the richest source of free energy in metabolism and can be catabolised by two major biochemical pathways: glycolysis and the citric acid cycle. Fatty acids can also be metabolised via the citric acid cycle, however less energy is extracted from these molecules in comparison with carbohydrates. Amino acids, the third most important class of small molecules in the living organisms are the least rich source of free energy. Nonetheless, amino acids serve for protein synthesis and therefore are essential for living organism. For example: tryptophan is an essential amino acid and has to be provided in the diet. In fact, prolonged tryptophan depletion causes death in animals; whereas acute tryptophan depletion influences mood and cognition.

1.2.1. Regulatory mechanisms in metabolism

At any given time, in every cell, thousands of metabolic transformations are taking place. Therefore, every biochemical reaction has to be precisely controlled. However, such control must be flexible (cells are exposed to a constantly changing environment) and fast enough to respond adequately to the constantly changing extracellular milieu. The term "**metabolic regulation**" refers to processes that serve to maintain homeostasis at the molecular level (Nelson 2008), in another words, to keep certain biochemical parameters (e.g. concentration of a metabolite) at a steady state level over time, even though the flow of metabolites through the pathway is changing (Nelson 2008). In contrast, the term "**metabolic control**" describes processes that cause a change in the output of a metabolic pathway over time, in response to some outside signal. Nonetheless, the distinction is not always easy to make. Moreover, the changes in the flow of intermediates (**flux**) through a pathway can be determined quantitatively using experimental methods like e.g. high pressure liquid chromatography (HPLC) and expressed in terms useful for predicting the flux when some factors involved in the pathway become changed. In general, this approach is described as "**metabolic control analysis**" (Nelson 2008). Experiments have confirmed predictions made by application of metabolic control analysis approach that the most efficient way of increasing metabolic flux toward a specific product is the raising the concentration of all enzymes in the pathway needed to achieve desired end product (Nelson 2008).

Although metabolic control analysis operates with a rather complicated mathematical apparatus and requires experimental data it is also possible to understand the basic concepts of this theoretical approach by three principal concepts. It can be assumed that metabolism is regulated by controlling: 1) the amounts of enzymes 2) their catalytic activities 3) the accessibility of substrates (Stryer 1995)

1.2.1.1. The amount of an enzyme

The amount of a given enzyme depends on the rate of its synthesis and degradation (Nelson 2008). Disused enzymes or those which lose their catalytic activity during the course of action can be either degraded in the proteosome or lysosomes. However, the vast majority of proteins are degraded in the proteasome in an ATP-dependent process; whereas in the lysosomes proteins are degraded by hydrolytic enzymes (Nelson 2008). Molecular mechanisms involved in targeting proteins into the proteasome or lysosomes are relatively well characterised. When protein undergoes monoubiquination it is highly likely to be transported into lysomoes. In contrast, when protein becomes polyubiquitinated it means degradation in the proteasome. Interestingly, it has been shown that external stimuli can trigger selective degradation of specific proteins in the proteasome by activation substrate specific enzymes involved in polyubiquitination (Nelson 2008).

Regulatory mechanisms responsible for enzyme synthesis are the most complex processes in the living organisms. However, study of gene regulation, from DNA to catalytically functional enzyme, can be intellectually rewarding and provides a beautiful narrative story in biology (the unified theory of gene expression) (Orphanides and Reinberg 2002).

In the inactive state, genes are densely packed in the chromatin, therefore are inaccessible for transcription from DNA into mRNA. Hence, for transcriptional activation, chromatin has to be remodelled. There are multiple mechanisms involved in this process. However, chemical modification of histones (histone code hypothesis) and ATP-dependent histone movement/replacement enzymes are the major players in the opening of chromatin. Once a gene is accessible for transcription, the successful binding of DNA-dependent RNA polymerase II (Pol II) to the gene promoter requires multiple other proteins which can be

classified into four groups: 1) basal transcription factors, 2) co-activators 3) transcriptional activators (transcriptional factors, TF). Nonetheless, sequence specific binding of TF's to the DNA sequence dictates localisation of transcriptional active sites on the chromatin. Immediately after initiation of transcription, mRNA undergoes profound modifications like: chemical modification of 5' cap on the mRNA, splicing, and polyadenylation. In fact, the formation of the polyadenylated 3' end of mRNA is inherently associated with termination of transcription (Orphanides and Reinberg 2002; Nelson 2008).

Mature mRNA transcripts are exported from the cell nucleus and transported in the specific regions in the cytoplasm in the multiple steps collectively referred to "RNA transport and localization control". The half-life of mRNA in cytoplasm is also under control of multiple factors and interactions between *cis* acting elements, which are nucleotide sequences of untranslated regions (UTR's) localised on the 5' and 3' ends of mRNA, and *trans* acting cytoplasmic proteins.

In addition, mRNA can undergo translational repression. Therefore, changes in the mRNA content for a given gene does not necessarily mean differences in the amount of enzyme encoded by this specific transcript. In fact, in eukaryotes, there are at least four major mechanisms responsible for translational regulation:

1) The rate of translation can be decreased by phosphorylation of translational initiation factors (TIF). This posttranslational modification usually makes TIF's less effective in the initiation of translation.
2) TIF's can be bound to other proteins e.g. 4E-BP's and therefore initiation of translation cannot proceed
3) Translational signals encoded in the UTR's of a given transcript can be masked by other proteins preventing initiation of translation.

4) RNA-mediated regulation of gene expression e.g. RNA interference (RNAi)

1.2.1.2. Regulation of the catalytic activity of enzyme

The efficacy of an enzymatic reaction depends on the catalytic properties of the enzyme and the concentration of its substrate. For example, when an enzyme follows Michaelis-Menten kinetics the rate of reaction reaches its half maximum when en enzyme is half saturated with its substrate. Such concentration of the substrate is referred to the Michaelis constant (*K*m). It is important to state that usually in cytoplasm the concentration of substrates is usually around or below *K*m, therefore, *in vivo* the rate of reaction is usually linearly dependent on the concentration of substrate (Nelson 2008).

However, the intrinsic activity of the enzyme can be either increased or decreased by an allosteric effector. The effect of an allosteric activator on the enzyme can be expressed with the Hill coefficient factor (n_H) derived from the Hill equation. When n_H =1 the binding of a ligand is not cooperative whereas n_H>1 indicates that the ligand can trigger positive effect on the substrate binding and therefore an enzyme exhibits sigmoid kinetic. In another words, the higher n_H factor the less substrate is required to increase the rate of enzymatic reaction from 10% to 90% of the maximal possible reaction rate for a given allosteric enzyme (Nelson 2008).

Binding of an allosteric modulator is always non covalent. However, covalent modifications can also influence on the catalytic activity of a given enzyme. There are at least 500 different types of covalent modifications of protein described so far. However, phosphorylation is one of the most common of regulatory strategies. This is because such modification is reversible and executed by protein phosphatises (Nelson 2008).

1.2.2. Metabolism of amino acids

In mammals, surplus fatty acids and glucose, unlike amino acids, can be stored in the body. Therefore, amino acids undergo oxidative degradation in all three major metabolic circumstances (Stryer 1995).

A) Amino acids are released from protein breakdown and are not needed for new protein synthesis
B) There is a dietary driven excess of amino acids
C) During starvation or upon inappropriate metabolism of carbohydrates

The first step in catabolism of amino acids is a biochemical removal of the α-amino group from the amino acid. This reaction is catalysed by the aminotransferases and α-amino groups are converted into urea in the series of biochemical reactions called the urea cycle. In contrast, the carbon skeleton of the amino acid from which α-amino group is removed can be converted into major metabolic intermediates e.g. pyruvate, acetyl CoA, and fumarate. Therefore, fatty acids, ketone bodies, and glucose can be formed from amino acids (Stryer 1995).

1.2.3. The kynurenine pathway

Tryptophan is one of the twenty other amino acids used for protein synthesis. However, unlike other biological amino acids (those used in translation), tryptophan exhibits a unique set of biophysical properties. For example, tryptophan is an essential amino acid for most mammals and therefore it has to be provided in the diet (Willcock 1906). In addition, tryptophan binds reversibly to albumin which serves as a "storage" molecule for free tryptophan (Mc and Oncley 1958; McMenamy 1965). However, it has been also reported that tryptophan can be displaced from albumin by some endogenous molecules e.g. non-esterified fatty acids (Cunningham et al. 1975) as well as by the certain types of drugs e.g. alclofenac

(Aylward 1975). Therefore, it is important to distinguish between free tryptophan and the total pool of tryptophan found in a given type of tissue and/or biological fluids e.g. serum. In the elegant study, (Smith and Pogson 1980) have demonstrated that tryptophan displacement can indeed play a role in the regulation of metabolic flow through the kynurenine pathway (Figure 1). In fact, this metabolic pathway is the major route of excessive tryptophan catabolism.

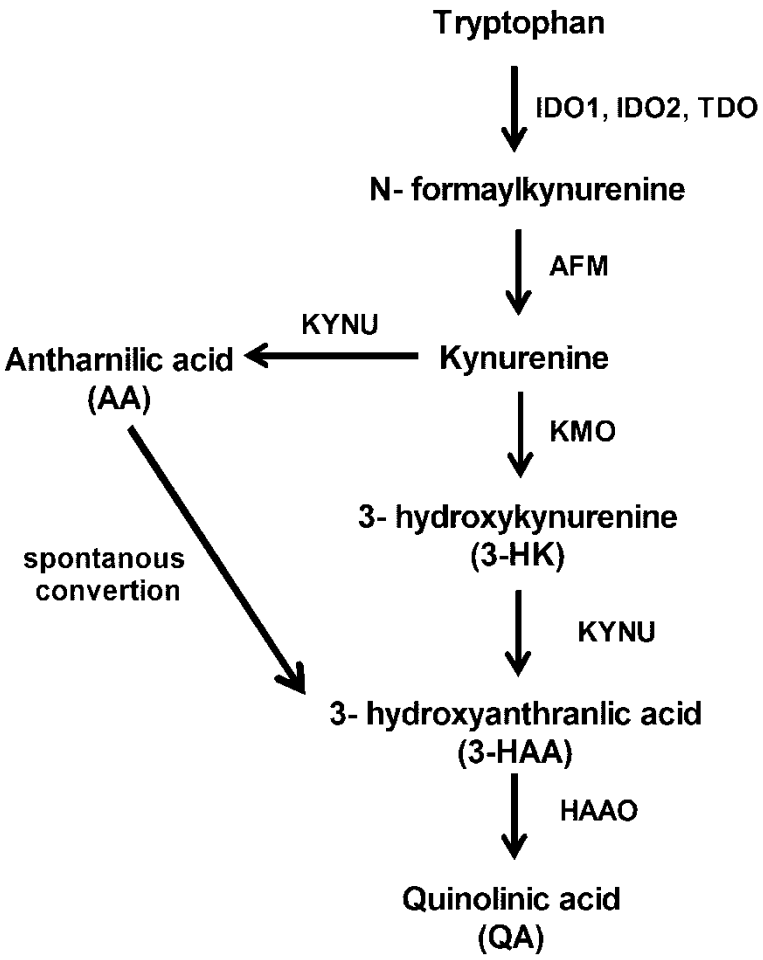


Figure 1 Schematic representation of the kynurenine pathway

1.2.3.1. Enzymes involved in the kynurenine pathway

IDO1 (EC 1.13.11.52) is a monomeric, cytosolic protein present in the placental mammals (Yuasa et al. 2007). Murine form of IDO1 is composed of 407 amino acids and of

molecular weight of 45.64 kDa (Grohmann and Bronte 2010). Human IDO1 shares 62% sequence identity with its mouse ortholog which is the lowest degree of similarity amongst other enzymes on the kynurenine pathway (Grohmann and Bronte 2010). (Ball et al. 2007) provided a detailed comparison between biophysical properties of human and mouse IDO1 enzymes is presented in the Table 1.

Table 1 Comparison of the selected biophysical and kinetic parameters of recombinant forms of human and mouse IDO1 enzyme

Murine b-end and human HBEC brain endothelial cell lines served as a source of *Ido1* mRNA for cloning of *Ido1* gene. Protein was expressed in *E.coli*. Based on (Ball et al. 2007)

Parameter	Human IDO1	Mouse IDO1
Kintetic parameter for tryptophan V_{max}/K_m($\mu M^{-1}min^{-1}$)	2.6	7.8
pH stability	More active in alkaline pH	More active in acidic pH
Thermal unfolding T_m	48^{o}C and 70^{o}C	60^{o}C

Although human and murine forms of IDO1 are not completely identical, in general, IDO1 enzyme has a broad substrate specificity for indoleamine derivatives of such as: D and L isomers of tryptophan, 5-hydroxytryptophan, tryptamine, and serotonin (Shimizu, Nomiyama et al. 1978). However, the maximal turnover number was obtained with L-tryptophan and this molecule is considerate as a primary substrate for IDO1 enzyme (Shimiz et al. 1978).

Although IDO1 was discovered in 1975 (Hayaishi et al. 1975) the chemistry involved in tryptophan catabolism remains not entirely understood. However, crystalographic studies of IDO1 have revealed that IDO1 consists of two distinct folds: small and large, separated by a loop made of 17 amino acids (Sugimoto et al. 2006). In the large domain, catalytic and

substrate binding sites are located, therefore this domain is involved in the catalytic cleavage of the indole ring (Sugimoto et al. 2006). In contrast, the function of the small domain is less clear. Nevertheless, (Pallotta et al. 2011) have recently shown that the small domain and the loop may play a role in the intracellular signalling processes. In fact, in this paper, for the first time, it has been shown that IDO1 can undergo phosphorylation in a FYN kinase dependent manner. In addition, these authors have demonstrated that phosphorylation of IDO1 can influence the non-canonical NF-κB pathway and therefore, result in sustained production of transforming growth factor –β (TGF-β), induction of type I interferons, and subsequent induction of regulatory phenotype in plasmacytoid dendritic cells (Pallotta et al. 2011).

IDO2 is relatively recently discovered enzyme of molecular weight of 45 kDa, which is also involved in the kynurenine pathway (Metz et al. 2007). Interestingly, phylogenetic analysis of the gene which encodes IDO2 has revealed that in fact *Ido2* gene might be evolutionary older than *Ido1*. On this basis, it is postulated that *Ido1* could have been created in a gene duplication event (Ball et al. 2009). However, the overall level of sequence conservation between human IDO1 and IDO2 is not particularly high (43% identical, whereas 63% is similar) (Grohmann and Bronte 2010). Therefore, it is possible that IDO1 displays slightly different biophysical properties from IDO2. In fact, this has been experimentally confirmed when the selected kinetic and biophysical parameters of IDO1 and IDO2 were compared in table 2 by (Austin et al. 2010).

Table 2 Comparison of the selected biophysical and kinetic parameters of recombinant forms of murine IDO1 and IDO2

IDO2 was expressed in KRX cells, purified and subjected to biochemical and biophysical studies described by (Austin et al. 2010).

Parameter	Murine recombinant IDO1	Murine recombinant IDO2
Structure α-helical random coil	 71% 10%	 75% 16%
Optimum pH	6 – 6.5	7.5
T_m	60°C	48°C
Kinetic V_{max} K_m	 0.12 ±001 29 ±9	 0.13 ±0.01 530 ±100

TDO (EC 1.13.11.11), like IDO1 and IDO2, can also catabolise tryptophan by incorporation of two molecules of the molecular oxygen into the double bond between carbon atoms localised in the 2nd and 3rd position in the indole ring (Smith and Pogson 1980). However, in contrast with IDOs, the functional form of TDO consists of four tetramers. The structure of each monomer resembles the large domain of IDO and is composed of 299 amino acids of total molecular mass 134 kDa (Grohmann and Bronte 2010). In addition, each monomer contains a heme binding site, which is located at the end of the long helical bundle (Zhang et al. 2007). TDO also displays high substrate specificity towards tryptophan in comparison with IDO (Capece et al. 2010). It has been shown that mammalian form of TDO

is related to the bacterial form of TDO indicating on an evolutionarily conserved nature of this enzyme (Dick et al. 2001). However, in mammals, unlike expression of IDO1, expression of TDO has been shown to be mainly confined to the liver (Dick et al. 2001), skin (Ishiguro, et al. 1993), and the brain (Ohira et al. 2010).

AFM (EC 3.5.1.9) is a 305 amino acid protein with an ancient evolutionary origin (Schuettengruber et al. 2003). In mammals, AFM is expressed predominantly in the kidneys and liver (Schuettengruber, Doetzlhofer et al. 2003), (Dobrovolsky et al. 2005). In addition, enzymatic activity for AFM is higher in the kidneys and liver than in other organs and tissues in which AFM is also expressed such as brain, sub-mandibular gland, heart, trachea, lung, thymus, oesophagus, stomach, intestine, cecum, colon, urinary bladder, testis, epididymis, seminal vesicle, and spleen (Takikawa et al. 1986; Dobrovolsky et al. 2005). At the intracellular level, AFM is predominantly expressed in the cytoplasm (Schuettengruber et al. 2003). Gene expression of AFM enzyme was reported to be restricted to non proliferating cells (Schuettengruber et al. 2003).

However, functional studies focused on the physiological role of AFM enzyme provide rather puzzling results *in vivo* (Dobrovolsky et al. 2003, Dobrovolsky et al. 2005). Nonetheless, an interesting comparison could be drawn between *Ido1* KO and *Afm* KO mice. In wild-type (WT) animals, pharmacological inhibition of either IDO1 or AFM has a minor effect in the experimental animals. Thus, it could be predicted that genetic deletion of *Ido1* or *Afm* gene could have a similar, rather mild effect (Dobrovolsky et al. 2003; Baban et al. 2004). As expected, the phenotype of naive *Ido1* KO mice is indistinguishable from WT mice (Baban et al. 2004). However, *Ido1* KO mice develop exacerbated immune responses when challenged with pathogens (Harrington et al. 2008) or immunised with antigens (Criado et al. 2009). However, in contrast with naive Ido1 KO mice, naive mice with *Afm* gene deletion

exhibit relatively severe abnormalities in their immune system and physiology (Dobrovolsky et al. 2003). *Afm* KO mice usually die at age of 6 months, develop (IgG but not IgM) spontaneous immune-complex mediated kidney failure, and exhibit reduced motor coordination. In the spleens isolated from *Afm* KO mice lymphoid atrophy was observed. Infiltration of lymphoid cells into the liver was noticed (Dobrovolsky et al. 2003). In addition, inflammation of arteries and myocardial arteriosclerosis was reported in these KO mice.

KMO (EC 1.14.13.9) is a protein of molecular mass of 55.8 kDa with localised on the outer mitochondrial membrane (Nishimoto et al. 1979). KMO requires nicotinamide adenine dinucleotide phosphate (NADPH) for its monooxygenase activity. As a consequence of the reaction between KMO, NADPH, and kynurenine, 3-HK and water is produced.

KYNU (EC 3.7.1.3) is a 52-kDa, cytoplasmic enzyme. In mammals, the enzymatic activity of kynureninase is low in comparison with other enzymes on the kynurenine pathway (Allegri et al. 2003).

The direct product of 3HAA catabolism executed by **HAAO** (EC 1.1311.6) is 2-amino-3-carboxymuconic semialdehyde. This molecule is further converted into QA as a result of non-specific cyclisation (Fig. 1). Thus, the rate of QA synthesis is primarily dependant on the activity of HAAO. It has been estimated that in rats, only 10% of injected 3-HAA was converted into QA and excreted in urine (Hankes and Henderson 1957). The remaining 3-HAA expired as carbon dioxide (CO_2) within 3 h after of the initial injection (Hankes and Henderson 1957). Thus, 3-HAA might be metabolised very efficiently in lungs.

1.2.3.2. The kynurenine pathway in physiology

Serotonin and kynurenines are metabolites of the essential amino acid tryptophan and influence a wide range of physiological processes, including mood (Russo et al. 2003; Kanai,

et al. 2009), blood pressure (Wang et al. 2010), and immunity (Moffett and Namboodiri 2003; Prendergast 2008). However, the biochemical pathways which are responsible for the production of serotonin and kynurenines are different. Serotonin is produced from tryptophan in two steps mediated by two distinct enzymes: tryptophan hydroxylase (EC1.14.16.4) and aromatic L-amino acid decarboxylase (EC4.1.1.28), respectively (Russo et al. 2003). In contrast, kynurenines are produced from tryptophan in a series enzymatic reactions collectively referred to as the kynurenine pathway (Fig. 1). The name of the pathway is derived from kynurenine, the most abundant molecule amongst kynurenines, which are by-products of tryptophan metabolism of this pathway (Beadle et al. 1947). Functionally, the kynurenine pathway can be grouped into three separate branches (Moffett and Namboodiri 2003). The first one is involved in the initiation of tryptophan metabolism and kynurenine production. Once kynurenine is produced, it can enter two other branches of the kynurenine pathway. Hence, either kynurenine can be metabolised into xanthurenic acid (XaA) and/or kynurenic acid (KA) (Amori et al. 2009). The formation of KA in particular was shown to play an important role in the central nerve system (CNS) (Perkins and Stone 1982; Schwarcz and Pellicciari 2002). KA is a neuro-protective molecule, which can reduce activation of N-methyl-D-aspartate receptors (NMDAR) (Nemeth et al. 2005). Thus, KA can protect neuronal cells from excitatory cell death evoked by over-activation of NMDA receptors (Schwarcz and Pellicciari 2002). In addition, it was shown that KA might be involved in early stages of neutrophil and monocyte adhesion to surfaces coated with fibrinogen upon physiological flow conditions (Barth et al. 2009). This process was shown to be dependent on G-protein coupled receptor 35 (GPR35) (Barth et al. 2009), which is activated by KA (Wang, Simonavicius et al. 2006). In addition, pre-treatment of mononuclear cells with KA effectively reduced tumour necrosis factor alpha (TNF-α) secretion of the kynurenine pathway from these cells upon lipopolysaccharides (LPS) stimulation (Wang et al. 2006).

Hence, KA may play an important but still not fully appreciated role in health and disease. Nonetheless, kynurenine catabolism to QA is a major route of kynurenine clearance (Saito et al. 1993). In addition, the biological activity of 3-hydroxykynurenine (3-HK) and 3-hydroxyanthranilic acid (3-HAA) is relatively well recognised (Stone and Darlington 2002).

It is estimated that only around 1% of dietary delivered tryptophan can be converted into serotonin (Russo et al. 2003). The remaining 99% is metabolised via the kynurenine pathway. Thus, increased production of kynurenine may result in an inadequate serotonin synthesis and predispose for certain psychiatric diseases like, e.g. depression (Russo et al. 2003). The causative relationship between increased tryptophan metabolism via the kynurenine pathway, depressive-like behaviour and the immune response is well established in the experimental animals. Mice infected with Bacillus Calmatte-Guérin or injected with LPS (O'Connor et al. 2009) develop depressive-like behaviour which is associated with decreased tryptophan and increased kynurenine concentrations in the serum. A similar observation was made when gerbils were injected with pokeweed mitogen (PWM) (Saito et al. 1993). In these animals, as in mice infected with Bacillus Calmatte-Guérin or injected with LPS, decreased tryptophan concentration resulted from increased gene expression and enzymatic activity of indoleamine 2,3 dioxygenase (IDO1). This is the first and rate limiting enzyme on the pathway which is activated by pro-inflammatory cytokines such as TNF-α and IFN-γ (Robinson et al. 2005). However, in gerbils the enzymatic activity of IDO1 was restricted to specific tissues, including: lungs, cecum, colon, and epididymis (Saito et al. 1993). In addition, Takikawa and colleagues have found that LPS could induce IDO1 enzyme activity only in specific tissues (Takikawa et al. 1986). However, this local induction of tryptophan metabolism resulted in a threefold increase in the concentration of kynurenine in sera taken from mice 24h after LPS injection (Takikawa et al. 1986). Thus, it has been suggested that tryptophan metabolism can be initiated locally; whereas kynurenine may diffuse into the bloodstream. Therefore,

increased kynurenine concentration in the serum can indicate increased tryptophan metabolism taking place in a specific tissue.

Upon normal conditions, kynurenine is readily cleared from blood in the liver and kidneys (Takikawa et al. 1986; Saito et al. 1993). This has been demonstrated by the intravenous administration of radioactively labelled [U-14C]kynurenine into naive mice (Takikawa, Yoshida et al. 1986). In this study, it was shown that 4h after initial injection, approximately 80% of the radioactivity was incorporated into XaA and excreted in urine. About 5–10% of 14C was expired as CO_2. LPS stimulation did not change these proportions but the level of XaA production in urine was increased approximately threefold. Nonetheless, upon LPS treatment, kynurenine turnover did not change substantially, from $5.3h^{-1}$ in naive mice to $6.1h^{-1}$ in the LPS challenged mice (Takikawa, et al. 1986). Thus, increased kynurenine concentration could result as a consequence of its higher production and inadequate to demand clearance from blood (Takikawa et al. 1986). Interestingly, increased excretion of kynurenine and XaA was reported in urine from rats (Takeuchi and Shibata 1984) and humans (Yeh and Brown 1977) loaded with tryptophan, but depleted of pyridoxal phosphate (PLP). This molecule is a cofactor for kynureninase (Jakoby 1954). Without PLP, kynureninase is inactive and kynurenine cannot be further converted into downstream metabolites (Yeh and Brown 1977). Thus, experimental depletion of PLP can abolish kynureninase activity and mimics the situation of insufficient metabolism of kynurenine. However, increased excretion of kynurenine and XaA in urine of PLP-depleted animals and humans could be a physiological route of kynurenine clearance upon its insufficient metabolism. In addition, Takikawa et al found that in the liver and kidneys, upon immune challenge, the enzymatic activities of the following enzymes on the kynurenine pathway: kynureninase, kynurenine 3-monooxygenase (KMO) and 3-hydroxyanthranilate 3, 4 dioxygenase (HAAO) were unchanged (Takikawa et al. 1986). A similar observation was

made in rabbits injected with LPS (Allegri et al. 2003). In addition, *in vitro* experiments with various cell lines have indicated that the enzymatic activity of kynureninase was not affected by IFN-γ in these cells (Heyes et al. 1997). Taken together, these findings suggest that inadequate activities of the downstream enzymes on the kynurenine pathway could be a limiting factor for kynurenine metabolism upon increased kynurenine production evoked by immune challenge. This may explain why, in sera from humans, accumulation of kynurenine is positively correlated with the level of neopterin, which is a biochemical marker of inflammation; (Iwagaki et al. 1995). Neopterin is a metabolite of guanosine triphosphate (GTP). The production of neopterin is significantly increased in the activated macrophages. Thus, increased neopterin is indicat an inflammatory reaction (Widner et al. 2002), whereas increased kynurenine indicates activation of tryptophan metabolism via the kynurenine pathway. Increased kynurenine concentration has been observed in many diseases, including RA (Schroecksnadel et al. 2003), systemic lupus erythematous (SLE) (Widner et al. 2000), sepsis (Pellegrin et al. 2005) and Huntington disease (Leblhuber et al. 1998).

Moreover, kynurenine and her downstream metabolites are biologically active. In the immune system, kynurenine and her metabolites are involved in the immunosuppression (Moffett and Namboodiri 2003). Therefore, reduced metabolism of kynurenine could dampen physiological role of the anti-inflammatory metabolites of kynurenine like, e.g. 3-HK and 3-HAA.

1.2.3.3. Physiological consequences of tryptophan starvation

The anti-proliferative function of decreased tryptophan concentration was shown for the first time in bacteria. In line with these observations, many contemporary publications emphasise an anti-proliferative role of reduced tryptophan concentration in the context of cancer and immune pathology. However, Muller et al. have shown that the concentration needed for anti-bacterial action of tryptophan depletion was 40 –fold higher than was

required for the anti-proliferative function of tryptophan depletion in lymphocytes. In this study, 50% reduction in bacteria cell growth was observed at 1.9 μM concentration of tryptophan, whereas 50% reduction in T cell proliferation was seen at 0.1 μM concentration of tryptophan (Muller et al. 2009).

As a result of tryptophan starvation, the pool of uncharged tRNA (free tRNA, without attached amino acid) is increased (Zaborske et al. 2009), (Munn et al. 2005). Such tRNA can bind into the histidyl-tRNA-synthetase (HisRS)related region located on the C-terminus of GCN2 kinase (Qiu et al. 1998). As a result of tRNA binding, GCN2 kinase undergoes conformational changes and becomes active (Qiu et al. 1998). Activated GCN2 can phosphorylate eukaryotic translation initiation factor 2A (eIF2a) and inactivate it (Qiu et al. 1998; Wek et al. 2006). As a consequence, translation of the vast majority of transcripts become inhibited and cell cycle is arrested (Munn et al. 2005).

1.2.3.4. Cellular and molecular consequences of activation of the kynurenine pathway

It has been shown that the longer T cells were kept under stimulatory conditions (anti-CD3) *in vitro,* the smaller doses of tryptophan metabolites (equimolar mixture of kynurenine, AA, 3-HAA, and QA) were required to induce cell death (Terness *et al.* 2002). It has been also reported that kynurenine was able to reduce proliferation of human peripheral blood lymphocytes (PBL) *in vitro* (Frumento et al. 2002). However, the effectiveness of kynurenine treatment was dependent on time. When kynurenine was present in the cell culture in the first 36h after phytohaemagglutinin (PHA) stimulation, the treatment resulted in decreased cell proliferation (Frumento et al. 2002). However, when exogenous kynurenine was added to the cell culture 36h after initial stimulation, the treatment did not reduce PBL proliferation (Frumento et al. 2002). Moreover, only activated cells were sensitive to the cytotoxic action of kynurenine, whereas naive T and NK cells were not affected by kynurenine (Fallarino et

al. 2002; Frumento et al. 2002). Nevertheless, accumulated kynurenine in the blood could immediately affect newly stimulated cells and limit the immune response.

However, the interpretation of *in vitro* results for the *in vivo* situation should be made carefully. In addition, kynurenine (and possibly N-formyl kynurenine (N-FK) and 3-hydroxykynurenine (3-HK) could be also involved in exacerbation of tryptophan starvation in T cells. In fact, the existence of a positive feedback between IDO1-mediated tryptophan metabolism in DCs and kynurenine-induced tryptophan starvation in CD98 expressing T cells has been proposed (Kaper et al. 2007). The CD98 complex is a Na^+-independent large neutral amino acid transporter able to transport neutral branched amino acids (valine, leucine and isoleucine) as well as aromatic amino acid like tryptophan (Speciale et al. 1989; Wagner, et al. 2001). CD98 is expressed on astrocytes (Speciale et al. 1989) and activated T cells (Wagner et al. 2001). It has been demonstrated that extracellular kynurenine can be exchanged for intracellular tryptophan in a LAT1-dependent manner (Kaper et al. 2007). LAT1 protein is a component of CD98 complex (del Amo et al. 2008). Thus, extracellular kynurenine could potentiate intracellular tryptophan starvation in cells expressing active CD98 complex by increasing tryptophan efflux (Kaper et al. 2007). As a consequence, local and/or systemic kynurenine concentration could be also regulated by the efficiency of kynurenine import into cells. On the other hand, extracellular kynurenine could potentiate intracellular tryptophan starvation in cells expressing active CD98 complex by increasing tryptophan efflux. Thus, this mechanism could account for the observation that kynurenine-dependent reduction in human T cell proliferation was potentiated by medium containing reduced tryptophan concentration (Terness et al. 2002). In this experimental model, kynurenine could have actively depleted T cells of tryptophan, which might have been exchanged for exogenous kynurenine. Also, kynurenine imported via the CD98 complex could have been converted into 3-HAA and further into QA. However, to the best of our

knowledge, it has not been tested yet if the expression of CD98 overlaps with the expression of kynureninase, KMO and HAAO enzymes in cells. Nevertheless, (Moffett et al. 1998) have found that, in rats, intraperitoneal injection of kynurenine resulted in increased concentration of QA in lymphoid organs, including thymus and spleen. In addition, accumulation of QA was observed in macrophages. Thus, these results suggest that kynurenine could be readily taken up and metabolised in various cells. Interestingly, kynurenine injection did not result in QA accumulation in hepatocytes (Moffett et al. 1998), suggesting that either kynurenine is not transported into these cells, or cannot be converted into QA. Moreover, intraperitoneal injection of tryptophan resulted in an increase in QA in hepatocytes but with mild effect on the QA in macrophages (Moffett et al. 1998). Thus, kynurenine is unlikely to be taken up and metabolised by hepatocytes. Moreover, the mechanism of kynurenine transportation into the immune cells described here may explain some of the therapeutic effects of exogenously administered kynurenine.

Treatment with kynurenine was found to ameliorate allergic airway inflammation (Taher et al. 2008), prolong transplanted skin graft survival in rats (Bauer, Jiga et al. 2005) and reduce severity of experimental arthritis (Criado et al. 2009). In addition, (Wang et al. 2010) have demonstrated that kynurenine is also involved in blood pressure regulation upon immune challenge. It has been shown that endothelial cells are primary sites of kynurenine production in an IDO1 dependant manner and IFN-γ can induce *Ido1* mRNA and protein expression in these cells (Wang et al. 2010). In addition, intravenous injection of kynurenine into rats with spontaneous hypertension resulted in a transient decrease in the mean arterial blood pressure. It has been also demonstrated that kynurenine is able to induce relaxation in pre-constricted porcine coronary arteries in a dose-dependant manner. This pharmacological effect of kynurenine was mediated by soluble guanylate cyclase (sGC), cyclic guanosine monophosphate (cGMP) and the protein kinase G (PKG) pathway. Thus, increased

kynurenine could account for hypotension observed in immunologically challenged mice, e.g. mice with sepsis or infected with Plasmodium berghei ANKA (PbA) (Wang et al. 2010).

Although downstream kynurenine metabolites like 3-HK, 3-HAA, and QA may not be involved in blood pressure regulation (Wang et al. 2010), they play a pivotal role in immune regulation (Stone and Darlington 2002). It has been demonstrated that T cell proliferation can be inhibited with micromolar concentrations of 3-HK (IC_{50} 187 μM) (Terness et al. 2002). The cytotoxic action of 3-HK can be attributed to the production of hydrogen peroxidase which results in the damaging action of free hydroxyl radical (Okuda et al. 1996; Okuda et al. 1998). As with kynurenine, exogenous administration of 3-HK effectively reduced symptoms in allergic airway inflammation (Taher et al. 2008).

In contrast to 3-HK, the toxic action of 3-HAA is more complex. Although the final effect of 3-HAA results in cell death of neurons, T cells (Fallarino et al. 2002), monocyte-derived macrophages (Morita et al. 2001) and thymocytes (Fallarino et al. 2002), the mechanisms involved in cell death may be cell-type specific. The formation of cytotoxic free hydroxyl radical might be involved in 3-HAA induced cell death in monocyte-derived macrophages (Morita et al. 2001). In contrast, (Lee et al. 2010) have shown that, in human T cells, 3-HAA could deplete cells of glutathione (GSH) resulting in apoptosis in these cells in a caspase 3-dependent manner. In addition, treatment of mice with 3-HAA increased the survival rate from in acute graft versus-host disease (Lee et al. 2010). However, in addition to GSH-dependant mechanism, 3-HAA can trigger apoptosis in T cells in another way. For example, in $CD4^+$ T cells and Jurkat cells stimulated with anti-CD3/anti-CD8, 3-HAA was shown to inhibit autophosphorylation of the serine 241 in PDK1 kinase (Hayashi et al. 2007). As an explanation of this observation, it has been suggested that 3-HAA forms hydrogen bounds with the following amino acids of PDK1: serine 160, alanine 162 and threonine 222.

This molecular interaction results in inhibition of PDK1 kinase and in an inadequate NFκB activation in response to anti-CD3/antiCD8 stimulation. As a consequence, Th1 and Th2 cells undergo apoptotic cell death upon stimulation (Hayashi et al. 2007). However, in addition to the free hydroxyl radical formation (Morita et al. 2001) and inhibition of autophosphorylation, 3-HAA can also induce apoptotic cell death in a caspase 8-dependent manner (Fallarino et al. 2002). This was observed in Th1 but not in Th2 cells and this may account for the prolonged graft survival in skin graft transplantation (Bauer et al. 2005) and reduced symptoms of allergic airway inflammation upon treatment with exogenous 3-HAA (Hayashi et al. 2007; Taher et al. 2008).

In addition, it has been shown that QA, like 3-HAA, can also induce cell death via caspase 8 and cytochrome c release in Th1 cells and thymocytes (Fallarin, et al. 2002). Interestingly, the involvement of QA in immune regulation was predicted before IDO1-dependant tryptophan depletion was shown to be immunosuppressive (Moffett and Namboodiri 2003). This prediction was based on the observation that of all the tissues tested, the concentration of QA was the highest in the spleen amongst other analysed tissues (Saito et al. 1993). However, the concentration of QA was increased in lymph nodes from mice injected with LPS (Espey et al. 1995). In fact, this was very first report showing accumulation of tryptophan metabolites in the secondary lymphoid organs upon immune challenge. QA, in addition to its immunomodulatory role, is also a natural agonist of the N-methyl-D-aspartate receptor (NMDA) which is primarily expressed in neuronal cells (Stone and Perkins 1981; Kincses et al. 2010). Thus, overproduction of QA can cause excitotoxic cell death in these cells (Stone et al. 2001).

1.2.3.4.1. Cumulative effects of kynurenines and tryptophan starvation on immune cells

Kynurenines can also exhibit a cumulative (additive) effect on T, B, and NK cells (Terness et al. 2002). (Desvignes and Ernst 2009) have demonstrated that an equimolar mixture of kynurenines (L-kynurenine, 3-HK, 3-HAA, anthranilic acid and QA) can inhibit IL-17 production in a dose-dependent manner with an IC_{50} value of 11.7 μM. However, when tested separately, 3-HAA was the most potent tryptophan metabolite with an IC_{50} value of 27.7 μM. Anthranilic acid and quinolinic acid on their own had no effect (Desvignes and Ernst 2009). Also, the differentiation of Th17 cells from naive $CD4^+$ T cells was reduced by the equimolar mixture of kynurenine. Interestingly, kynurenines were able to abrogate the Th17-promoting capacity of IL-23 in Th17 cells. However, the mechanisms responsible for this effect remain unknown (Desvignes and Ernst 2009). In addition to the above findings, Fallarino *et al*. (2006) have shown that in long-term cell culture (7 days), low tryptophan concentration (35 μM) and an equimolar (10 μM) mixture of kynurenine, AA, 3-HK, 3-HAA, and QA promote conversion of naive $CD4^+$ T cells into $CD25^+$ $Foxp3^+$ regulatory T cells (Treg). Tregs are a subset of T cells which are able to reduce immune response by promoting tolerogenic signals in the immune system (Fallarino et al. 2002). When tested *in vivo*, these cells were able to protect NOD-SCID mice from diabetes transfer in a CTLA-4 and IL-10 dependent manner (Fallarino et al. 2006). Therefore, in the long-term, decreased tryptophan concentration and increased concentration of kynurenines could promote tolerance in the immune system. Similarly, $CD8^+$ T cells, exposed to medium containing a suboptimal concentration of tryptophan and increased concentrations of kynurenines, were characterised by the decreased expression of receptor δ, which is a part of the T cell receptor complex (TCR) (Fallarino et al. 2006). As a result, $CD8^+$ T cells exhibited reduced lytic activity and reduced production of IFN-γ and interleukin 2 (IL-2). Proliferation of $CD8^+$ but not $CD4^+$ T cells was also affected by decreased tryptophan concentration and increased kynurenines

upon anti-CD3 or concanavalin (Con A) stimulation. However, when $CD8^+$ and $CD4^+$ T cells were stimulated with PMA and calcium ionophore, using the same culture conditions as for anti-CD3 stimulation, neither cell type was affected (Fallarino et al. 2006).

1.2.3.5. Regulation of the kynurenine pathway

1.2.3.5.1. The amount of enzymes on involved in the kynurenine pathway

In mice, *Ido1* gene contains ten exons and spans 10 kb in the chromosome 8 in mice (Grohmann and Bronte 2010). Interestingly, in the mesenteric lymph nodes, IDO1 has been reported to be expressed constitutively (Onodera et al. 2009), whereas in the antigen presenting cells, mRNA expression for *Ido1* gene has been shown to be inducible by IFN-γ (Munn et al. 1999) , type I interferons (IFN-α and IFN-β) (Adams et al. 2004), and Toll-like receptor 7 (TLR-7) (Furset et al. 2008) and TLR-9 (Fallarino et al. 2009). It has been also shown that in DC exposed to tumour growth factor β (TGF–β) the transcription of *Ido1* gene could be induced by phosphatidylinositol 3-kinase (PI3K) (Belladonna et al. 2008), noncanonical NF-κB pathway (Pallotta et al. 2011), human chorionic gonadotropin (Ueno et al. 2007), and estrogens (Zhu et al. 2007). In addition to the transcriptional regulation of IDO1, post-translational regulation of IDO1 has been also reported. (Emmons et al. 2008) have shown that 3' region of mRNA for *Ido1* contains an AU rich element, which controls stability of mRNA in a TTP-dependent manner. In addition, it has been shown that either upon IL-6/CD28-Ig stimulation (Orabona et al. 2008) or exposure to sodium butyrate (Jiang et al. 2010) IDO1 can undergo proteosomal degradation in a suppressor of cytokine signalling 3 (SOCS3) dependent manner.

In contrast to IDO1, in mice infected with *Plasmodium berghei* ANKA (PbA) mRNA expression for *Ido2* has been reported to be not inducible by IFN-γ (Ball et al. 2007). However, (Metz et al. 2007) have shown that in the pre-dendritic cell line (JAWII) mRNA

and protein for IDO2 was expressed constitutively, whereas stimulation with IFN-γ, IL-10, and LPS resulted in a moderate increase in mRNA and protein expression for *Ido2*.

Transcription of the *Tdo2* gene, in contrast to the IDO enzymes, has been reported to be not inducible by cytokines (Wirleitner et al. 2003). However, an increased concentration of tryptophan (Sadler, Weiner et al. 1984; Sainio and Sainio 1990), corticosteroids (Nakamura et al. 1987), insulin and glucagon (Nakamura et al. 1980) have been shown to be a potent inducers of *Tdo2* mRNA and protein expression.

The murine *Afm* gene is localised on chromosome 11 and consists of 10 exons (Schuettengruber et al. 2003). The *Afm* gene shares the same gene promoter as the T*hymidine kinase* (*Tk*) gene. The sites of initiation of transcription of *Tk* and *Afm* genes are separated from each other by 172-bp-long nucleotide sequence (Schuettengruber *et al.* 2003). Reduced acetylation of the histone H4 on this bidirectional gene promoter drives expression of Afm, whereas its hyperacetylation results in *Tk* gene expression (Schuettengruber *et al.* 2003). Two separate transcription initiation sites drive expression of the *Afm* gene. The first one is located in the bidirectional promoter and gives a 2.6 kb transcript. A 2.9 kb transcript is produced when transcription of *Afm* gene starts in the second exon of *Tk* gene. However, both transcripts, 2.6 and 2.9 kb, encode the same open reading frame of the AFM enzyme (Schuettengruber et al. 2003). In addition, transcription of the longer and shorter transcripts is regulated in an SP1-dependent manner. SP1 transcription factor can bind into the GC-rich sequences like: CACCC and GC boxes and induce expression of various genes involved in cell growth and metabolism (Black *et al*. 2001).

Although inhibition of KMO could be a therapeutically important target (Zwilling et al. 2011) not much is known how expression of the *Kmo* gene could be regulated. Nevertheless, it has been shown that 4h after LPS injection, the expression of mRNA for *Kmo* was

significantly reduced in the cortex but not in the hippocampus of mice (Connor et al. 2008). In contrast, 24h after LPS injection, *Kmo* gene expression was markedly increased in both brain structures: the cortex and hippocampus (Connor *et al*. 2008). Interestingly, mRNA expression for the pro-inflammatory cytokines like: TNF-α, IFN-γ, and IL-6 were significantly increased in the cortex 4h after LPS stimulation, suggesting that these cytokines could be important for *Kmo* gene expression. However, in the hippocampus mRNA expression for *Ifn-γ* was neither changed 4h nor 24h after immune stimulation suggesting that IFN-γ may not be involved in the initiation of the *Kmo* gene transcription in this brain structure. Moreover, it has been demonstrated that LPS can induce *Kmo* gene expression in the microglia *in vitro* (Connor *et al.* 2008). Taken together, these results suggest that in the brain, *Kmo* mRNA expression is tightly regulated in the tissue and in a cell-type specific manner. It has been also shown that in human monocytes, taken from atopic individuals, *Kmo* gene expression was initiated 24h but not 4h after activation of the high-affinity receptor for IgE (FcεRI) receptor (von Bubnoff et al. 2002). In addition, in the non-atopic donors, *Kmo* gene was constitutively expressed in human monocytes. Moreover, in healthy donors, (FcεRI stimulation did not result in increased transcription of the *Kmo* gene. Therefore, increased expression of the *Kmo* gene might be restricted to the pathological situation. Nonetheless, further studies are needed to fully understand FCεRI-induce *Kmo* gene expression.

Although pro-inflammatory signals were not found to increase kynureninase activity in organs isolated from experimental animals (Takikawa et al. 1986; Saito *et al*. 1993), another study showed that TNF-α and a TLR3 ligand (PolyI:C), induced *Kynu* mRNA expression in mature DC's *in vitro* (McIlroy et al. 2005). However, , mRNA expression for *Ido1* and *Kmo* genes was the highest 2h after stimulation; whereas *Kynu* mRNA expression peaked 12h after initial stimulus (McIlroy et al. 2005). In addition, Belladonna et al. (2006)

have found that, in splenic $CD8^+$ DCs, kynurenine could be detected 5h after initiation of tryptophan metabolism induced by IFN-γ. In contrast, QA was detected 18h after IFN-γ stimulation. Thus, this shows that the kinetic of *Kynu* mRNA expression may account for an increased kynurenine concentration in the immune system. In addition, previous *in vivo* observations of delayed kynurenine clearance from sera of immune challenge animals may suggest that accumulation of kynurenine may play some physiological role. For example, immune cells could be exposed to kynurenine for a longer time. Thus, from the resolution of inflammation point of view, it might be beneficial to delay kynurenine metabolism in order to produce toxic metabolites sometime after initial stimuli.

Not much is known about the regulation of *Haao* mRNA and protein expression. Nonetheless, (Huang et al. 2010) have demonstrated that the *Haao* gene promoter is hyper-methylated in endometrioid endometrial carcinoma (Huang et al. 2010). As a result of this epigenetic modification, *Haao* mRNA expression is lost in cancerous tissues (Huang et al. 2010). Hypermethylation of *Haao* gene has been also proposed as a biomarker of ovarian cancer (Huang, et al. 2009).

1.2.3.6. Regulation of catalytic activities of enzymes on the kynurenine pathway

Post-translational control of IDO1 activity is well recognised since it has been found that not always protein expression for IDO1 directly corresponds to its enzymatic activity (Belladonna et al. 2006). The major and the rate limiting factor which may determine the rate of IDO1 efficacy may be the incorporation of heme, a prosthetic group, into the IDO1 protein (Shimizu et al. 1978; Samelson-Jones and Yeh 2006). In addition, superoxide is regarded as a co-factor and even an activator of IDO1, whereas nitrosilation of IDO1 is considered to reduce IDO1 activity (Samelson-Jones and Yeh 2006).

In mice, the activity of KMO is higher in the kidneys 901.50 ±73.50 nmol/(min/g) than the liver 656.55 ±18.99 nmol/(min/g) (Allegri et al. 2003). Interestingly, in rats, it has been shown that the activity of KMO was reduced in the liver during ageing (Comai et al. 2005). Stroke, which is a primary source of ischemic brain damage, is more likely to occur in older people. Thus, reduced KMO activity could be protective in patients affected by stroke. However, KMO activity in humans has not been assessed yet.

In mammals, the enzymatic activity of KYNU is the lowest in comparison with other enzymes on the kynurenine pathway (Allegri et al. 2003). In murine kidneys the enzymatic activity of kynureninase was found to be 1.43 ± 0.04 nmol/ (min/g) tissue, whereas in the liver: 10.69 ± 0.26 nmol/ (min /g) tissue (Allegri et al. 2003). Thus, KYNU may be considered as a rate limiting enzyme involved in the catabolism of kynurenine (Salter et al. 1986). (Comai et al. 2005) have also reported that in rats, enzymatic activity of KYNU decreased in the liver with ageing. In contrast, in the kidneys, the activity of KYNU was increased in 18-month-old rats in comparison with 1-week-old animals (Comai et al. 2005). Thus, in old animals, kynurenine could be preferentially metabolised in the kidneys rather than in the liver. In addition, it has been reported that 3-HAA can inhibit KYNU in porcine liver (Tanizawa and Soda 1979). This observation suggests that KYNU activity may be regulated by the auto-inhibitory loop. However, this has to be validated with more contemporary methods and in other tissues and species.

Therefore, not surprisingly, HAAO was found to exhibit the highest enzymatic activity amongst kynurenine pathway enzymes (Allegri et al. 2003). In murine liver, the activity HAAO was reported to reach 4,803 ± 256 nmol/(min g) tissue whereas in the kidneys this value was 1,108 ± 59 nmol/(min g) tissue (Allegri et al. 2003). Comai et al. (2005) have demonstrated that, in the liver and kidneys of aging rats, the specific activity of HAAO

enzyme was increased. Thus, efficiency of 3-HAA metabolism may be higher in old animals in comparison with younger ones. This may have physiological implications since 3-HAA is biologically active. It is also possible to reversibly inhibit HAAO enzyme activity by administration of the synthetic HAAO inhibitor, NCR-631 (Walsh et al. 1991). It has been shown that NCR-631 effectively protected organotypic hippocampal cultures from LPS and interleukin 1 beta (IL-1β)-induced cell death (Luthman et al. 1998). In addition, pre-treatment of mice and rats with NCR-631 reduced severity of pentylenetetrazol (PTZ)-induced seizures (Luthman 2000). A similar observation was made in DBA/2J mice in which pre-treatment with NCR-631, 30 or 15 min before sound-induced seizures, exhibited an anti-convulsive effect. However, the therapeutic effect of NCR-631 has been shown to wear off quickly. 60 min after drug administration seizures were comparable with vehicle-treated animals (Luthman 2000). Thus, pharmacological intervention into 3-HAA metabolism may not be feasible in the long-term. In contrast, modulation of *Haao* mRNA and protein expression could be a more effective strategy.

1.2.3.7. The kynurenine pathway in the experimental medicine

The kynurenine pathway has been extensively investigated in the past few decades and there are at least three drugs available which are derived from catabolites of kynurenine: tranilast (Konneh 1998), ponstan, and arlef (Barnardo et al. 1966). Hence, not surprisingly, catabolites of tryptophan have attracted substantial attention and have been tested in the multiple animal models of human disease (Table 3).

Table 3 Therapeutic applications of the kynurenines in animals

Tryptophan metabolite	Experimental model	Effect	Reference
Kynurenine	Allergic airway inflammation Skin graft transplantation CIA	Reduced eosinophilia, Reduced TH2 cytokine production Prolonged graft survival Reduce severity of disease	(Taher, Piavaux et al. 2008) (Bauer, Jiga et al. 2005) (Criado, Simelyte et al. 2009)
3 - HK	Allergic airway inflammation	Reduced eosinophilia, Reduced TH2cytokine production	(Taher, Piavaux et al. 2008)
3-HAA	Allergic airway inflammation Allergic airway inflammation Skin graft transplantation	No Reduced symptoms, T_H2 cell death Prolonged graft survival	(Taher, Piavaux et al. 2008) (Hayashi, Mo et al. 2007) (Bauer, Jiga et al. 2005)
QA	Allergic airway inflammation Carrageenan-induced inflammation	No Reduced inflammation	(Taher, Piavaux et al. 2008) (Heyliger, Mazzio et al. 1999)
KyA	Allergic airway inflammation	NO	(Taher, Piavaux et al. 2008)
XaA	Allergic airway inflammation	Reduced eosinophilia, Reduced TH2 cytokine production	(Taher, Piavaux et al. 2008)

1.3. Arthritic diseases

1.3.1. Joints and arthritic diseases

In the anatomic nomenclature the term "joint" refers to the functional unit which connects two or more parts of the skeleton. Synovial joints (diarthroses) evolved to promote movement and have a joint cavity which is enclosed by a fibrous capsule linking the skeletal elements. The capsule itself is lined by a synovial membrane that secretes fluid which has lubricating and nutritive functions. In healthy joints, the synovium membrane (intima) is a fine film, one or two cell layers thick. The normal intima has no basement membrane and is made of comprises type A and type B synoviocytes lying on a bed of loose connective tissue with a network of small blood vessels (the subintima). Type A synoviocytes are macrophage – like cells and type B synoviocytes (fibroblast – like cells) are of mesenchymal origin (Taylor 2007). Therefore, it is important to bear in mind that the joint needs to be considered as a whole organ in which several types of different tissues/structures act together and constitute a functional unit.

Arthritis is a collection of pathological conditions affecting joint function and therefore directly impairing patient ability to move and perform everyday tasks. There are various arthritic diseases with multiple clinical manifestations, prognosis, and aetiology. Nonetheless, based on the cellular and molecular mechanisms involved in the diseases, arthritic pathology can be divided into three distinct groups: metabolic driven arthritis e.g. gout, injury induced arthritis e.g. osteoarthritis and inflammatory arthritic diseases e.g. RA and psoriatic arthritic (PsA).

1.3.2. Rheumatoid arthritis

RA is the most common form of inflammatory arthritis and effects around 1% of the population of European descent. The disease is characterised by chronic inflammation of

synovial joints involving infiltration of activated T cells (Th1 and Th17) and macrophages. Once established, RA is characterised by a deforming symmetrical polyarthritis of varying severity and clinical symptoms. In fact, the word "*rheum*" (in Greek: ρευμ) means "to flow" and reflects relapsing and self-remitting nature of RA (Taylor 2007). The primary manifestations of RA are: synovitis of joint, loss of articular cartilage, and formation of bone erosions. When the disease is left untreated or sub-optimally managed it becomes progressively disabling and this contributes to the tremendous suffering of the patient and his/her next of kin (Taylor 2007).

Although more than two centuries passed since RA was clinically described (Garrod 1888; Landre-Beauvais 2001) the causative factors involved in the disease remain unknown. Nonetheless, molecular and cellular mechanisms responsible for propagation of the pathology in RA are relatively well characterised. In the established RA, the synovial membrane is inflamed (synovitis) and infiltrated by blood derived cells, e.g. T cells, B cells, macrophages, and plasma cells. $CD4^+$ T cells represent the majority (50 – 70 %) of the cellular infiltrate with macrophages comprising an additional 20%. Interestingly, neutrophils are rarely retained within the subintimal layer, however they comprise the majority cell type in synovial fluid. The remaining pool of cells in the synovial fluid is made of $CD4^+$, $CD8^+$, macrophages, dendritic cells, and synoviocytes. The protein level in the synovial fluid has been shown to be elevated. In contrast, the glucose level may be lower in comparison with healthy synovial fluid. In RA, the synovial fluid is rich in pro-inflammatory cytokines and immune complexes containing rheumatoid factor (Taylor 2007).

Pannus, defined as synovitis which locally adhere to cartilage and invade it, is considered as an invasive front of rheumatoid tissue. The destructive lesion typically occurs at the circumferential attachment of the joint capsule, just below and adjacent to the articulate cells at the cartilage-pannus junction. Interestingly, the cellular composition of the pannus

depends on the anatomical localization of this highly pathological form of tissue. For example, it has been shown that at the cartilage–pannus junction, it is compromised of synoviocytes and macrophages, whereas the pannus–invading subchondral bone is enriched with osteoclasts (Taylor 2007).

In RA, bone erosions and cartilage damage is mediated by several families of proteolytic enzymes, including serine proteases, matrix metalloproteinases (e.g. collagenases, stromelysin, and gelatinase). Nonetheless, exacerbated activity of aggrecanase is believed to play a primary pathological role in cartilage degradation. However, the reciprocal relation between the degree of inflammation, formation of bone erosions, and cartilage damage is far from being comprehensively understood (Taylor 2007).

Although pathological changes in RA are perpetuated by the various families of enzymes and cell types the activity of a particular effecter mechanism depends on the local milieu of signalling molecules. Cytokines are small, short lived proteins and important players in the intercellular communication between cells. In addition, certain types of cytokines exhibit pro-inflammatory activities whereas other types of cytokines are important mediators of anti-inflammatory responses. Nonetheless, it is worth keeping in mind that the particular role of a given cytokine depends on the molecular context in which the cytokine operates. For example, IFN-γ is considered as a major pro-inflammatory cytokine, whereas it has been shown that anti-IFN-γ treatment exacerbates severity of CIA. In addition to IFN-γ and TNF–α, the inflamed synovium is characterised by increased concentration of other pro-inflammatory cytokines, including IL-1, IL-6, IL-8, and granulocyte macrophage colony–stimulating factor (GM-CSF) (Taylor 2007).

1.3.2.1. Pharmacotherapy of RA

The successful therapy of RA aims to chive four goals: 1) to control symptoms and signs 2) to retard and/or prevent of structural damage in the joints 3) to preserve and improve

function of the affected joints 4) to induce a remission. In fact, drug therapy for RA can be grouped into one of five categories (listed below). However, it is important to state that there is no correlation between the aims of therapy and the type of treatment (Taylor 2007).

Non-steroidal anti-inflammatory drugs (NSAIDs) e.g. aspirin are weak organic acids that bind to serum proteins and may accumulate preferentially in the inflamed joints and persist there longer than would be predicted on the basis of their serum half-life. The primary anti-inflammatory action of NSAIDs is mediated by inhibition of cyclo-oxygenases (COXs). COXs are important in inflammation because these enzymes participate in productions prostanoids which acerbate the inflammatory reaction (Greene et al. 2011).However, there are two different types of COX proteins, COX-1 and COX-2, respectively. These two enzymes are encoded by two distinct genes. *Cox-1* is constitutively expressed, whereas *Cox-2* has been shown to be inducible e.g. by pro-inflammatory cytokines. However, the first generation of NSAIDs targeted both enzymes causing severe side effects e.g. peptic ulceration with bleeding. Nevertheless, currently, there are available specific and selective inhibitors of COX-1 and COX-2. In the line with this, indomethacin and naproxyn have been proven to be able to inhibit COX-1 selectively, whereas nabumetone, meloxican, and etodolac selectively inhibit COX-2. In addition, it has been demonstrated that etoricoxib and lumeracoxib can specifically inhibit COX-2 which reduces risks associated with non-specific inhibition of COX-1. However, NSAIDs can only effectively reduce symptoms of RA (e.g. reduced inflammation and analgesia) whereas they have no effect on disease progression (Taylor 2007).

Corticosteroids belong to a family of drugs chemically related to steroids such as cortisone which is an endogenous hormone in the adrenal cortex. Anti-inflammatory mechanisms of corticosteroid are mediated by the various mechanisms. Nonetheless, the most

important one involves the selective binding of corticosteroids to the intracellular receptor localised in the cytoplasm. Subsequently, this complex translocates into the cell nucleus and binds to the steroid response elements in the promoters of genes. In line with this model, it has been shown that transcriptional activation of IκB promotes down-regulation of a number of key pro-inflammatory pathways, including expression pattern for adhesion molecules and secretion of pro-inflammatory cytokines e.g. IL-1 and TNF-α. As a result, recruitment and migration of inflammatory cells is reduced. In addition, upon treatment of macrophages and granulocytes with corticosteroids, a reduction in the rate of phagocytosis has been also reported. Corticosteroids can also reduce proliferation of T cells, induce slower rate of IL-2 secretion, and increase the rate of lymphocyte apoptosis. However, administration of steroids has a number of side effects, some of them being serious (e.g. glucose intolerance, osteoporosis, and infection) (Taylor 2007).

Disease modifying anti-arthritic drugs (DMARDs) are able to reduce the rate of structural joint damage. This is in contrast to the NSAIDs which do not reduce structural joint damage. Currently available drugs in the category of DMARDs include methotrexate (MTX), sulphasalazine, hydroxychloroquine, leflunomide, D-pennicillamine, and injection with gold salts. However, in the clinical practice, MTX is the most commonly prescribed drug. At the higher doses (used in cancer therapy) MTX reduces the rate of purine nucleotide synthesis by inhibition of dihydrofolate reductase. In addition, at the lower doses (used in the therapy of RA), MTX may also stimulate the release of adenosine which has multiple anti-inflammatory functions. In fact, it is postulated that MTX-driven adenosine release could be mediated by a pharmacologically active metabolite of MTX which is 5-aminoimidazol-4-carboxamide ribonuleotide (AICAR). This substance is a substrate for AICAR transformylase which can be also inhibited by MTX (Taylor 2007).

Biologics are protein based drugs derived from living organisms and designed either to inhibit or augment a specific component of the immune system. The advantages of biologics rely on the fact that it is possible to design and produce very selective molecules, which can recognise and neutralise biological activities of their targets. The binding between biologics and their targets utilise the same biophysical principles as described for interactions between antigen/antibody and ligand/receptor. For example, Infliximab (Remicade®) and Adalimumb (Humira®) are monoclonal anti-TNF-α antibodies which bind and inactivate biological activities of TNF-α. In contrast, Etanercept (Enbrel®) is a dimer and fusion protein which is composed of p75 TNF receptor of fully human amino acid sequence linked to the Fc fragment of human IgG_1. Therefore, etanercept acts as a competitive inhibitor of TNF-α and lymphotoxin β (LT-β). However, in contrast to infliximab and adalimumab, etanercept forms relatively unstable complexes with TNF-α. Nonetheless, all TNF inhibitors drive deactivation of cascades of the pro-inflammatory cytokines at the site of inflammation and therefore prevent joint from (cellular and enzymatic driven) destruction. These effects of biologics are primarily mediated by the reduced traffic of leukocytes to the inflamed joints as shown in an open label clinical trial. In this particular study, it has been demonstrated that two weeks after treatment with infliximab the retention rate of autologous indium-111 labelled granulocytes in the hands, wrists, and knees was decreased by up to 50% (Taylor 2007).

Combinatory therapy of RA with biologics and DMARDs has been shown to be superior over mono-therapy either with DMARDs or biologics. In addition, it has been confirmed in the multiple clinical trials that early and aggressive therapy with combination of biologics and DMARDs (mainly methotrexate) provides the best therapeutic outcome (Taylor 2007; Smolen et al. 2010).

1.3.3. Animal models of RA

Animal models of human diseases serve as an important experimental tool mimicking human diseases. Therefore, it is possible to investigate molecular and cellular mechanisms responsible for propagation of pathological features observed in human diseases in a rigorous scientific manner. In fact, drug testing in experimental animals is an indispensable step during drug development. However, it is important to recognise and appreciate that human disease cannot be exactly mimicked by the any of the existing animal models. Nevertheless, animal models of human diseases are valuable source of information regarding biology of the disease and efficacy of novel drug candidates (Bolon et al. 2011).

Currently, several types of animal models of RA are available. Historically, one of the first models of RA was known as antigen–induced arthritis (AIA). In this model, animals (e.g. guinea pigs, mice or rabbits) were injected with fibrin (protein of extracellular matrix) dissolved in complete Freund's adjuvant (CFA) followed by intra-articular injection of fibrin 2-3 weeks later (Dumonde and Glynn 1962). Interestingly, it has been shown that fibrin could be successfully replaced with other antigens like e.g. methylated bovine serum albumin. Histopathological examination of joints with AIA reveals many similarities to RA, including hyperplasia of synovial lining layer, perivascular infiltration with lymphocytes and plasma cells, formation of lymphoid follicles, cartilage erosions and pannus (Williams 1995). In addition, AIA in rabbits, like RA in humans, is chronic, with synovitis lasting for long periods. However, unlike RA, AIA, is a monoarticular disease (affecting only the injected joint) and is not associated with MHC class II genes (Henderson et al. 1993).

Adjuvant arthritis is another animal model of RA. In this model, rats are injected with single dose of CFA. Polyarthritis begins 10-45 days after injection and usually lasts for a month. Adjuvant arthritis is an acute disease characterised by oedema, infiltration into the

joint of mononuclear and polymorphonuclear cells, and formation of pannus, cartilage and bone erosions. Susceptibility to adjuvant arthritis is MHC-linked and the disease involves inflammatory and necrotic changes in multiple sites, including the gastrointestinal and genitourinary tracts, skin and eyes (Kaklamanis 1992).

Streptococcal cell wall–induced arthritis in rodents, like human RA, is a severe chronic polyarthritis, characterised by remissions and exacerbations. The pathological features of streptococcal cell wall – induced arthritis include infiltration of polymorphonuclear cells, $CD4^+$ T cells and macrophages. Histological analysis of inflamed joints reveals hyperplasia of the synovial lining layer, formation of pannus, bone, and cartilage erosions (Bolon et al. 2011).

Pristane-induced arthritis, as RA, is a chronic form of arthritis that fluctuates in disease activity. The disease can be evoked in genetically susceptible mice 65 to 300 days after intraperitoneal injection of 2,6,10,14-tetramethylpentadecane (pristane). Like other models of RA, histopatological changes observed in this model are similar to those seen in human RA. However, molecular and cellular mechanisms of pristine-induced arthritis remain unclear (Wooley et al. 1989; Holmdahl et al. 2001).

It is also possible to induce inflammatory arthritis in rodents by immunisation of animals with joint specific antigens. Proteoglycan-induced arthritis (PIA) has been described in BALB/c mice following repeated injections with human foetal cartilage proteoglycans (Mikecz et al. 1987). Clinical manifestations of the disease include progressive inflammation of the joints in the limbs with formation of bone and cartilage erosions. The development of PIA is associated with both humoral and cellular immunity to human and murine proteoglycans. Collagen induced arthritis (CIA), like PIA, is also associated with both humoral and cellular autoimmune mechanisms (Mikecz et al. 1987; Williams 1995).

1.3.3.1. Collagen induced arthritis

1.3.3.1.1. Induction and pathogenesis of CIA

The development of CIA in different species depends on the ability to induce and maintain an immune response to autologous type II collagen. Thus, this suggests CIA may depend on the activation of autoreactive T cells and can be only developed in genetically susceptible mice. In fact, it has been shown that H-2^q, H-2^r, H-2^{w3}, and H-2^{w17} haplotypes make mice prone for CIA and these gene variants are localised in the MHC class II locus (Holmdahl et al. 1988; Durie et al. 1994). Interestingly, in CIA, like in RA, there is a sex-dependant linkage in the susceptibility to arthritis. However, in mice, unlike in humans, males are more susceptible to the disease (Williams 1995).

During CIA, there is a pronounced T and B cell response to type II collagen (Stuart et al. 1982). However, the increased activity of T cells isolated from draining lymph nodes is generally only detectable for a relatively short time period (two weeks after immunisation) and returns to the normal levels before clinical manifestations of arthritis becomes apparent (Stuart et al. 1982). However, it has been well recognised that inflamed joints are the sites where activated T cells accumulate and are involved in bone damage. In line with these observations, it has been observed that immediately before the onset of CIA activated $CD4^+$ T cells could be found in close proximity to class II expressing cells in the synovium (Holmdahl et al. 1988).

T cells are also likely to contribute to the induction of the inflammatory responses in CIA by activating macrophages and fibroblast in the synovium. This process could be mediated by the release of the pro-inflammatory cytokines such as IL-1, IFN-γ, and TNF-α. In addition, T cells can also contribute to the development of CIA by activation of B cells. The interaction between T and B cells has been shown to be required for the induction of CIA

because arthritis may be prevented by treatment with antibodies against CD40 ligand. This molecule is specifically expressed on the surface of T cells and is necessary for T cell dependent B cell activation (Durie et al. 1993).

1.3.3.1.2. A comparison between CIA and RA

Although CIA is one of the most relevant animal models of RA, there are also profound differences between this animal model and human disease. For example: in CIA the inflammatory infiltrate contains large numbers of polymorphonuclear leucocytes (Caulfield et al. 1982), whereas the infiltrate in RA is dominated by mononuclear cells (Janossy et al. 1981). In addition, unlike RA, CIA is not characterised by prolonged inflammatory activity or fluctuations in disease activity (Holmdahl et al. 1989). However, both diseases have periods of remission and auto-antibodies can be detected (Holmdahl et al. 1989). In CIA, the antibody response is directed against native type II collagen, whereas only 10-15% of sera from RA patients are positive for anti-native type II collagen antibodies (Morgan et al. 1987). In addition, type II collagen is the antigen driving the T cells response in CIA, whereas a joint specific T cell antigen has not been convincingly identified in RA (Williams 1995).

1.4. Imaging methods in RA and CIA

1.4.1. Overview of the existing imaging modalities

Based on the physical principles applied for imaging of RA it is possible to classify imaging strategies into the six different modalities (Gomples et al.2011) (Figure 2). However, in clinical practise, only three of them are commonly applied for diagnosis and monitoring progression of the disease. These are: magnetic resonance imaging (MRI), x-ray radiography, and imaging with ultrasound (Fouque-Aubert et al. 2010).

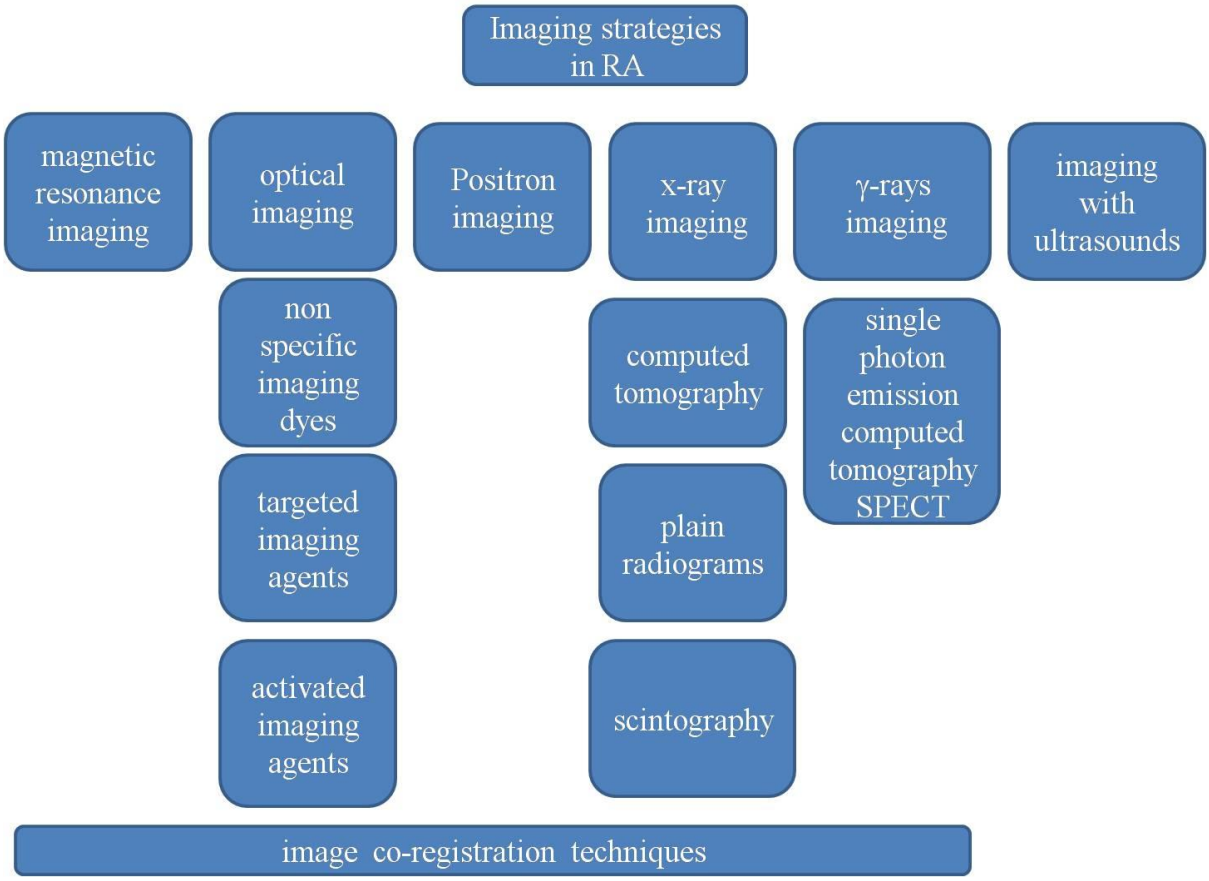


Figure 2 Various types of imaging modalities applied in clinical and preclinical medicine of RA

Historically, imaging of RA with x-rays was the first method applied in the clinical practise (Kellgren 1956). In fact, for the first time, semi-quantitative assessment of plain radiograph showing arthritic pathology in hands and foots was introduced in the 1950's and since then is a gold standard method in clinical trials and as well as in the routine assessment of RA (Kellgren 1956; Smolen and Aletaha 2011). However, the limitation of this technique relies on the fact that only profound changes in the joint integrity (e.g. narrowing of the joint space and large erosions in the cortical bone) can be visualised and scored. Therefore, mild and subclinical pathological changes may be underestimated.

Application of x-ray imaging is associated with exposure to damaging radiation. In contrast, imaging with ultrasounds is harmless and has been shown to provide pivotal

information about bone damage, synovial thickness, and functional changes in the blood flow in the inflamed joints (Finzel et al. 2011; Iagnocco et al. 2011).

Magnetic resonance imaging (MRI) is another method for imaging of synovitis and tenosynovitis in clinical practise of inflammatory arthritis (Fouque-Aubert et al. 2010). The majority of the scoring systems developed for assessments of RA with MRI rely on measurements of the synovial membrane thickness and signal intensity upon intravenous contrast administration. In addition, using MRI and histochemical analyses of synovial biopsies, a correlation between the degree of inflammation and the vascularity of synovium has been demonstrated (Ostergaard et al. 1997).

As has been stated in the previous two paragraphs, plain radiograms and MRI are well established imaging modalities in the clinical assessment of RA. However, there are other methods available and experimental approaches towards imaging of RA (Figure 2). For example, positron emission tomography (PET) has been successfully applied for imaging of cell proliferation in the joints with RA (Andersson et al. 1998). In this particular study, using radioactively labelled glucose (^{18}Fluorodeoxyglucose, ^{18}F-FDG) and choline (methyl-^{11}C-choline) metabolism of glucose and choline (indispensable component of cell membrane) was investigated. In addition, in this study, patients were subjected to MRI imaging and results showed high correlation between volume of inflamed synovium and turnover of cell membranes in the inflamed joints and glucose metabolism (Roivainen et al. 2003).

1.4.2. Micro-computed tomography in clinical medicine of RA

Microscopic computer tomography (μCT) is a term which refers to the technique of imaging objects with submillimetre spatial resolution using x-rays (Ritman 2011). However, in fact, there are three levels of μCT: mini-CT (200 – 50 μm), micro-CT (50 -1 μm), and nano-CT (1 -0.1 μm). Nonetheless, usually, μCT refers to the imaging with x-rays within the

range of 50 to 1 μm (Ritman 2011). It has also been shown that μCT provides reliable results (Liu and Morgan 2007; MacNeil and Boyd 2007) which are highly correlated with traditional 2D histomorphometric studies in animals, human specimens, and biomechanical properties of bones (Marechal et al. 2005; Teo et al. 2006; Yeom et al. 2008). Therefore, not surprisingly, μCT became a gold standard in the studies aiming to assess bone phenotype. However, in the past, application of μCT was primarily restricted to the *ex vivo* studies. This was mainly due to the high dose of exposure to the x-ray radiation. Moreover, recently, a new generation of μCT scanners has been constructed which enable researcher to perform μCT *in vivo* (Laperre et al. 2011) and on humans (Liu et al. 2010; Wang et al. 2010). Interestingly, (Finzel et al. 2011) have demonstrated that bone erosions are not restricted to the arthritic patients but also could be seen in the healthy volunteers. However, in this study, it was not addressed if these bone erosions could overlay with the "nutrient foraments", the places where blood vessels enter the bones. Nevertheless, application of μCT in patients with inflammatory arthritis has revealed that in RA bone erosions may have distinct appearance from those observed in PsA, (Figure 3 and Table 4).

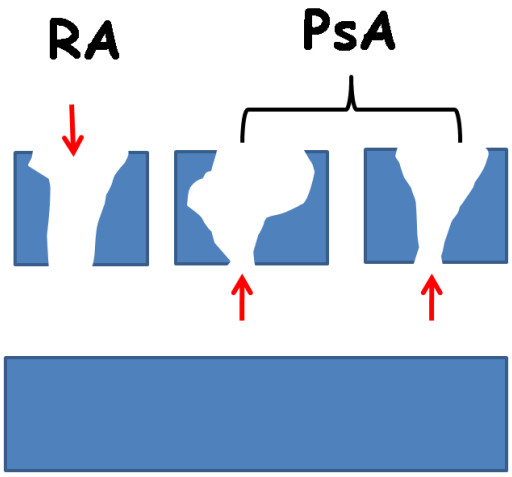


Figure 3 Schematic representations of bone erosions and their origin in two types of inflammatory arthritis.

In RA bone erosions usually have U shape, whereas in PsA two types of bone erosions have been reported: Ω and T shape. Red arrows indicate on the origin of bone erosions. Blue shows cortical bone. Based on the information provided by (Finzel et al. 2011).

Table 4 Quantitative comparison of bone erosions observed in two types of inflammatory arthritis

Comparison is based on the single publication using μCT techniques (Finzel et al. 2011).

Parameter	PsA	RA
Number of bone erosions	6.3 ±1.3	6.1 ±0.9
Percentage of bone erosions with diameter bigger than 2mm	39.7%	60.2%
The size of mean cortical breaks	1.33 mm	2.3 mm
The size of mean cortical deepness of cortical break	0.86 mm	2.2 mm

In addition, these authors also postulated that in PsA bone erosions could be initiated from the endosteal sites of bone. In contrast, in RA, it is well established that bone erosions are triggered by interactions between T cells (mainly Th1 and Th17 cells) and osteoclastic/osteoclastic cells (see section 1.2.2) on the periosteal site of the bone (Figure 3). However, (Finzel et al. 2011) has shown that in patients with RA, treated with anti-TNF inhibitors (adalimumab, etanercept, infliximab, and certolizumab), the healing of bone erosions started from the endosteal site of cortical bone. Interestingly, treatment with methotrexate only has been reported to be ineffective in the initiation of bone erosion healing.

1.5. Objectives and an outline of the thesis

In conclusion to information presented in the introduction, the following objectives have been made:

1) To compare changes in mRNA expression for the kynurenine pathway enzymes in the secondary lymphoid organs (lymph nodes and the spleen), paws, liver, and the kidneys during CIA[2] in comparison with naïve tissues.

2) To compare changes in protein expression for enzymes on the kynurenine pathway in these organs during CIA and healthy animals.

3) To quantify changes in tryptophan, kynurenine, AA, and 3-HAA in sera and tissues taken from naïve mice and those with CIA

4) To test anti-arthritic properties of 3-HAA in mice with CIA

5) To test if novel pathological features of bone pathology in patients with RA can be also seen in mice with CIA

6) To test if novel pathological features of bone pathology in mice could be prevented by anti-TNF therapy

In the next six chapters materials and methods are described together with experimental results showing original data needed to fulfil objectives specified to this project. In line with this:

[2] In this thesis, healthy animals, purchased and kept together with mice with arthritis are defined as naïve. During CIA, two separate groups were selected. Pre-arthritic animals (14 days after immunisation) and those with established CIA (10 days after onset of disease). Such classification is based on the previous findings showing functional differences at these time points (Stuart, J. M., A. S. Townes, et al. (1982). "Nature and specificity of the immune response to collagen in type II collagen-induced arthritis in mice." J Clin Invest **69** (3): 673-683.

Chapter 2 "Methods"

In this chapter, materials and methods used in this project have been described. The chapter starts from the description of animals and detailed information about *in vivo* experiments which were conducted to fulfil objectives specified to this project. Next, the establishment of the quantitative HPLC and immunohistochemical methods have been described.

Chapter 3 "Systemic changes in the concentartion of tryptophan and its metabolites during arthritis"

In this chapter, changes in the concentration of tryptophan, kynurenine, AA, and 3-HAA in serum, liver, and the kidneys during CIA are presented. In addition, I have measured changes in the expression of mRNA for subsequent genes on the kynurenine pathway during the disease in the liver and kidneys.

Chapter 4 "Comparative study of tryptophan catabolism via the kynurenine pathway in the secondary lymphoid organs and inflamed paws during arthritis"

Activity of the kynurenine pathway in the immune system has been previously well documented. Thus, it was of interest to measure the concentration of tryptophan, kynurenine, AA, and 3-HAA in the iLN, spleens, and inflamed paws isolated from mice with pre-arthritic stage of CIA as well as from animals with established CIA and naive mice.

Chapter 5 "Evaluation of the therapeutic potential of kynurenine catabolites in collagen induced arthritis"

Formation of bone erosions in the diarthrodial joints is a primary manifestation of inflammatory arthritis. μ-CT is a well established method for imaging of bone pathology. Hence, it was of interest to establish this method in the Kennedy Institute of Rheumatology and assess the outcome of the anti-inflammatory treatment with catabolites of kynurenine

(AA and 3-HAA) on bone pathology. As a positive control, treatment with TNF-α inhibitor, etanercept, had been applied.

Chapter 6 "General discussion and future directions"

In this chapter, I have described how my original results contribute to the existing knolwaleadge about the kynurenine pathway in the immune system and an animal model of rheumatoid arthritis. In addition, the limitations of my my experimental methods as well as future plans had been presented.

Chapter 7 " Bibliography"

In this chapter the existing literatuture relevent to this projcets is presented.

Chapter 2

Methods

2.1. Experimental animals

DBA/1 mice (H-2^q MHC haplotype), C57BL/6 mice (WT), and *Ido1* KO C57BL/6 mice (8-12 weeks of age) were used throughout my PhD project. Apart from *Ido1* KO mice which were bred at the Kennedy Institute of Rheumatology, the remaining mice were purchased from Harlan (Bicester), UK. Mice were housed in groups of 6-8, and maintained at 21°C ±2°C on a 12 hour light/dark cycle (7am – 7pm) with food and water *ad libitum*.

All experimental procedures were approved by the UK Home Office and performed on male mice because it has been previously reported that female mice exhibit reduced onset of CIA (Staines and Wooley 1994; Williams 1995). The microbiological quality of the mice colony was screened on a routine basis. This is necessary because it has been previously reported that infection of mice with *Mycoplasma spp, Saldactoadenitis sendai, and hepatitis spp viruses* reduces susceptibility to CIA (Williams 1995).

2.1.1. Genotyping of Ido1 KO mice

Genomic DNA was extracted from the murine tails using REDExtract-N-Amp™ Tissue PCR kit (Sigma). PCR reaction was performed as described in a subsequent section with the primers indicated in Table 5.

.

Table 5 Oligonucleotide sequences used for Ido1 KO mice genotyping

Nucleotide sequences of the primers are provided on the Jacksons Laboratory website. This company provides Ido1 KO mice to the scientific community

WT (forward)	5'TGG AGC TGC CCG ACG3'
WT (reverse)	5'TAC CTT CCG AGC CCA3'
Ido1 KO (forward)	5'CTT GGG TGG AGA GGC3'
Ido1 KO (reverse)	5'AGG TGA GAT GAC AGG3'

DNA Engine DYAD^{TM} thermo cycler was used for the reverse transcription reaction. The reaction was carried out using MangoMix (Bioline). PCR products were resolved in 2% agarose/TBE gel with ethidium bromide. UV light in a transilluminator was used to visualise 400 bp and 300 bp long DNA fragments. A representative result is shown in Figure 4.

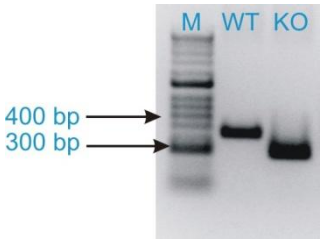


Figure 4 Genotyping of Ido1 KO mice

A representative picture showing results of genotyping of WT and Ido1 KO mice using PCR technique followed by DNA electrophoresis in an agarose gel. The band corresponding to the 400 bp is characteristic for WT mouse whilst the band which corresponds to the 300 kb indicates an *Ido1* KO mouse because exons 3 to 5 are deleted in mutated mice.

2.2. Collagen-induced arthritis

As has been described in the first chapter, CIA is a commonly used animal model of RA. However, the severity of the disease as well as the incidence highly depends on the type of the collagen used for immunisation. For example, it has been shown that type IX and XI collagens are poorly arthritogenic, whereas type II collagen is a potent inducer of inflammatory arthritis (Williams 1995). However, it has been observed that immunisation with heterologous type II collagen results in more robust arthritis than immunisation with autologous type II collagen (Williams 1995). For example, in DBA/1 mice, immunisation either with chicken or bovine type II collagens was shown to be effective. In contrast, in C57BL/6 mice only immunisation with chicken type II collagen could induce arthritis. Thus, selection of particular source of type II collagen is important for induction of the disease in specific strains of mice (Inglis et al. 2007; Inglis, 2008).

2.2.1. Extraction of type II collagen

Type II collagen was purified from the knee joints of one week old calves or adult chicken sternums. Interestingly, it has been previously observed that cartilage obtained from neonatal or very young animals provided the most consistent results. In addition, young cartilage provided the highest yield of type II collagen (Williams 1995; Inglis, Simelyte et al. 2008).

In this project, the following protocol was used for purification of type II collagen:

1. Cartilage (white colour) was dissected from the bones (pink colour) using a scalpel.

2. Cartilage was chopped into small pieces and then powdered using a liquid nitrogen freezer-mill (Spex Industries Inc, Metuchen, NJ, USA).

3. In the next step, proteoglycans were removed by stirring the finely-powdered cartilage in 5 volumes of 4M guanidine-HCl in 0.05M Tris-HCl (pH 7.5) overnight at 4 ^{0}C. The suspension of cartilage was then centrifuged at 20,000 g for 1h at 4 ^{0}C. The supernatant was discarded and the sediment was washed three times in 0.5M acetic acid. To ensure better removal of proteoglycans, extraction with guanidine-HCl and washing steps were repeated three times.

4. The insoluble cartilage residue was added to a solution of pepsin in 0.5M acetic acid (1 mg/ml) and left to stir for 24h at 4^{o}C. Insoluble material was removed by centrifugation and the supernatant was retained.

5. Type II collagen was precipitated by adding NaCl to give a 0.9M solution. Following centrifugation, the precipitate was re-dissolved in 0.05M Tris plus 0.5M NaCl (pH7.5) to inactivate residual pepsin.

6. The type II collagen was then dialysed exhaustively against acetic acid (0.5M) and freeze-dried. Collagen was stored in a desiccator at 4^{o}C.

2.2.2. Induction of arthritis

DBA/1 mice were immunized subcutaneously at the base of the tail with bovine type II collagen (200 μg) emulsified in complete Freund's adjuvant (CFA 3.3 mg Mycobacterium tuberculosis per ml of oil; Difco, West Molesley, UK). In contrast, *Ido1* KO mice and C57BL/6 mice (WT) were immunised with type II chicken collagen in emulsified in complete Freund's adjuvant.

2.2.3. Assessment of arthritis

The clinical progression of arthritis was monitored on daily basis for a period of 10 days after the onset of the disease and animals were concious during the measurements. In order to comapre the clinical severity of arthritis the following scorring system was used:

0 = no obious pathology

1 = slight swelling/or erythema

2 = pronounced swelling

3 = ankylosis

Results were presented as changes (Δ) in clinical scores. However, to make observation of the progression of the disease more quantitative measurements of paw swelling was done using calipers ("Pocotest" Kroeplin Langenmesstechnik). This device measures the size of the inflammed paws and results are presented in milimiters (mm). Such simple readout well reflects the degree of oedema and the increased cellularity in affected paws.

2.3. Tissue collection and processing

2.3.1. Serum

Blood was taken from experimental animals, which were unconscious, by cardiac puncture, transferred into 1.5 ml eppendorfs and left in room temperature to coagulate for 15 minutes. Samples were also protected from daylight. In the next step, eppendorfs filled with blood were centrifuged at 6000 g for 5 minutes. The straw-coloured supernatant (serum) was collected, placed in smaller eppendorfs and frozen on dry ice. Samples were stored for future analysis at -80^{o}C.

2.3.2. Tissues

Kidneys, livers, inguinal lymph nodes (iLN), spleens, and paws were taken from previously sacrificed animals and immediately frozen on dry ice. Samples were stored for future analysis at -80 ^{0}C.

2.3.3. Collection of hind paws for ex vivo imaging and histological assessment

The first affected hind paw of a given mouse with CIA was removed *post mortem* and fixed in buffered formalin (10%). Some paws were scanned using μCT, whereas others were decalcified in a solution of EDTA (10%w/v) in buffered formalin (5.5% w/v) for three weeks. Next, hind paws were embedded in paraffin. Next, sectioned (each slice of 10 μm thick) and stained either with haematoxylin and eosin (H&E) or Safranin O according to the protocols provided by the manufacturer of the dyes (Leica, London, UK).

2.4. Micro-computed tomography

Hind paws were scanned using HMX ST system (Nikon Metrology, Tring UK), (Figure 5), X-ray voltage 180 kV, current 170 μA. μCT scans were reconstructed with CT PRO 2.1 (Nikon Metrology, Tring UK). The resulting voxels were isotropic (10 mm^3), providing an effective spatial resolution of about 20 mm^3. Three-dimensional models were rendered as images and movies using VG Studio Max 2.1 (Volume Graphics, Heidelberg, Germany).

2.4.1. Recording of movies and preparation of figures

Movies showing rotating (360^o) reconstructed paws were stored as AVI and QuickTime Movie files. Figures were prepared with Adobe Photoshop, however no contrast or brightness enhancement has been applied.

2.4.2. BoneJ

Bone cortical parameters were measured with boneJ (slice geometry), a freely available plug-in to ImageJ (Doube, Klosowski et al. 2010; M 2010). The mean cortical thickness in the 3rd metatarsal bone from the hind paw was determined on the randomly selected, 10 out of 300 cross sectional slices of 2D μCT scans (Figure 5). Results were presented as a mean for each sample.

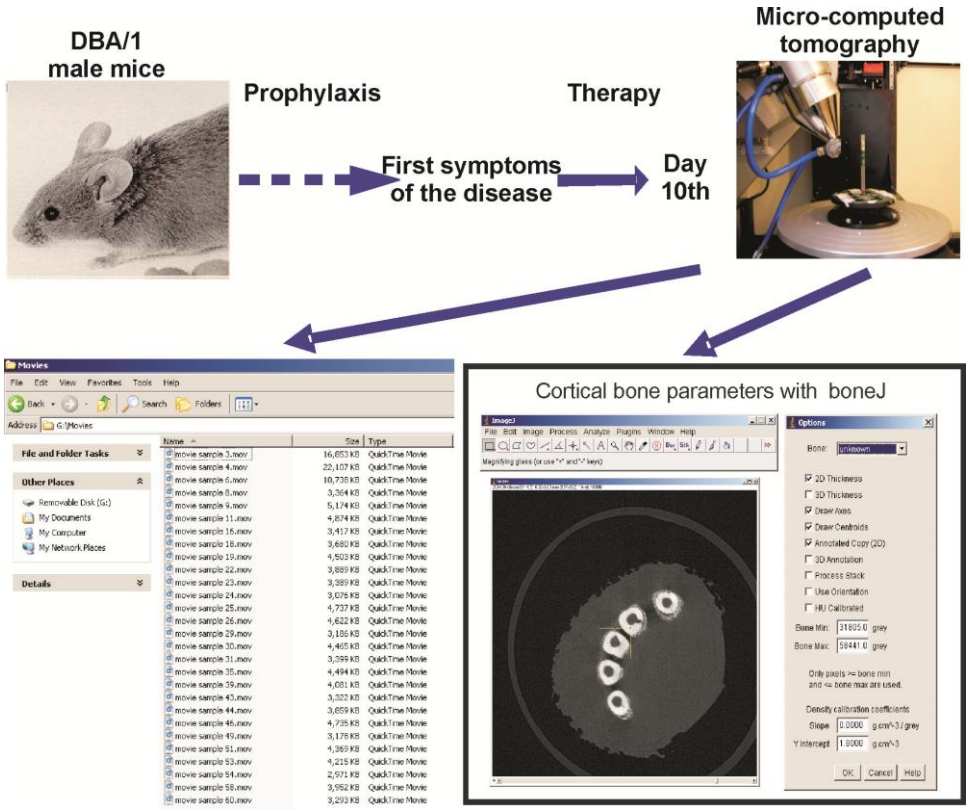


Figure 5 Application of μCT and boneJ in CIA

DBA/1 mice with CIA are routinely used for the study of prophylactic as well as anti-arthritic treatment with novel drug candidates for the therapy of RA. μCT can be used as a read-out for assessment of bone pathology in the experimental animals. Results can be stored and displayed as movies in 2D and 3D. In addition, using boneJ, it is possible to quantify changes in the parameters of cortical bone e.g. the mean cortical thickness.

2.5. Histological assessment of inflamed paws with CIA

Unlike μCT, histological sectioning of the inflamed paws reveals joint pathology in 2D. In addition, histological assessment requires sectioning of the diseased paws and is prone to potential artefacts from the cutting process as well as sampling errors. Nevertheless, application of histological methods can provide information about cell infiltration into the affected joints and destruction of the cartilage and the extent of bone erosions.

2.5.1.1. Assessment of joint damage using histological scores

In this method, the extent of joint damage in the various experimental groups was assessed using staining of the paraffin embedded sagittal cross section of the proximal interphalangeal (PIP) joint in the middle digit of the hind paw (Williams 1995). The assessment was carried out in this way to ensure that comparisons were made always between the same joints and that duration of arthritis was identical in each joint examined. The PIP joint was chosen because erosions were found in this joint in more than 85% of untreated arthritic mice 10 days after onset of clinical arthritis.

The sagittal cross section of PIP joint were stained with H&E. Haematoxylin binds to the nucleoproteins and therefore stains cell nucleus with a blue colour. In contrast, eosin Y dye stains cytoplasm and extracellular matrix with intense red and pink colour. Thus, using combination of haematoxylin and eosin days it is possible to visualise bone erosions and cellular infiltration into the joint cavity. Based on the numerous cross sections analysed in the past (Williams 1995) it was possible to design a semi quantitative histological scoring system, (Table 6 and Figure 6).

Table 6 Description of histological grades assigned to the arthritic PIP joints

Grade	Description
0	No obvious pathology
1	Slight synovitis, no erosive changes
2	Severe synovitis, bone erosions readily visible, however, joint architecture preserved
3	Severe synovitis, joint architecture difficult to recognise

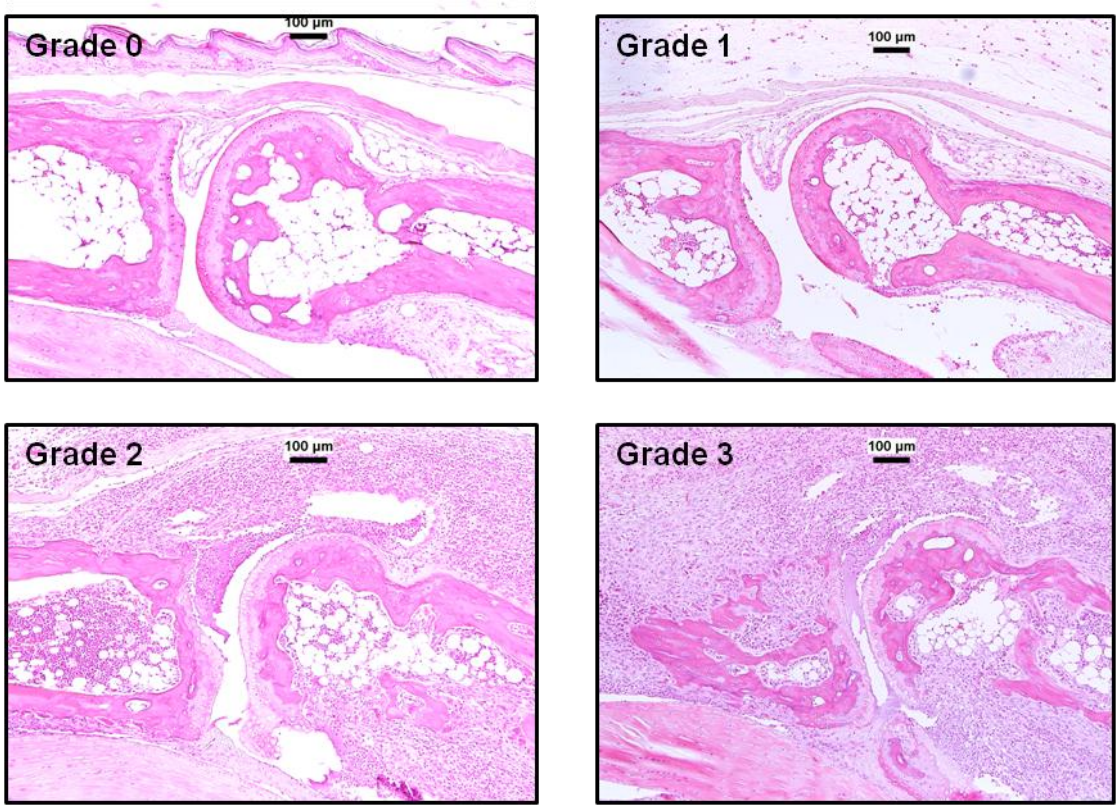


Figure 6 Sagittal cross sections of PIP joint stained with H&E

CIA was developed in DBA/1 mice. Hind paws were taken from mice of various stages of the disease, sectioned, and stained with H&E. Severity of joint damage was assessed using four grade system, ranging from 0 (no obvious pathology) to 3 (joint architecture lost).

2.5.1.2. Assessment of cartilage damage in CIA using Mankin scale

Although cartilage damage can be revealed by the H&E staining routinely cartilage involvement in arthritis is assessed using a Mankin's scale (Table7). In this method, saggital cross sections of PIP joints are stained with Safranin O (Figure 7). This dye specifically binds to proteoglycans from tissues in a linear manner. Thus, the intensity of the staining reflects proteoglycan content in the cartilage. Arthritic pathology is usually associated with the loss of proteoglycans in the cartilage which leads to the loss of its function. Therefore, the Mankin's scale is routinely applied for assessment of cartilage damage in joints with OA. However, in this project, the scale was applied for assessment of cartilage damage in PIP joints taken from mice with CIA, (Mankin et al. 1971; Pritzker et al. 2006).

Table 7 Semi-quantitative assessment of cartilage damage using Mankin's scale

Grade	Features of Cartilage Damage
0	No Damage
0.5	Mild Proteoglycan (Safranin O staining) loss
1	Roughened articular surface and small fibrillations
2	Fibrillation down to the layer immediately below the superficial layer and some loss ofsurface lamima
3	Mild loss of cartilage, with no loss of calcified cartilage i.e. Down to the tidemark.
4	Major fibrillations down to the calcified cartilage
5	Moderate loss of cartilage, involving loss of calcified cartilage
6	Severe loss (more than 80% thickness) of cartilage e.g. down to the subchondral bone

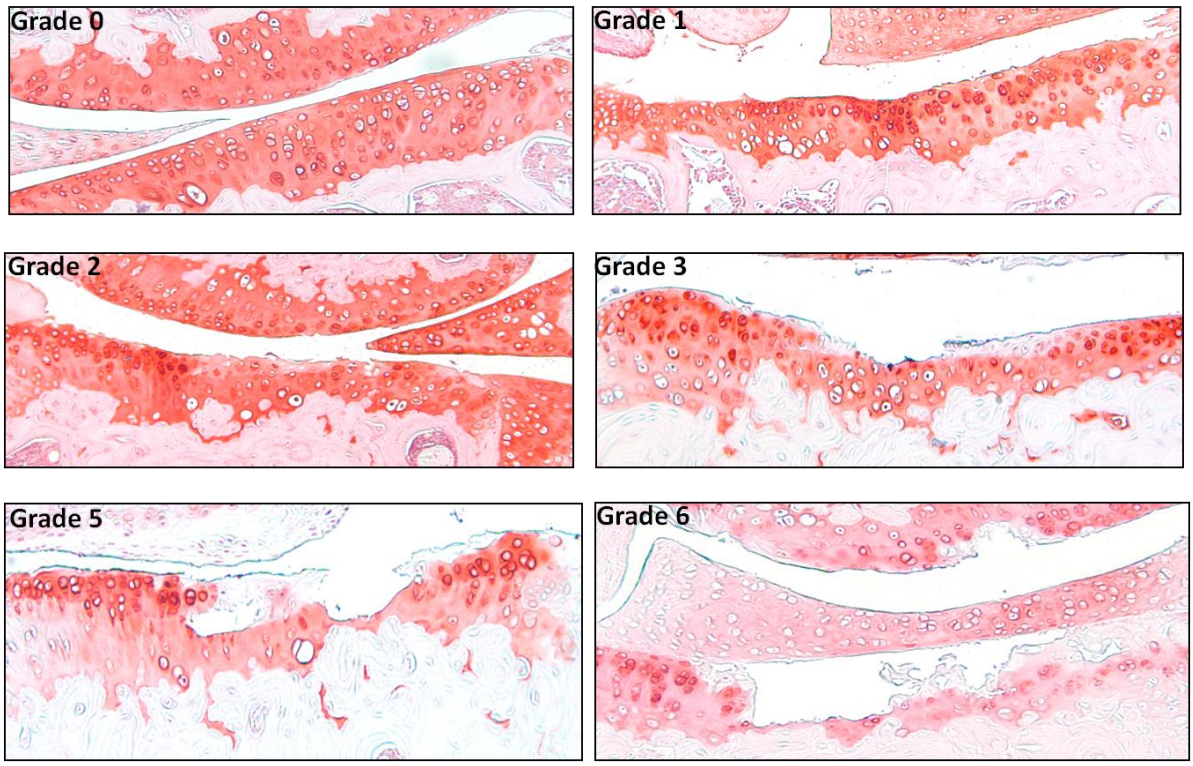


Figure 7 Representative pictures of cartilage assigned with Mankin's grades (based onMankin *et al.* 1971; Pritzker *et al.* 2006)

2.6. Therapy of mice with kynurenines and etanercept

When the first symptoms of CIA were observed in DBA/1 mice with CIA, animals were treated daily for subsequent 10 days with one of these substances: AA and 3-HAA (Sigma, UK) dissolved in 1% $NaHCO_3$ (Sigma, UK), 1% $NaHCO_3$ on its own (vehicle treated group), and etanercept (Wyeth Pharmaceutical, Taplow, UK). Drugs were administrated by intraperitoneal injections. The general health of the animals was assessed during the entire experiment.

2.7. Biochemical analysis of collected tissues

2.7.1. Isolation of mRNAand real-time PCR

Frozen tissues were homogenised using PRECELLYS^{R} 24 lyser/homogeniser machine (Bertin Technologies, France). Briefly, samples were placed into the grinding tubes containing porcelain beads. Tubes were moving up and down with speed reaching up to 6200 cycles per minute. Two cycles, each lasting for 45s and separated with 20s brake, were applied. Tissues were macerated by physical forces acting between shacking beads. RNA was extracted using RNA-Stat60 reagent (ams Biotechnology (Europe) Ltd) according to the manufacturer's instructions. cDNA was transcribed using the Applied Biosystems Reverse Transcription System. Briefly, the reaction mix was prepared according to the manual provided with the kit. Total volume of reaction was 50 µl (30 µl of reaction mix with 20 µl of RNA solution). DNA Engine DYAD^{TM} thermo cycler was used for reverse transcription reaction. Settings used for this purpose are presented in the (Table 8).

Table 8 Settings applied for RNA reverse transcription

No	Stage	Temperature	Time (min)
1	To equilibrate temperature of all samples	25 ^{o}C	10
2	Annealing and elongation	48 ^{o}C	30
3	Separation of RNA from cDNA	95 ^{o}C	5

Real time PCR reaction was done with the gene specific TaqMan probes (Applied Biosystems). Probes with references numbers are presented in Table 9.

Table 9 **TaqMan probes with their reference numbers bought from Applied Biosystems Company**

Gene	Symbol
Hprt1	Mm00446968_m1
Td2o	Mm00451266_m1
Ido1	Mm00492586_m1
Ido2	Mm00524206_m1
Kmo	Mm00505511_m1
Kynu	Mm00551012_m1
Haao	Mm00517945_m1

The total volume of qRT-PCR reaction was 10µl. (0.5µl primer probe, 5µl Applied Biosystems Mastermix, 2µl cDNA template, 2.5µl RNAse free water). PCR was performed in a Corbett Rotor-gene 6000 thermocycler (Corbett Lifesciences, Sydney) under the following conditions; 10 min hold at 95°C, then 95°C for 1 second and 60°C for 20 seconds for 45 cycles. Analysis of the reaction was conducted using the Rotor-gene 6000 series software 1.7 (Corbett Lifesciences, Sydney) for the ΔΔCt method. Gene expression in the naive animals deviated from 1 because Rotor-gene 6000 series software 1.7 enabled to randomly select a single animal as a reference (automatically assigned with 1 as a relative expression unit) to which gene expression in other naive animals was compared to. The gene expression in the remaining naïve animals was automatically compared to the referee animal (that one which was assigned with 1 as a relative expression unit). There were usually 3 to 5 naïve animals. Thus, mRNA expression in the naïve animals expressed as relative units can be close to 0.

Similarly, there is no limit on the maximal value. Therefore, theoretically, the maximal value for expression units can be close to the infinity. Nonetheless, it is possible to get the mean value of the relative units by adding up the individual values for all naïve animals divided by their total number. Let suppose: there were 4 naïve animals assigned with the following relative expression units: 1 + 1.5 + 0.5 + 1. 1. Thus, the relative gene expression for hypothetical naïve animals was of 1.025.

2.7.2. Tissue homogenisation and metabolite extraction

Isolated organs (kidneys, livers, iLN, spleens and paws) were kept at -80^{0}C. Paws were powdered using a mechanical pulveriser and the procedure was carried out on liquid nitrogen. The powdered paws were collected and stored in eppendorfs at -80^{0}C for further analyses. Kidneys, livers, LN, spleens, and powder from the paws were homogenised in buffer containing: 50 mM Tris-HCl pH=7.7, 150 mM NaCl (Sigma, Poole, UK), 5 mM $CaCl_2$ (Sigma) using the PRECELLYS^R 24 lyser/homogeniser (Bertin Technologies, Paris, France) with two cycles of shaking separated by 20 seconds apart, each lasting for 45 seconds in the room temperature. After homogenisation, samples were centrifuged at 14,000 g and the supernatant was collected and mixed with 150 μl of a solution containing: 2 mM ascorbic acid (Sigma), 240 μM 3-nitrotyrosine (3-NT); (Sigma), 4 M perchloric acid (PA); (AnalaR) (Forrest, Mackay et al. 2010). All procedures related to the isolation of tryptophan and its catabolites were carried out in the room temperature. However, samples were protected from light. The samples were then vigorously vortexed for 30 seconds and centrifuged at 5000 g for 15 min. The supernatant was collected and the pellets were resuspended in 150 μl of 4M PA, vortexed for 30 seconds and centrifuged at 5000 g. This procedure was repeated three times in order to ensure efficient recovery of metabolites. Finally, pooled supernatants were transferred into the filtration tubes (0.22 mm cellulose acetate, Spin-X^R Costar^R) and centrifuged at 3000 g.

2.7.3. Development of the quantitative HPLC

Before I started this project there was no method established for a quantification of tryptophan, AA, and 3-HAA in the Kennedy Institute. Therefore, using available literature about chromatographic techniques suitable for the quantification of tryptophan, AA, and 3-HAA I have developed and validated experimental protocols required to accomplish this project.

HPLC with the reverse-phase has been chosen for the analysis of tryptophan, AA, and 3-HAA. In this technique, the stationary phase is non-polar whereas the mobile phase is made of polar compounds. Hence, based on the partition coefficients between a polar mobile phase and a hydrophobic stationary phase molecules of interest could be seperated. In this type of HPLC the more polar molecules are eluted more readily than less polar chemical entities. Therefore, various molecules can be identified and separated from each other by the different retention time (t_R) on the column packed with the hydrophobic stationary phase. In fact, t_R parameter is defined as the time between injection of the sample and the maximum of the peak. In particular, t_R depends on the strength of the mobile phase, the nature of stationary phase, and the temperature. In this project I have used a C18 column (Acclaim 120, Dionex) 3 mm, 120Å; 4.6x150 mm and an injection volume of 10 μL. An HPLC machine was bought from (UltiMate 3000, Dionex, Camberely, UK) which allowed me to conduct all chromatographic procedures at 37^0C. I have also used a C18 column (Acclaim 120, Dionex) 3 mm, 120Å; 4.6x150 mm and an injection volume of 10 μL.

The most common type of mobile phase applied for analysis of tryptophan by HPLC has been reported to be made of 50 mM acetic acid, 100 mM zinc acetate, and 3% acetonitrile. In contrast, mobile phase applied for analysis of AA and 3-HAA by HPLC has been reported to be composed of 25 mM sodium acetate and 1 mM acetic acid. The pH of

this mobile phase was adjusted to 5.5. The rate of flow of these mobile phases has been reported to be 1 ml/min. Thus, taken together, it was reasonable to apply similar conditions in my HPLC protocols. Representative chromatograms are shown on figure 8.

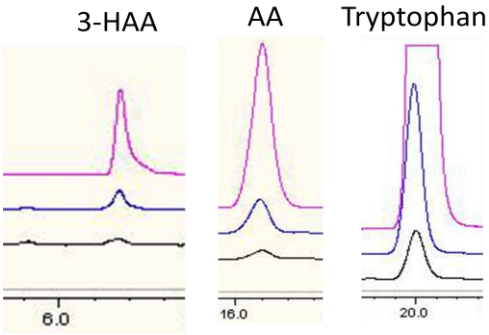


Figure 8 Representative pictures of chromatograms with 3-HAA, AA, and tryptophan

Tryptophan, AA, and 3-HAA were isolated from the kidneys and analysed with an HPLC technique. Subsequent numbers (6.0, 16.0, and 20.0) indicate on the time (min) after the sample was injected and the peak appeared, which stands for a Rt factor. A black colour indicates on the original sample. In blue samples spiked with the pure chemicalas are shown. In pink pure chemicals (3-HAA, AA, and tryptophan) are shown.

All chromatographic procedures were performed at 37^{o}C. Tryptophan concentration was determined by HPLC with fluorescence detection (excitation λ=284 nm; emission λ=365 nm). The mobile phase (1 ml/min flow rate) consisted of 50 mM acetic acid, 100 mM zinc acetate, and 3% acetonitrile). The limit of detection (LoD) was 1.5 nM and the limit of quantification (LoQ) was 3 nM. These parameters were derived from chromatographic analyses of solutions containing known concentrations of tryptophan. The concentration of AA and 3-HAA was determined by HPLC with fluorescence detection (excitation λ=320 nm; emission λ= 420 nm). The concentration of tryptophan, AA, and 3-HAA in tissues were calculated based on the standard curves derived from analysis of pure substances provided by

Sigma and adjusted according to the tissue mass. In order to increase precision and reduce errors due to the differences in small molecule recovery 3-NT (present in the homogenisation solution) was used as an internal/external standard.

2.7.4. Determination of kynurenine concentration

Concentration of kynurenine could be determined either by using an HPLC method or by a colorimetric assay (Hara, Yamakura et al. 2008). However, it has been previously shown that in acid conditions (pH <4) kynurenine can react with nitric oxide (NO). As a result, kynurenine is converted into the diazotized derivative which cannot be detected using fluorometric detection at 360 nm (Hara et al. 2008). NO is a commonly produced by various types of cells, whereas pro-inflammatory stimuli can trigger increased production of NO (Hara et al. 2008). Hence, in this study, it was likely that the production of NO could be increased, therefore a colorimetric assay was applied. An equal volume (100 μl) of Ehrlich reagent (0.4% *p*-dimethylaminobenzaldehyde in acetic acid) was mixed with the tissue homogenate (100 μl). Absorbance was determined at 490 nm. Kynurenine concentration in the biological samples was calculated from the standard curve prepared from pure kynurenine (Sigma) and adjusted according to the tissue mass.

2.7.5. Immunohistochemistry

Protein expression for enzymes on the kynurenine pathway could be investigated either by application of western blotting method or immunohistochemistry. However, using western blotting, I could not detect proteins for the kynurenine pathway enzymes in the iLN, whereas in the homogenates from the livers this method worked perfectly (data not shown). Thus, it was of interest to test if the kynurenine pathway enzymes could be detected in iLN using immunohistochemistry. In addition, this approach could reveal localisation of the kynurenine pathway enzymes in tissues and, at least, indirectly indicate on changes in protein

expression between experimental conditions. Therefore, I tried to establish experimental protocols for detection of 4 enzymes on the kynurenine pathway, IDO1, IDO2, KYNU, and HAAO in iLN and inflamed paws. As a positive control small intestine was chosen. The source of antibodies and their characteristic is presented in Table 10.

Table 10 Primary antibodies used for detection of the kynurenine pathway enzymes in iLN, inflamed paws, and small intestine

Enzyme	Antibody	Type of antibody	Supplier	Catalogue number
IDO	Anti human-IDO	Sheep polyclonal	Hycult Biotechnology	HP5004
KYNU	Anti-human KYNU	Goat polyclonal	R&D Systems	AF4887
HAAO	Anti human-HAAO	Rabbit (polyclonal)	ProteinTech Group	12791-1-AP

For detection of protein expression using immunohostochemistry the following protocol was established:

2.7.5.1. Tissue collection and processing

iLN, small intestine, and paws were taken either from naive mice or animals with established CIA and placed in the pots containing buffered formalin (10%). Tissues were embedded in paraffin and sliced into 10 μm cross sections.

2.7.5.2. De-paraffinizing and hydrating of tissue sections

Slides were placed in the incubator (+60 ^{0}C) for 20 minutes, after which slides were soaked

in xylene for a few minutes. To hydrate tissue slides, samples were placed in pots containing decreasing concentration of ethanol (staring from 95% to 60%). In each concentration, slides were incubated for at least 5 minutes. In a next step, slides were rinsed in distilled water for 5 minutes.

2.7.5.3. Retrieving antigen epitopes

Tissue slides were placed in a container filled with 1x citrate buffer (pH 6.0) and microwaved for 30 minutes at maximal settings. Next, tissue slides were allowed to cool to room temperature.

2.7.5.4. Staining

At this step, slides were rinsed in TBS buffer 4 to 5 times and incubated with 3% H_2O_2 in methanol for 30 minutes. This step was necessary to block an endogenous activity of peroxidase. Next, slides were rinsed with 1x TBS buffer 4 to 5 times and incubated with 5% serum taken from animals in which secondary antibody was raised (Table 11) for 40 minutes. Then, tissues were incubated with diluted primary antibodies against selected enzymes on the kynurenine pathway (Table 11) over night at +4 ^{0}C. As a negative control isotype matched antibodies were applied e.g. in slides incubated with anti-human IDO antibodies sheep polyclonal IgG were applied diluted to the same concentration as primary anti IDO antibodies. On the next day, slides were rinsed with TBS buffer 4 to 5 times and incubated with diluted secondary antibody for 40 minutes a room temperature. Secondary antibodies (Table 11) were conjugated with avidine.

Table 11 Primary antibodies used for detection of the kynurenine pathway enzymes in iLN, inflamed paws, and small intestine

Primary antibody	Concentration of primary antibody	Supplier and catalogue number	Secondary antibody (1: 2000)	Supplier and catalogue number
Anti human IDO	1: 100	Hycult®Biotech (HP5004)	Anti Sheep	Vector laboratories BA-6000
Anti human KYNU	1:50	R&D systems (AF4887)	Anti Goat	Vector laboratories BA-9500
Anti human HAAO	1:20	Abcam	Anti Rabbit	Vector laboratories BA-1100

In a next step, tissue sections were subjected to the ABC method using Universal Elite ABC Kit (Vector laboratories, catalogue number: PK – 6200) and rinsed in 1x TBS solution 4 -5 times and remaining water was removed. Reaction was developed using colorimetric method using (DAB) staining solution purchased from Vector laboratories (catalogue number: SK – 4100) according to the manual provided by the manufacturer. The excess of the solution was removed by washing tissues in distilled water and stained with H&E stains according to the well established protocol in the Department of Histopathology in the Charing Cross Hospital.

2.7.5.5. Dehydration and mounting of tissue sections

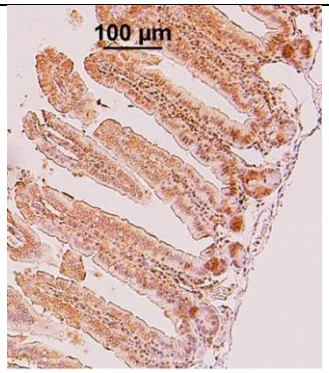
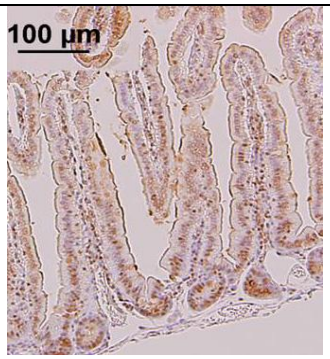
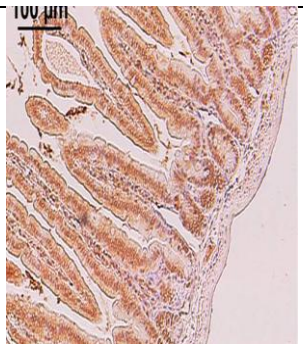
Tissues slides were dehydrated, mounted, and cover slipped using Integrated Workstation Leica ST5010 – CV5030 machine placed in the Department of Histopathology in the Charing Cross Hospital.

2.7.5.6. Limitation of the immunohistochemistry

Unfortunately, for IDO enzymes and HAAO control reaction with isotype matched antibodies provided almost identical results on the cross sections of the small intestine (Table 12) and lymph nodes (data not shown). The small intestine was chosen because IDO, kynureninease and HAAO were shown to be expressed in this tissue. However, when cross sections of the joints were subjected to the immunohistochemical reactions with isotype controls t some unspecific binding was observed. This might be due to the differences in the type of tissue and tissue processing for histological analyses (e.g. decalcification of paws). Therefore, I studied protein expression for the kynurenine pathway enzymes in paws during CIA (see chapter 5, section 4.2.3)

Table 12 Establishment of immunocytochemical reactions using antibodies against selected enzymes on the kynurenine pathway

The kynurenine pathway enzymes have been shown to be expressed in the small intestine. Therefore, immunohistochemical reactions were developed on this type of tissue.

Enzyme	Primary antibody	Isotype control	Result
IDO1 and IDO2			No obvious difference between isotype control and slides treated with primary antibody
KYNU			difference between isotype control and slides treated with primary antibody
HAAO			No obvious difference between isotype control and slides treated with primary antibody

2.8. Statistical analysis and data presentation

Exploratory data analysis (box and whisker plot) was initially carried out to determine which data sets approximated to a normal distribution. The two-sample *t* test was used to compare differences in paw thickness, which conformed to a normal distribution. The two-sample *t* test was applied without pooling of standard deviations, as the standard deviations of the different treatment groups were not assumed to be equal or similar. This gives a more conservative estimate of the *P* value.Comparisons of medians of non-parametric data (e.g. clinical scores and numbers of arthritic limbs) were made using the Mann-Whitney *U* test. When there were more than two groups, one way ANOVA was carried out followed by the Dunnetts multiple comparison test, where appropriate. Figures were prepared using Adobe Photoshop and Correl Draw. However, no image enhancemnet was used in figures showing bone pathology obtained from μCT.

Chapter 3

Systemic changes in levels of tryptophan and its metabolites during arthritis

3.1 INTRODUCTION

The kynurenine to tryptophan ratio is a commonly accepted indicator of the activity of IDO1 dependent tryptophan catabolism (Widner et al. 2002; Schrocksnadel et al. 2006; Gupta et al. 2011). The application of this readout is based on the observation that upon immune challenge (e.g. intraperitoneal injection of LPS) the serum concentration of kynurenine increased, whereas the concentration of tryptophan decreased (Takikawa et al. 1986; Saito et al. 1993). An increased kynurenine to tryptophan ratio has been also found in sera taken from patients suffering from various diseases, including RA (Kurz et al. 2011), major depression (Myint et al. 2007), and several types of cancers (de Jong et al. 2011). Thus, measurements of the concentration of tryptophan and its catabolites via the kynurenine pathway in serum might be of clinical importance. Previously, it has been shown that upon inflammation, increased concentration of kynurenine positively correlated with increased production of neopterin (Fuchs et al. 1991). Neopterin is a catabolite of guanosine triphosphate (GTP) and is produced in excess by activated macrophages. Therefore, increased concentration of kynurenine can be an indirect indicator of systemic inflammation.

Interestingly in the context of RA, it is known that *in vitro* and *in vivo* the balance between pro-arthritogenic Th17 cells and anti-arthritic Treg cells can be modulated by the ratio of kynurenines to tryptophan. It has been also shown that tryptophan starvation can reduce the efficiency of Th17 cell differentiation whereas kynurenine can hamper differentiation of Th17 cells in a dose dependent manner. In line with these observations, in previous work from our laboratory, decreased kynurenine concentration has been reported in sera from DBA/1 mice with CIA (Criado et al. 2009). However, this observation remains controversial, because it is against the currently held view that upon immune stimulation, the concentration of tryptophan in serum should have been reduced. Similarly, the concentration

of kynurenine should have been increased. Nevertheless, very early studies of kynurenine metabolism in patients with RA demonstrated accumulation of 3-HAA in urine(Spiera 1963; Labadarios, 1978) . Thus, it might be speculated that kynurenine, like 3-HAA, could be also accumulated in urine but not in sera. In addition, (Kanai et al. 2009) have shown that in mice, deletion of the *Tdo2* gene but not *Ido1* resulted in the increased concentration of tryptophan in the sera. As has been mentioned in the first chapter, expression of TDO is almost exclusively restricted to the liver, an organ primarily responsible for regulation of tryptophan concentration in the serum. In line with this observation, it has been shown that in TDO deficient mice and in animals expressing a non-inducible from of TDO the excessive tryptophan concentration is toxic. Hence, it is more likely that the tryptophan concentration in serum is regulated in a TDO, rather than an IDO1 dependent manner.

To study changes in the concentration of tryptophan and its catabolites via the kynurenine pathway in serum during inflammatory arthritis I have applied a CIA model in DBA/1 mice. Therefore, the concentrations of tryptophan, kynurenine and its catabolites, AA and 3-HAA, were measured in sera taken from naive mice, pre-arthritic mice, and animals with established CIA. I have also investigated whether CIA could influence on tryptophan catabolism via the kynurenine pathway in the liver and kidneys. Hence, the concentrations of tryptophan and kynurenines were determined in the liver and kidneys taken from mice with CIA. Finally, changes in mRNA expression for the kynurenine pathway enzymes were assessed in these organs during CIA.

3.2. RESULTS

3.2.1. Changes in the concentration of tryptophan and kynurenines in sera from mice with CIA

In the sera taken neither from pre-arthritic mice nor those with established CIA, the concentration of tryptophan was significantly changed, when compared to naive animals, (Table 13). In contrast, the mean concentration of kynurenine was significantly decreased ($p<0.05$) in sera either taken from pre-arthritic mice or those with established CIA in comparison with healthy mice, (Table 13). A similar decreasing trend was observed for AA and 3-HAA isolated from sera of mice with CIA. However, unlike with kynurenine, the concentration of AA was only significantly reduced ($p<0.05$) in sera from mice with established CIA, (Table 13). Interestingly, the concentration of 3-HAA, unlike AA, but similar to kynurenine, was significantly decreased in pre-arthritic and arthritic mice, (Table 13).

Table 13 The concentration of tryptophan was not changed, whereas the concentration of kynurenines was decreased in sera from mice with CIA

CIA was induced in DBA/1 mice and sera was taken either from pre-arthritic mice (n=5) or animals with established CIA (n=5). Results were compared with sera taken from naive mice (n=3). Tryptophan, AA, and 3-HAA were isolated from sera and their concentration were measured by HPLC. The concentration of kynurenine was measured in sera by a colorimetric method. Results were statistically assessed using one way ANOVA with Dunnetts multiple comparison test. * $p<0.05$, ** $p<0.01$

Compound	Naive	Pre-arthritic	Established CIA
Tryptophan μM	53.25 ± 3.44	46.24 ± 14.72	50.56 ±5.17
Kynurenine μM	2.17 ± 1.16	0.75 ± 0.29 *	0.74 ± 0.28 *
AA nM	420.37 ± 68.34	316.11 ± 123.01	230.02 ±53.9 *
3-HAA nM	38.27 ± 5.59	20.8 ± 6.42 **	23.69 4.9 *

In a next step, it was of interest to test if deletion of *Ido1* could have an impact on the concentration of tryptophan and kynurenines in sera from mice with established CIA. The disease was induced in *Ido1* KO mice and WT animals. Results are presented in Table 14.

Table 14 The concentration of kynurenine was decreased in sera from arthritic *Ido1*-/- mice but not from the WT mice

CIA was induced in *Ido1* KO mice and WT animals. 10 days after first symptoms of the disease became apparent mice were sacrificed and sera taken. Tryptophan, AA, and 3-HAA were extracted from sera and measured with HPLC. In contrast, kynurenine concentration was measured in sera with a colorimetric method. Results were statistically assessed using t-test. *** $p<0.001$

Compound	WT mice with established CIA (n=4)	*Ido1* KO mice with established CIA (n=3)
Tryptophan (μM)	59.73 ± 9.84	59.4 ± 20.95
Kynurenine (μM)	1.85 ± 0.27	0.64 ± 0.14 ***
AA (nM)	474 ± 72.25	371 ± 157.71
3-HAA (nM)	71.71 ± 7.27	56.67 ± 15.84

As could be predicted from previous results (Baban et al. 2004), the mean concentration of tryptophan in the serum from diseased WT mice was not significantly changed in comparison with sera taken from *Ido1* KO mice with established CIA. However, in contrast to tryptophan, the mean concentration of kynurenine was significantly decreased ($p<0.001$) in sera taken from *Ido1* KO mice with established disease but not WT animals. In addition, the concentration of AA and 3-HAA in sera from *Ido1* KO mice with established CIA followed a similar, decreasing, trend as observed for kynurenine. However, the results were not significant.

3.2.3. The involvement of the liver in tryptophan metabolism via the kynurenine pathway during CIA

The liver is a primary organ involved in the regulation of tryptophan concentration in serum. Therefore, it was of interest to test if catabolism of tryptophan via the kynurenine

pathway could be affected in the liver during CIA. Hence, livers were taken from the same mice from which sera were taken for analysis. Interestingly, unlike in sera from the diseased mice, in the liver from mice with CIA, the mean concentration of tryptophan exhibited a decreasing trend in both experimental groups: pre-arthritic mice and animals with established CIA. However, the decrease in tryptophan concentration was only statistically significant ($p<0.05$) in the mice with established CIA in comparison with naive animals. In the livers of healthy mice the mean tryptophan concentration was 9.76 ± 5.11 nmol/g of wet tissue, whereas in the livers of mice with established CIA the mean tryptophan concentration dropped to 4.31 ± 1.94 nmol/g of wet tissue. In the livers from pre-arthritic mice the mean concentration of tryptophan was 5.22 ± 1.72 nmol/g of wet tissue (Figure 9A).

The concentration of kynurenine followed a similar pattern to that one described for tryptophan. In both experimental groups (pre-arthritic and mice with established CIA) the concentration of kynurenine was significantly ($p<0.01$) decreased in comparison with naive mice. In the livers from healthy animals, the mean concentration of kynurenine was 13.92 ± 1.94 nmol/g of wet tissue, however, in livers taken from pre-arthritic mice, the mean kconcentration of kynurenine concentration was 8.44 ± 2.24 nmol/g of wet tissue. In the livers taken from mice with established CIA the mean kynurenine concentration was 8.3 ± 2.7 nmol/g of wet tissue (Figure 9B). Therefore, not surprisingly, when compared with naive mice, the kynurenine to tryptophan ratio was not significantly changed in the livers either taken from pre-arthritic or mice with established CIA (Figure 9C).

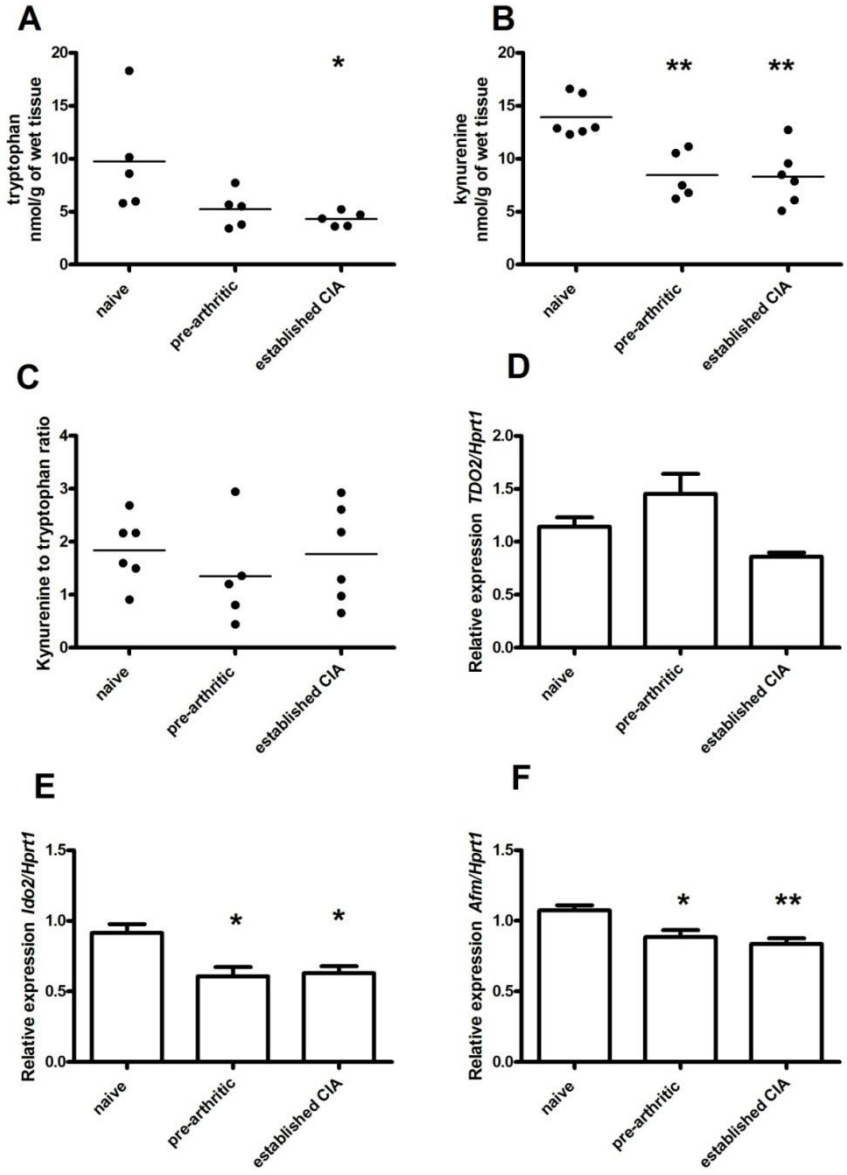


Figure 9 Unchanged kynurenine to tryptophan ratio in the livers of mice with CIA

CIA was induced in DBA/1 mice and livers were taken from mice (n=4) 14 days after immunisation (a pre-arthritic stage of CIA) and animals (n=5) with established CIA (10 days after first onset of disease become apparent). Results were compared with livers from naive mice (n=5) and statistically assessed as previously described, Table 13. **A)** tryptophan was extracted from livers and its concentration was determined with an HPLC method. **B)** kynurenine was extracted from livers and its concentration was determined with colorimetric assay. **C)** kynurenine to tryptophan ratio. mRNA expression for **D)** *Tdo2,* and **E)** *Ido2* **F)** *Afm* was measured with qRT-PCR technique on cDNA prepared with total RNA isolated from livers. Expression of these genes was normalised to *Hprt1* transcripts. Values represent arbitrary units with SEM provided as results of mRNA expression analysis with ΔΔCt method. * $p<0.05$, ** $p<0.01$

Decreased tryptophan concentration in the livers from mice with CIA could indicate an increased metabolic flux through the kynurenine pathway during the disease. Thus, it was of interest to assess changes in mRNA expression for enzymes involved in the initiation of tryptophan catabolism. However, mRNA expression for *Tdo2* did not reach significance in neither of experimental groups (pre-arthritic and mice with established CIA) in comparison with naive mice (Figure 8D). However, mRNA expression for two other enzymes *Ido2* and *Afm* was significantly decreased ($p<0.05$) in pre-arthritic and mice with established CIA in comparison with naive samples (Figure 9E and 9F, respectively).

Decreased mRNA expression for the initial enzymes on the kynurenine pathway in the liver of CIA could explain decreased kynurenine concentration in this organ during the disease. Alternatively, in the livers taken from mice with CIA, kynurenine could be catabolised into AA and 3-HAA much faster than in naive mice. Therefore, it was of interest to measure the concentration of these molecules in the livers with CIA. In the livers of naive mice the mean concentration of AA was of 3.66 ±0.54 nmol/g of wet tissue, whereas in pre-arthritic animals the mean concentration of AA was 3.2 ± 0.5 nmol/g of wet tissue. In contrast, in the livers taken from mice with established CIA the mean concentration of AA was decreased to 0.38 ±0.15 nmol/g of wet tissue (Figure 10A). This change was significant ($p<0.001$).

In contrast to AA, the mean concentration of 3-HAA was not significantly changed in tissues from either arthritic or pre-arthritic mice compared with tissues from naive mice (Figure 10B). In the livers taken from healthy animals the mean concentration of 3-HAA was 735.41 ±183.68 pmol/g of wet tissue, whereas in the organs taken from pre-arthritic mice the mean concentration of 3-HAA was 504.78 ±122.9 pmol/g of wet tissue. In mice with established CIA, the mean concentration of 3-HAA was 565.2 ±182.72 pmol/g of wet tissue.

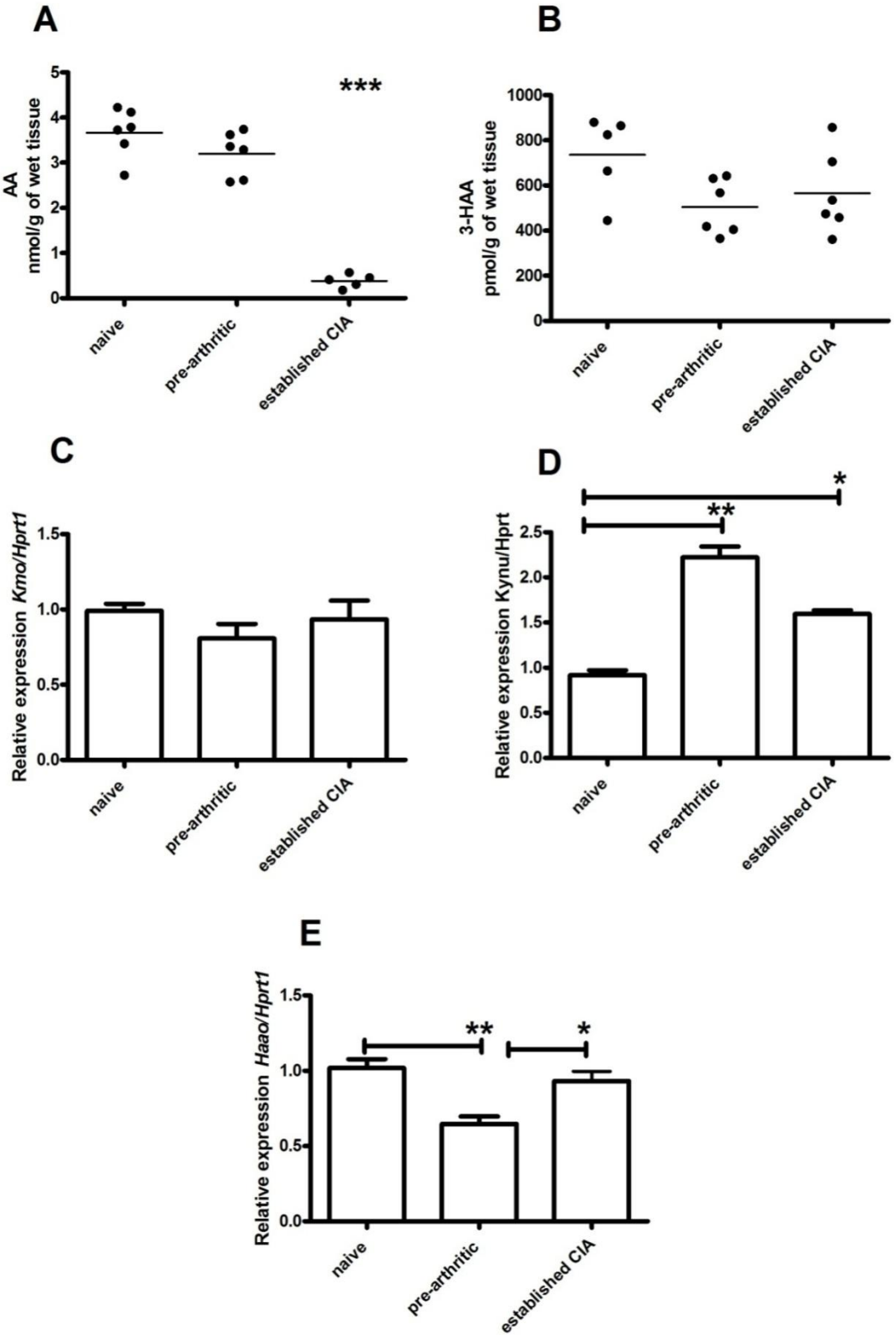


Figure 10 Catabolism of kynurenine in the livers taken from mice with CIA

CIA was induced in DBA/1 mice and livers were taken (n=4) 14 days after immunisation (pre-arthritic stage of CIA) and animals (n=5) with established CIA (10 days after onset of disease). The results were compared with naive livers (n=5) and statistically assessed using one way ANOVA with Dunnetts multiple comparison test. In addition, some livers came from the same animals as used for measurements of tryptophan and kunurenines in sera, Table 13 **A)** AA and **B)** 3HAA were extracted from livers and their concentration were determined with HPLC. mRNA expression for **C)** *Kmo*, **D)** *Kynu*, and **E)** *Haao* was measured with qRT-PCR technique as previously describe.* $p<0.05$, ** $p<0.01$

To complete the study of kynurenine catabolism in the liver during CIA mRNA expression for *Kynu, Kmo,* and *Haao* was assessed in the livers from mice CIA. Interestingly, mRNA expression for *Kynu* was significantly increased in both pre-arthritic ($p<0.05$) and arthritic ($p<0.01$) mice (Figure 10C). In contrast, mRNA expression for *Kmo* was not significantly changed in pre-arthritic or arthritic mice compared to naive mice (Figure 10D). However, in contrast to *Kmo,* mRNA expression for *Haao* was significantly decreased in the livers of pre-arthritic mice. In the livers from mice with established CIA *Haao* mRNA expression became normalised to the control level (Figure 10E).

3.2.4. The involvement of the kidneys in tryptophan catabolism via the kynurenine pathway during CIA

The kidneys are organs in which toxic products of metabolism are disposed in urine whereas vital nutrients like e.g. amino acids are reabsorbed from the primary ultra filtrate. Thus, it was of interest to test if CIA could affect tryptophan catabolism via the kynurenine pathway in the kidneys. In fact, some kidneys used in this study came from the same study, in which I have measured concentration of tryptophan and kynurenine in sera, see Table 13.

The concentration of tryptophan was found to be significantly ($p<0.01$) increased in the kidneys taken from mice with established CIA in comparison with naive organs. In the kidneys of healthy mice, the mean tryptophan concentration was 39.39 ± 1.72 nmol/g of wet tissue, whereas in the organs taken from animals with established CIA the mean concentration of tryptophan was increased to 69.46 ± 17.97 nmol/g of wet tissue. In the kidneys taken from pre-arthritic mice the mean concentration of tryptophan was 48 ± 4.24 nmol/g of wet tissue (Figure 11A).

However, unlike tryptophan, the concentration of kynurenine was not significantly changed in pre-arthritic mice or arthritic mice. In the kidneys taken from naive mice the mean

concentration of tryptophan was 91.95 ± 15.97 nmol/g of wet tissue, whereas in the kidneys taken from animals with established CIA the mean concentration of kynurenine was 63.99 ± 25.2 nmol/g of wet tissue. In the kidneys taken from pre-arthritic mice the mean kynurenine concentration was 73.72 ± 23.76 nmol/g of wet tissue (Figure 11B).

The increased concentration of tryptophan in the kidneys from mice with established CIA but not changed concentration of kynurenine in these organs suggested that the concentration of tryptophan could not undergo metabolic regulation. To test this hypothesis, mRNA expression for the initial enzymes on the kynurenine pathway was assessed. Not surprisingly, mRNA expression neither for *Ido1* nor for *Afm* was changed in the kidneys taken from naive, pre-arthritic or mice with established CIA (Figure 11C and 11D, respectively). Nonetheless, mRNA expression for *Ido2* was found to be significantly ($p<0.05$) decreased in the kidneys taken from pre-arthritic mice (Figure 11E). In contrast, in mice with established CIA, mRNA expression for *Ido2* was not significantly changed in comparison with naive organs.

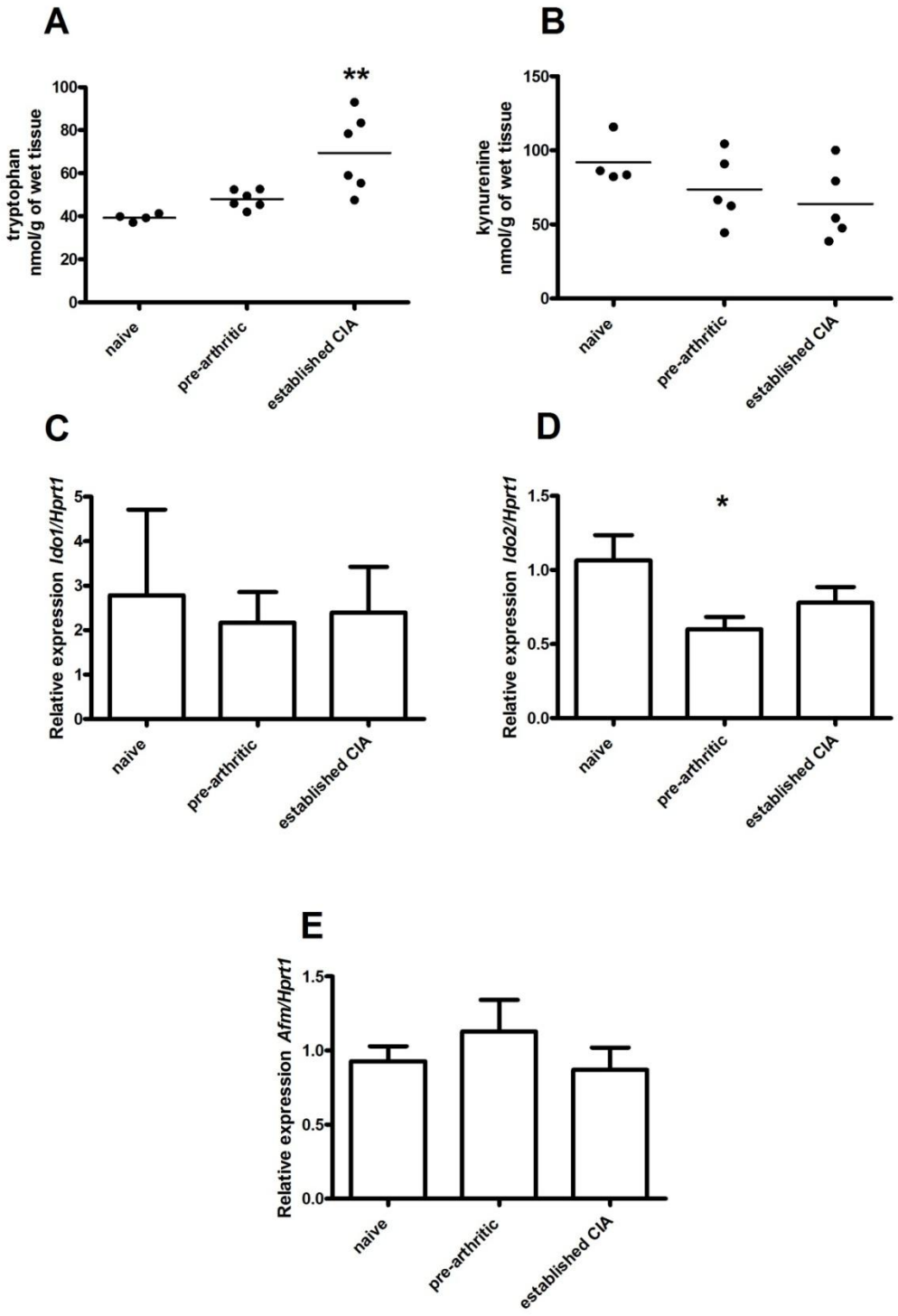


Figure 11 Increased levels of tryptophan in the kidneys from mice with established CIA

CIA was induced in DBA/1 mice and kidneys were taken from mice and subjected to the biochemical analyses describe on the Figure 8 and Table 13. **A)** concentration of tryptophan **B)** concentration of kynurenine. mRNA expression for **C)** *Ido1*, **D)** *Ido2*, and **E)** *Afm* Expression of these genes was

normalised to *Hprt1* transcripts. Values represent arbitrary units with SEM provided as results of mRNA expression analysis with ΔΔCt method. * $p<0.05$, ** $p<0.01$

Previous studies indicated on the increased extrection of kynurenine and its catabolites in the urine from patients with RA. Therefore, it was of interest to study catabolism of kynurenine in the kidneys taken from mice with CIA. The concentration of AA was not significantly changed between experimental groups in comparison with naive mice. In the kidneys from healthy animals, the mean concentration of AA was around 0.34 ± 0.23 nmol/g of wet tissue, whereas in the organs taken from pre-arthritic mice the concentration of AA was of 0.5 ± 0.17 nmol/g of wet tissue. In the kidneys taken from mice with established CIA the mean concentration of AA reached 1.13 ±1.14 nmol/g of wet tissue (Figure 12A). Moreover, changes in the concentration of 3-HAA in the kidneys of mice with CIA exhibited a very distinct pattern from that one observed for tryptophan and other kynurenines during CIA. In the kidneys taken from pre-arthritic mice the mean concentration of 3-HAA was increased to 59.57 ±10.64 pmol/g of wet tissue; whereas in the kidneys taken from animals with established CIA the mean concentration of 3-HAA was 53.68 ±31.13 pmol/g of wet tissue. In contrast, the mean concentration of 3-HAA in the kidneys of naive mice was 12.45 ±6.79 pmol/g of wet tissue. Thus, the concentration of 3-HAA was significantly increased in the kidneys taken from pre-arthritic mice ($p<0.01$) and animals of established CIA ($p<0.05$) in comparison with kidneys taken from healthy animals (Figure 12B).

To test if CIA could influence mRNA expression for genes encoding enzymes involved in the catabolism of kynurenine, changes in their mRNA expression were assessed. Interestingly, unlike in the liver, *Kmo* mRNA expression was slightly increased in the kidneys isolated from pre-arthritic mice. However, this change was not significant (Figure 12C). However, in the kidneys from mice with established CIA, *Kmo* mRNA expression was indistinguishable from that observed in the kidneys isolated from naive mice (Figure 12C). In contrast, mRNA expression for *Kynu* and *Haao* followed a similar pattern. In the kidneys from pre-arthritic animals, mRNA expression for *Kynu* and *Haao* was significantly reduced,

($p<0.01$) and ($p<0.05$), respectively. Nonetheless, like the mRNA expression for *Kmo*, mRNA expression of *Kynu* and *Haao* was normalised in the kidneys taken from mice with established CIA (Figure 12D and 12E, respectively).

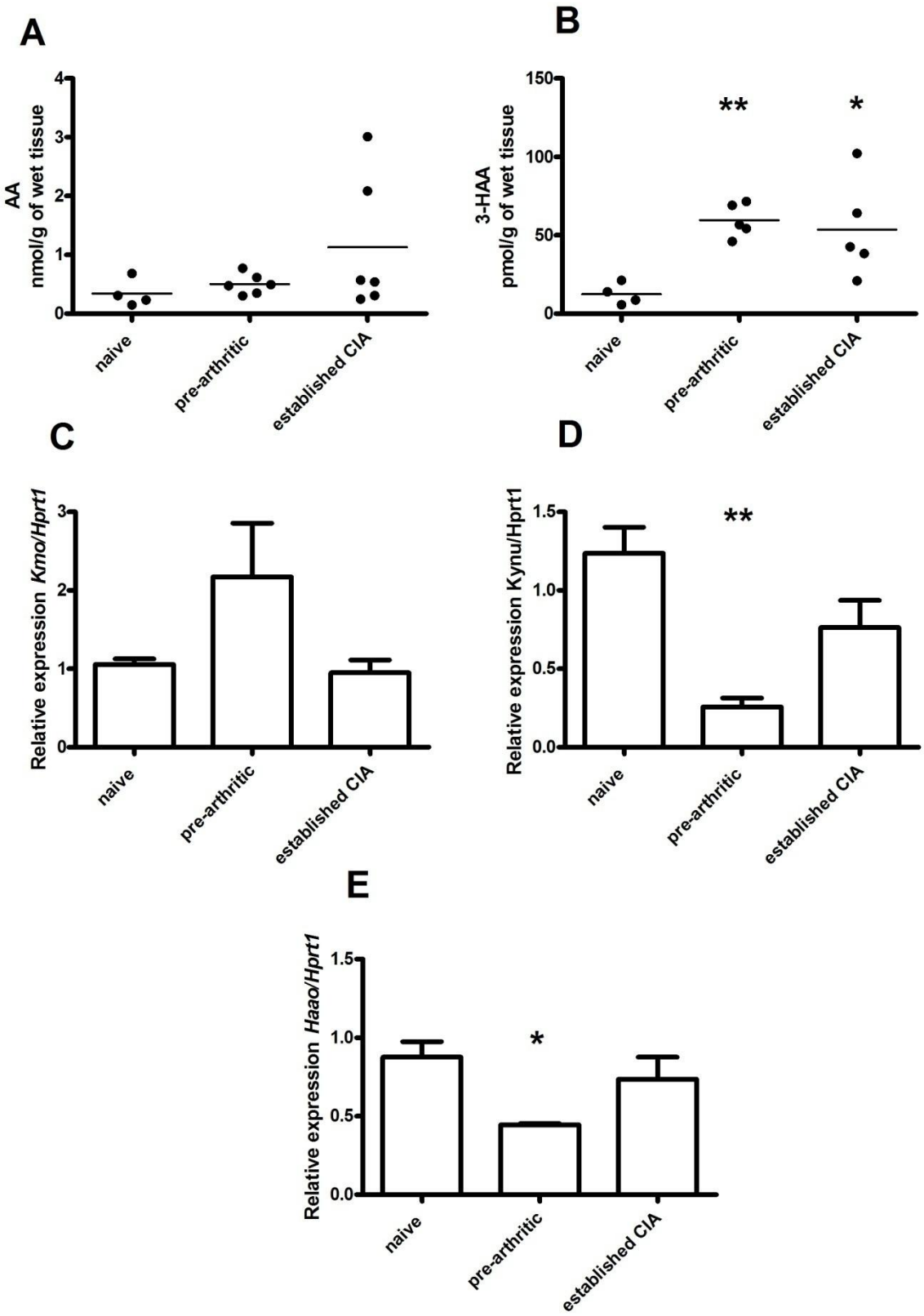


Figure 12 Increased levels of 3-HAA inthe kidneys of mice with CIA

CIA was induced in DBA/1 mice, kidneys were taken from mice (n=4) 14 days after immunisation (a pre-arthritic stage of CIA) and animals (n=5) with established CIA (10 days after first onset of disease become apparent). The same animals were used as in the first experiment described in this thesis. Results were compared with naive kidneys (n=5).Concentration of **A)** AA and **B)** 3-HAA. mRNA expression for **C)** *Kmo*, **D)** *Kynu*, and **E)** *Haao* was measured with qRT-PCR. * $p<0.05$, ** $p<0.01$

3.3. DISCUSSION

In this chapter I addressed the question of whether the inflammation observed in DBA/1 mice with CIA could influence systemic tryptophan metabolism via the kynurenine pathway. First, I measured the concentration of tryptophan and kynurenines in the sera from pre-arthritic and arthritic mice. The results were compared to levels found in the sera of naive mice. Stimulation of the immune system results in the activation of IDO1, leading to a reduction in tryptophan level and an increase in kynurenines. It is surprising therefore that the concentration of tryptophan was unchanged and the concentration of kynurenine was decreased in sera from arthritic animals. As the concentration of tryptophan and kynurenine may also be controlled by enzymatic activity in the liver and kidneys, I addressed the question of whether the rate of tryptophan catabolism changes in these organs in arthritis.

The concentration of tryptophan and kynurenine was decreased in the livers of pre-arthritic or arthritic mice in comparison to livers from naive mice. Thus, the kynurenine to tryptophan ratio was unchanged in arthritic mice compared to healthy mice. This shows that kynurenine to tryptophan ratio may be a parameter of limited sensitivity when it comes to assessment of tryptophan catabolism via the kynurenine pathway. Moreover, the decreased concentration of tryptophan and kynurenine detected in the livers of mice with CIA could indicate a reduced activity of the kynurenine pathway in the livers of arthritic mice. This is supported by assessment of mRNA expression for the initial enzymes on the kynurenine pathway (TDO, IDO2, and AFM). As expected, in the livers of mice with CIA, mRNA expression for *Tdo2* was not significantly changed in comparison with organs taken from naive animals. This result is in agreement with previous results which have shown that *Tdo2* mRNA expression is driven by hormonal stimulation (e.g. glucocorticoids) (Schutz et al. 1975), whereas immune challenge (e.g. intraperitoneal injection of LPS) could not drive

transcription of this gene (Berry and Smythe 1964). Nonetheless, results presented in this chapter have shown, for the first time, that mRNA expression for the *Ido2* and *Afm* were significantly reduced in the livers of mice with CIA but not in livers taken from naive animals. Therefore, it is possible that in the livers of mice with CIA at least two processes take place. First, tryptophan might be less efficiently absorbed from the hepatic portal vein and, secondly, catabolism of tryptophan via the kynurenine pathway could be reduced.

In contrast to the changes in mRNA expression for *Ido2* and *Afm*, mRNA expression for *Kynu* was found to be significantly increased in the livers from mice with CIA (pre-arthritic and those of established disease). This observation might be interpreted as an adaptive response to the decrease concentration of kynurenine observed in the livers from mice with CIA. However, the concentration of AA was found to be significantly decreased in the livers of mice with established CIA. AA is an immediate by-product of kynurenine catabolism by KYNU. Therefore, currently, it is difficult to explain and interpret this observation. Nevertheless, it was found that the decreased concentration of AA in the livers of mice with established CIA correlated with the decreased concentration of AA in sera of mice with established CIA.

The physiological consequences of decreased concentration of 3-HAA in sera are unknown. Equally puzzling is the observation of decreased mRNA expression for *Haao* in the livers from pre-arthritic mice but not in those taken from mice with established CIA when compared with naive tissues. Moreover, changes in *Haao* mRNA expression did not result in statistically significant changes in the concentration of 3-HAA in the livers of mice with CIA.

Measurements of the concentration of tryptophan and kynurenines in the kidneys of mice with CIA revealed that tryptophan accumulated in the kidneys of arthritic but not pre-arthritic mice. The lack of changes in mRNA expression for the initial genes on the

kynurenine pathway (*Ido1*, *Ido2*, and *Afm*) in the kidneys from mice established CIA could suggest that accumulation of tryptophan may result from non-metabolic mechanisms e.g. higher rate of tryptophan absorption from the primary ultra filtrate. However, this hypothesis has to be confirmed. Nevertheless, the finding showing significant accumulation of 3-HAA in the kidneys from mice with CIA (pre-arthritic and those of established CIA) is in agreement with previous observations showing increased accumulation of 3-HAA in urine from patients with RA (Spiera 1963; Labadarios, 1978). Thus, discoveries made in the 1960's have now been reproduced in CIA. Moreover, it is important to state that concentration of 3-HAA in the kidneys may not necessarily reflect concentration of 3-HAA in urine. Nevertheless, a statistically significant decrease in the concentration of 3-HAA in the sera of mice with CIA was associated with increased accumulation of 3-HAA in the kidneys taken from these mice. Hence, it is possible that the decreased concentration of 3-HAA in serum could be triggered by increased excretion of this molecule by the kidneys.

Chapter 4

Comparative study of tryptophan catabolism via the kynurenine pathway in the secondary lymphoid organs and inflamed paws during arthritis

4.1 INTRODUCTION

The results presented in the previous chapter indicate that systemic catabolism of tryptophan via the kynurenine pathway may play only a limited anti-inflammatory role during CIA. The concentration of kynurenines in sera was found to reach the nanomolar range (see table 13, page 91), whereas anti-inflammatory actions of kynurenines have been reported to be restricted to the milimolar range. However, as it has been mentioned before, *Ido1* KO mice have been found to be more susceptible to CIA and the disease is more severe than in WT mice (Criado et al. 2009). In line with these findings, it has been shown that administration of a pharmacological inhibitor of IDO1, 1MT tryptophan, to DBA/1 mice with CIA resulted in the increase in the severity of CIA, as observed in *Ido1* KO mice (Criado et al. 2009). Conversely, administration of IDO-containing exosomes reduced the severity of CIA (Bianco et al. 2009). Hence, IDO1 mediated tryptophan catabolism is likely to play at least some anti-arthritic role.

Kynurenine, 3-HAA, and AA have all been shown to have immunomodulatory properties. Interestingly, Belladonna *et al*. have demonstrated that dendritic cells express enzymes involved in the metabolism of kynurenine (Belladonna et al. 2006). These authors have also shown that IFN-γ is able to induce transcription of the initial genes on the kynurenine pathway (*Ido1*, *Ido2*, and *Afm*) as well as genes involved in the catabolism of kynurenine (*Kmo*, *Kynu*) and 3-HAA (*Haao*). This proves that catabolism of kynurenine, as in the case of tryptophan degradation, is inducible and therefore may influence T cells in the secondary lymphoid organs and inflamed paws with CIA.

Hence, to further explore the role of the kynurenine pathway in CIA I have aimed to:

1) Measure the concentration of tryptophan and kynurenine in the iLN, spleens, and inflamed paws

2) Assess mRNA expression for all three enzymes involved in the initiation of tryptophan catabolism via the kynurenine pathway (IDO1, IDO2, and AFM).
3) Test if kynurenine catabolism could undergo metabolic regulation in the secondary lymphoid organs and inflamed paws of CIA.

4.2. RESULTS

4.2.1. Tryptophan catabolism in the inguinal lymph nodes

The concentration of tryptophan in iLN during the pre-arthritic phase and in established arthritis was significantly lower than in iLN from naive mice. In iLN taken from naive mice, the mean concentration of tryptophan was 75.86 ±9.22 nmol/g of wet tissue, whereas in iLN isolated from mice during the pre-arthritic phase of arthritis, the mean concentration of tryptophan was significantly decreased ($p<0.05$) to 53.92 ±8.47 nmol/g of wet tissue, (Figure 13A). The same trend was observed in the established CIA. In iLN isolated from mice of established disease, the mean concentration of tryptophan was decreased to 40.74 ±8.47 nmol/g of wet tissue. When compared with iLN from naive mice this change was also significant ($p<0.01$) (Figure 13A).

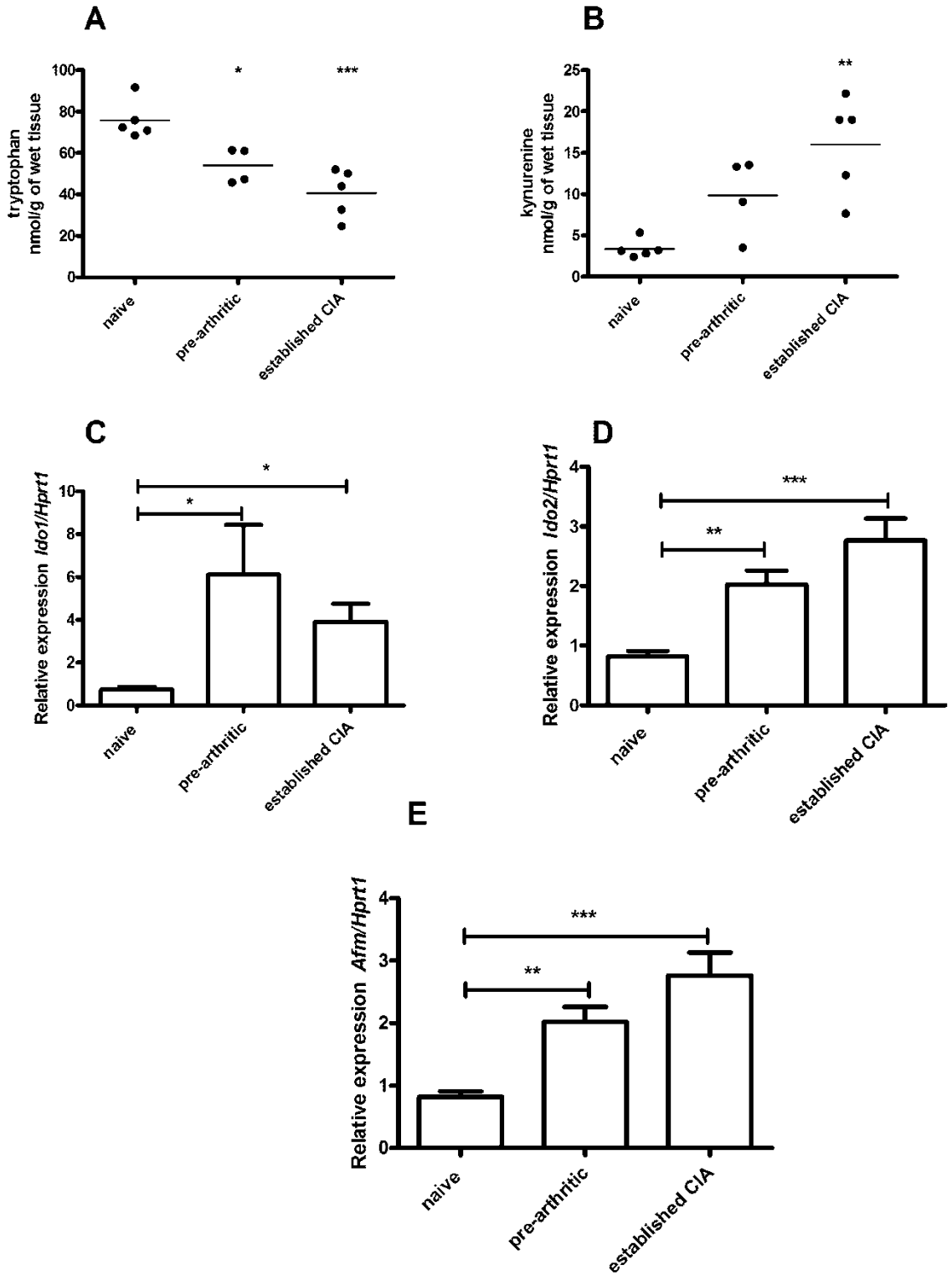


Figure 13 Increased initiation of tryptophan metabolism via the kynurenine pathway in lymph nodes of mice with CIA

CIA was induced in DBA/1 mice and inguinal lymph nodes (iLN) were taken from mice (n=4) 14 days after immunisation (pre-arthritic stage of CIA) or mice with established CIA (n=5) (10 days after

onset of arthritis). The results were compared with iLN from naive mice (n=5). **A)** Concentration of tryptophan. **B)** Concentration of kynurenine. mRNA of **C)** *Ido1*, **D)** *Ido2* **E)** *Afm*. Expression of these genes was normalised to the expression level of (*Hprt1*). Values represent levels of mRNA expression using the ΔΔCt method and are expressed as arbitrary units (mean ±SE). * $p<0.05$, ** $p<0.01$

Next, kynurenine was measured in the iLN isolated from naive mice, pre-arthritic mice, and animals with established CIA. There was a trend towards increased concentration of kynurenine during the pre-arthritic phase. However, a significant ($p<0.01$) increase in the concentration of kynurenine was observed only in iLN taken from mice with established phase of CIA (Figure 13B). In iLN from naive mice the mean concentration of kynurenine was 3.62 ±1.53 nmol/g of wet tissue, whereas in iLN taken from mice with pre-arthritic phase of CIA, the mean concentration of kynurenine was increased to 9.86 ±4.69 nmol/g of wet tissue. In contrast, in iLN taken from mice with established stage of CIA, the mean concentration of kynurenine was increased to 15.28 ±6.55 nmol/g of wet tissue. When compared with iLN taken from naïve mice this change turned out to be significant ($p<0.05$), (Figure 13B).

A decreased concentration of tryptophan and accumulation of kynurenine indicates on the increased rate of tryptophan catabolism. In order to confirm this hypothesis I compared mRNA expression for all three initial genes on the kynurenine pathway in iLN during CIA with iLN from naive mice. In comparison with naive iLN mRNA expression for *Ido1* was significantly ($p<0.05$) increased in the iLN isolated from pre-arthritic mice and in the iLN from mice with established CIA (Figure 13C). IDO2, a recently described homologue of IDO1, may be also involved in the initiation of tryptophan catabolism via the kynurenine pathway. Thus, I measured *Ido2* mRNA expression in iLN during CIA. mRNA expression for *Ido2* was significantly increased in iLN from pre-arthritic mice ($p<0.01$) and animals with established CIA ($p<0.001$) (Figure 13D).

N-formylkynurenine is produced as a result of IDO1 and IDO2 activity and serves as a precursor for the synthesis of kynurenine in an AFM dependent manner. Thus, mRNA expression of *Afm* was assessed in iLN isolated from naive, pre-arthritic mice, and animals with established CIA. The results were compared with iLN from naive mice. Like for *Ido1*

and *Ido2*, mRNA expression for *Afm* was significantly increased in pre-arthritic mice ($p<0.01$) and in mice with established CIA ($p<0.001$) compared to iLN from naive mice (Figure 13E).

Hence, in CIA, mRNA expression for the all three initial genes on the kynurenine pathway (*Ido1*, *Ido2*, and *Afm*) was significantly increased in iLN. Consistent with these findings, the concentration of tryptophan was significantly reduced in iLN in CIA. However, the concentration of kynurenine was significantly increased only in iLN taken from mice with established CIA, although there was a strong trend towards increased kynurenine levels before disease onset (Figure 13).

4.2.1.1. Accumulation of AA and 3-HAA in iLN of mice with established CIA

I then studied the catabolism of kynurenine in iLN mice with CIA. Kynurenine may be catabolised by KYNU to yield AA or by KMO to yield 3-HK. 3-HK is further catabolised by KYNU and 3-HAA is produced. Hence, the generation of both, AA and 3-HAA, is regulated by the activity of KYNU. It was therefore of interest to measure the concentration of AA, 3-HK, and 3-HAA in iLN of mice with CIA and naive animals. However, because of technical problems (I did not have access to the electrochemical detector required for detection and quantification of 3-HK within the physiological concentration range) it was not possible to measure concentrations of 3-HK. Thus, only the concentration of AA and 3-HAA was determined by HPLC. In addition, I assessed mRNA expression for *Kmo* and *Kynu*. In addition, *Haao* mRNA expression was measured because HAAO catalyses the catabolism of 3-HAA.

The concentration of AA was significantly higher in iLN taken from mice with established CIA than in naive mice. In contrast, the concentration of AA was unchanged during the pre-arthritic phase of CIA in comparison with naive iLN (Figure 14A).

A similar pattern was observed for 3-HAA. In iLN isolated from mice with established CIA, the concentration of 3-HAA was significantly increased in comparison with naive mice (Figure 14B). However, although there was a trend towards increased concentration of 3-HAA during the pre-arthritic phase of CIA, it was not significantly changed in comparison with naive mice or mice with established CIA (Figure 14B).

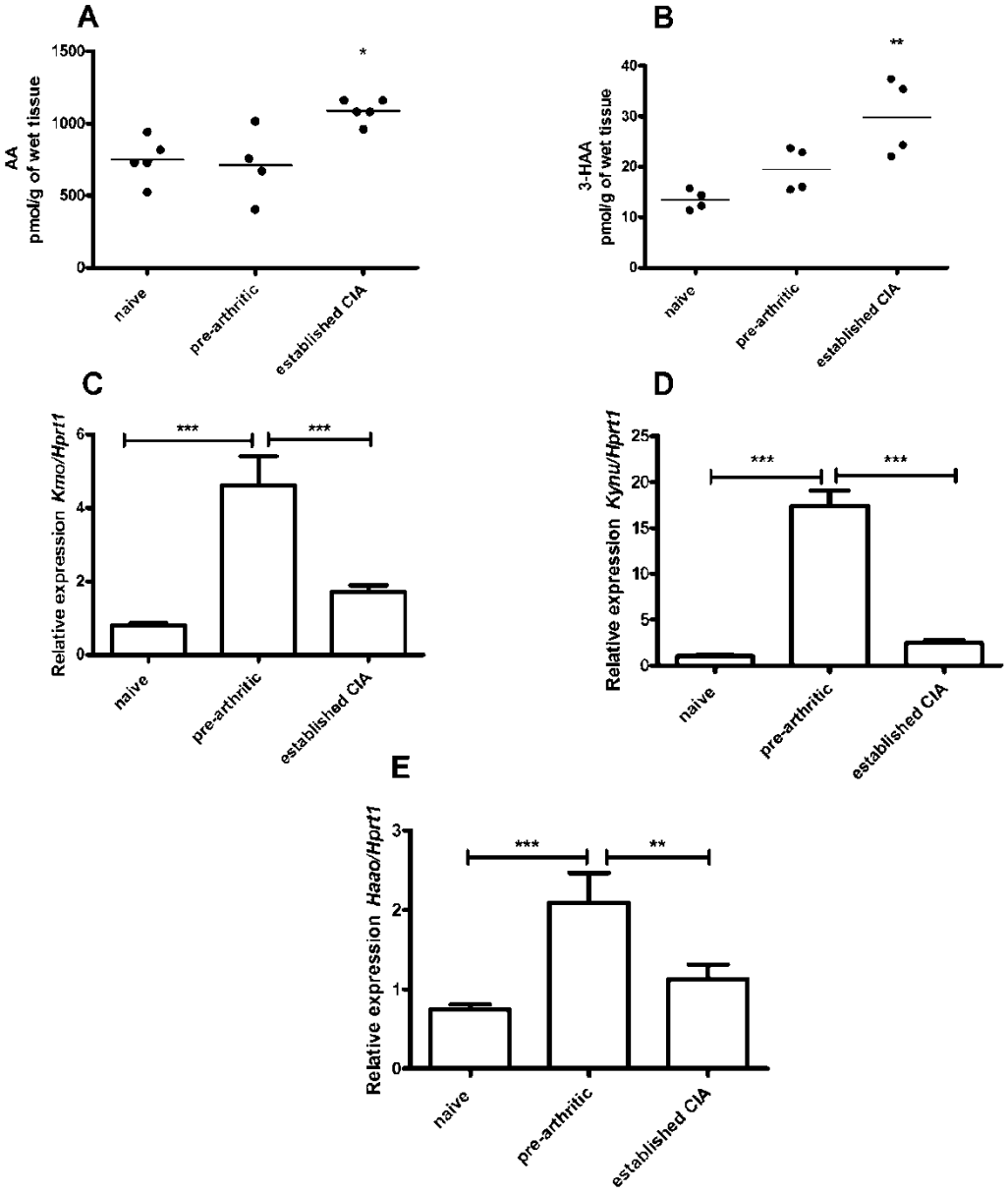


Figure 14 Catabolism of kynurenine in lymph nodes of mice with CIA

CIA was induced in DBA/1 mice and inguinal lymph nodes (iLN) were taken from mice (n=4) 14 days after immunisation (pre-arthritic stage of CIA) or from animals with established CIA (n=5) (10 days after onset of disease). The results were compared with iLN from naive mice (n=5). **A)** Concentration of AA **B)** Concentration of 3-HAA. mRNA expression for **C)** *Kmo*, **D)** *Kynu* **E)** *Haao*. mRNA expression was measured by qRT-PCR on cDNA prepared from total RNA isolated from iLN and normalised to hypoxanthine guanine phosphoribosyltransferase (*Hprt1*). Values represent levels of mRNA expression using the ΔΔCt method and are expressed as arbitrary units (mean ±SE), * $p<0.05$, ** $p<0.01$

In order to establish an association between the accumulation of kynurenines (kynurenine, AA, and 3-HAA) and the expression of enzymes responsible for their metabolism, mRNA expression for *Kmo*, *Kynu*, and *Haao* was assessed. In iLN taken from pre-arthritic mice, mRNA expression for all three genes: *Kmo* (Figure 14C), *Kynu* (Figure 14D), and *Haao* (Figure 14E), followed the same pattern. In the iLN isolated from pre-arthritic mice mRNA expression for all three genes was significantly ($p<0.01$) increased in comparison with naive mice (Figure 14C-E). However, in the iLN taken from mice with established CIA, mRNA expression for *Kmo*, *Kynu*, and *Haao* was normalised to the control level.

Taken together, in the iLN taken from mice with established CIA not only was there accumulation of kynurenine but also the concentration of its catabolites, AA and 3-HAA, was increased. In addition, mRNA expression for genes involved in the catabolism of kynurenine was normalised to the control level during established phase of CIA. However, this normalisation was preceded by an increase in mRNA expression for these genes in the iLN taken from pre-arthritic mice (Figure 14).

4.2.2. Tryptophan catabolism in the spleen during CIA

The secondary lymphoid organs are made of lymph nodes and the spleen. Thus, it was of interest to test if tryptophan catabolism via the kynurenine pathway could be also affected in the spleens from mice with CIA. To address this question, CIA was induced in DBA/1 mice and spleens were taken from pre-arthritic mice and mice with established CIA. As before, tryptophan was isolated from tissues and its concentration was measured with by HPLC, whereas the concentration of kynurenine was determined in the crude homogenates with a colorimetric method. The results were compared with spleens taken from naive mice and are presented in Table15. In contrast to the iLN from mice with CIA, the concentration of

tryptophan and kynurenine was significantly changed neither during the pre-arthritic nor established phases of CIA in comparison with spleens from naive mice (Table 15).

Table 15 In the spleen, during CIA, the concentration of tryptophan and kynurenine was not changed

Spleens were homogenised and the concentration of tryptophan was measured by HPLC and the concentration of kynurenine was measured by a colorimetric method.

Compound	**Naive (n=5)**	**Pre-arthritic (n=4)**	**Established CIA (n=5)**
Tryptophan (nmol/g of wet tissue)	29.38 ±11.35	30.86 ±15.49	49.87 ±5.87
Kynurenine (nmol/g of wet tissue)	55. 64 ±44.10	57.10 ±37.82	33.9 ±8.24

The lack of statistically significant changes in the concentration of tryptophan and kynurenine in the spleens from mice CIA prompted me to hypothesise that mRNA expression for the initial genes on the kynurenine pathway (*Ido1*, *Ido2*, and *Afm*) would also be unchanged. To test this hypothesis, the changes in mRNA expression for *Ido1*, *Ido2*, and *Afm* were assessed in the pre-arthritic and arthritic spleens. The results were compared with spleens taken from naive mice. I have found that mRNA expression for all three initial genes on the kynurenine pathway, *Ido1*, *Ido2* and *Afm* was in deed unchanged in comparison with naive samples (Figure 15).

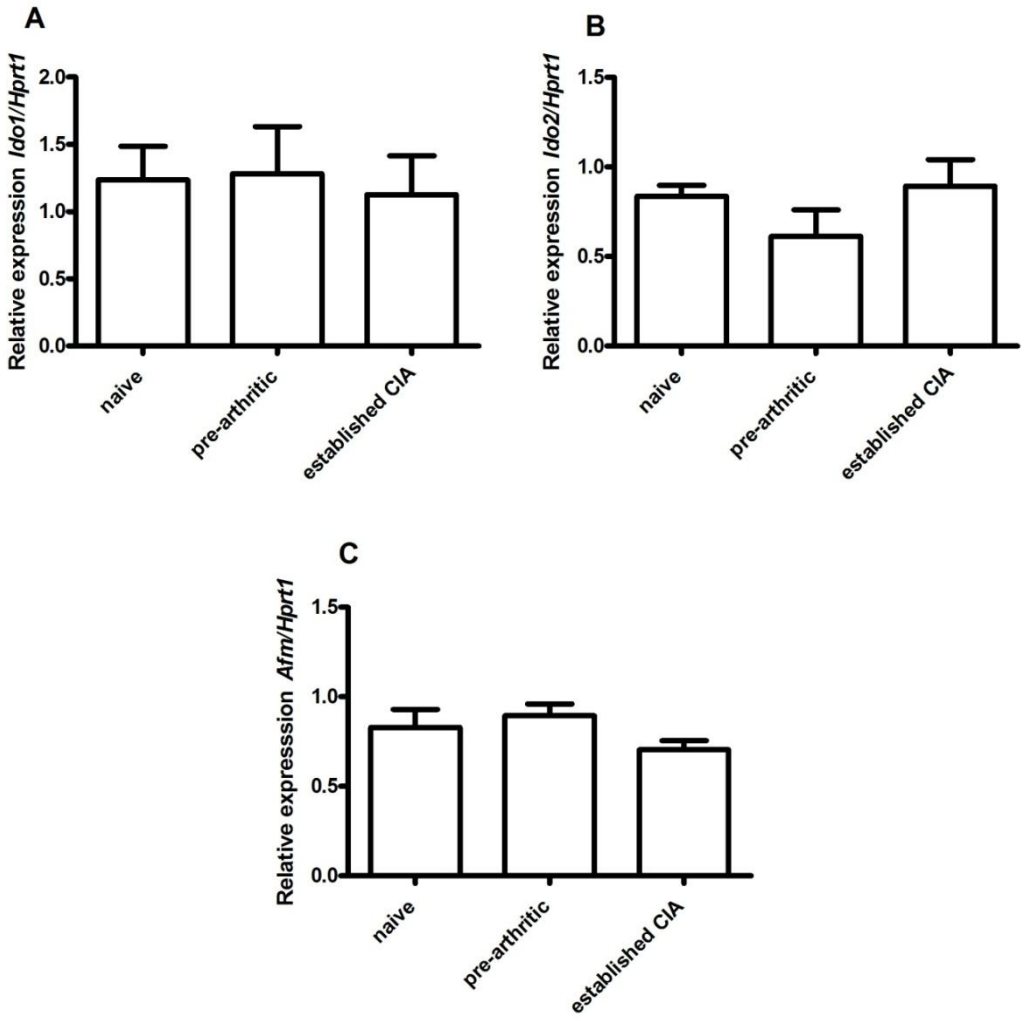


Figure 15 mRNA expression for the initial enzymes on the kynurnine pathway was unchanged in spleens of mice with CIA

CIA was induced in DBA/1 mice and spleens were taken from mice 14 days after immunisation pre-arthritic stage of CIA (n=4) and animals (n=5) with established CIA (10 days after first onset of disease become apparent). Results were compared with naive spleens (n=5) and statistically assessed using one way ANOVA with Dunnetts multiple comparison test. mRNA expression for **C)** *Ido1*, **D)** *Ido2*, and **E)** *Afm* was measured with qRT-PCR technique on cDNA prepared with total RNA isolated from spleens. Expression of these genes was normalised *Hprt1* transcripts. Values represent arbitrary units with SEM provided as results of mRNA expression analysis with ΔΔCt method.

To complete the study of tryptophan catabolism via the kynurenine pathway in the spleens taken from mice with CIA I addressed the question of whether the downstream catabolism of kynurenine was also unchanged. Thus, the concentrations of AA and 3-HAA were measured by HPLC. Spleens were either taken from the pre-arthritic mice or animals with established CIA. However, the concentration of AA and 3-HAA was found to be unchanged in pre-arthritic and arthritic mice compared to naive mice (Table 16).

Table 16 In the spleen during CIA the concentration of AA and 3-HAA was not changed

Anthranilic acid (AA) and 3-hydroxyanthranilic acid (3-HAA) were extracted from spleens and their concentration was measured by HPLC. Results were compared between spleens taken from naive, pre-arthritic, and mice with established CIA. One-way ANOVA with Dunnetts multiple comparison test was applied for statistical analysis.

Compound	**Naive (n=5)**	**Pre-arthritic (n=4)**	**Established CIA (n=5)**
AA (nmol/g of wet tissue)	0.20 ±0.15	0.34 ±0.06	0.26 ±0.13
3-HAA (fmol/g of wet tissue)	1.85 ±0.57	1.94 ±0.66	1.37 ±0.26

The next step was to establish whether the lack of changes in the concentrations of AA and 3-HAA in the spleens from mice with CIA could coincided with unchanged rate of mRNA expression of the genes involved in the catabolism of kynurenine and 3-HAA. Hence, mRNA expression for *Kynu, Kmo,* and *Haao* was assessed in the spleens taken form naive, pre-arthritic, and mice with established CIA. mRNA expression for only *Haao* was significantly ($p<0.05$) increased in the spleens taken from pre-arthritic mice. However, mRNA expression for this gene was normalised to the control level in the spleens taken from mice with established CIA. Interestingly, mRNA expression for genes responsible for

catabolism of kynurenine (*Kmo* and *Kynu*) was unchanged in the spleens taken from either pre-arthritic or arthritic mice compared to naive mice (Figure 16).

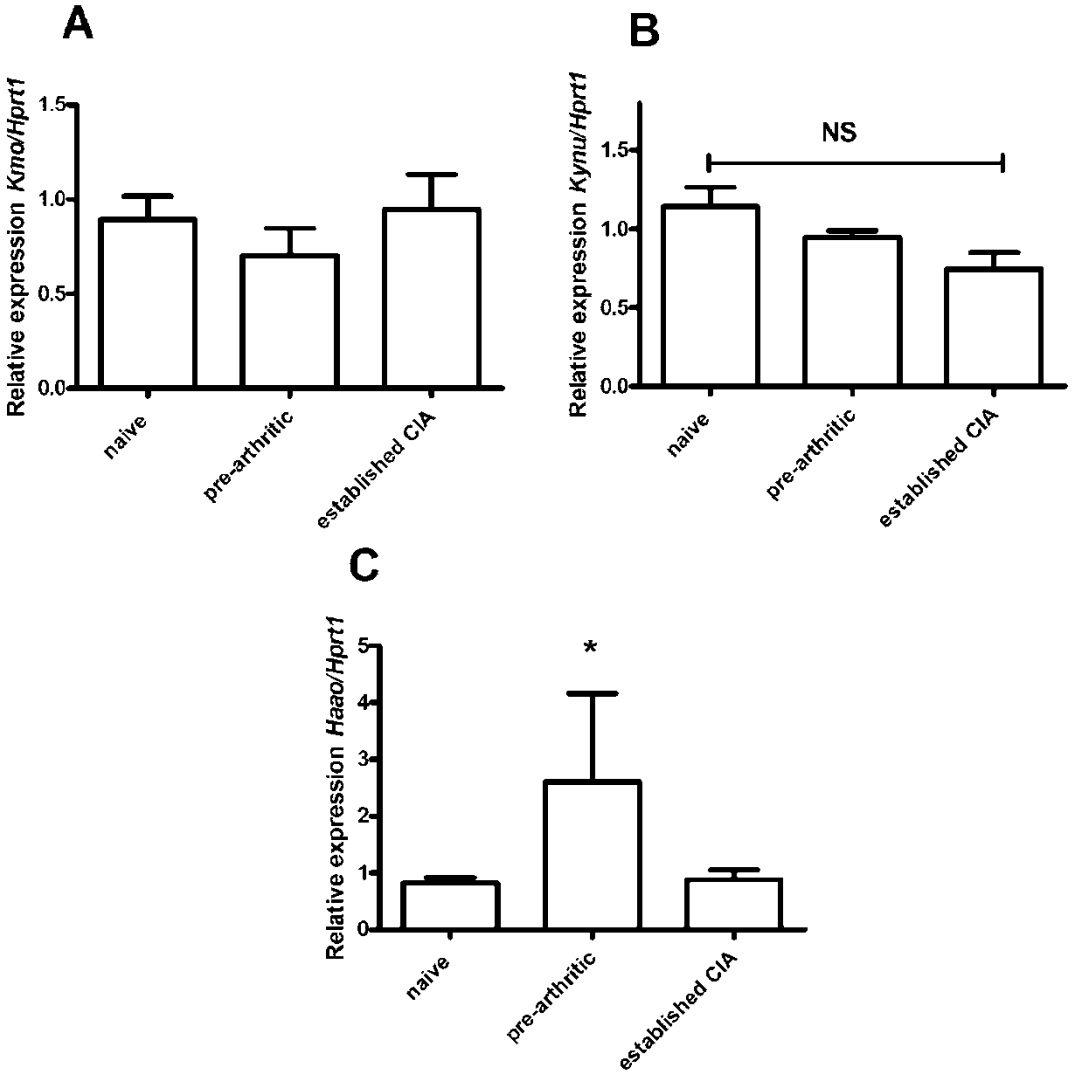


Figure 16 Expression of genes encoding KMO, Kynureninase, and HAAO in spleens of mice with CIA

CIA was induced in DBA/1 mice and spleens were taken from mice (n=4) 14 days after immunisation (a pre-arthritic stage of CIA) and animals (n=5) with established CIA (10 days after first onset of disease become apparent). Results were compared with naive spleens (n=5).Gene expression for **A)** *Kmo*, **B)** *Kynu*, and **C)** *Haao* was measured with qRT-PCR technique on cDNA prepared with total RNA isolated from iLN. Values represent arbitrary units with SEM provided as results of mRNA expression analysis with ΔΔCt method. * $p<0.05$

4.2.3. Tryptophan catabolism in the inflamed paws during CIA

Having investigated the kynurenine pathway in the several types of organs during CIA, it was of also of interest to test if this metabolic pathway could be affected in the inflamed paws, which are of course the main sites of the disease activity. Hence, in the first sets of measurements, the initiation of tryptophan catabolism via the kynurenine pathway was studied. However, because of technical difficulties (no amplification signal for mRNA encoding IDO1, IDO2, and HAAO) it was not possible to use qRT-PCR with TaqMan probes. Similarly, using RT-PCR technique, I was unable to detect *Ido1* mRNA expression. Using immunochistochemistry I have showed the lack of significant protein expression for IDO1 and IDO2 in paws.

Interestingly, the mean concentration of tryptophan was higher in the paws taken from mice with established CIA than in the paws taken either from naive mice or pre-arthritic animals (Figure 17A). In the paws of mice with established CIA, the mean concentration of tryptophan was 128.19 ±19.91 nmol/g of wet tissue. However, in the paws isolated from naive mice, the mean concentration of tryptophan was 93.54 ±16.07 nmol/g of wet tissue (Figure 16A). Therefore, the difference between paws from healthy mice and paws taken from the diseased animals was statistically significant ($p<0.05$). In the paws taken from pre-arthritic mice, the mean concentration of tryptophan was 95.46 ±18.59 nmol/g of wet tissue. In contrast, the concentration of kynurenine was not significantly different between groups although there was a trend towards increased concentration of kynurenine in the paws isolated from pre-arthritic and arthritic groups (Figure 17B). *Ido1* mRNA expression was not detectable by RT-PCR in the paws either taken from naive mice or animals with CIA (Figure 17C). The absence of mRNA expression for *Ido1* was supported by the absence of IDO1 and IDO2 expression in the paws taken from naive mice and animals with established CIA (Figure 17D).

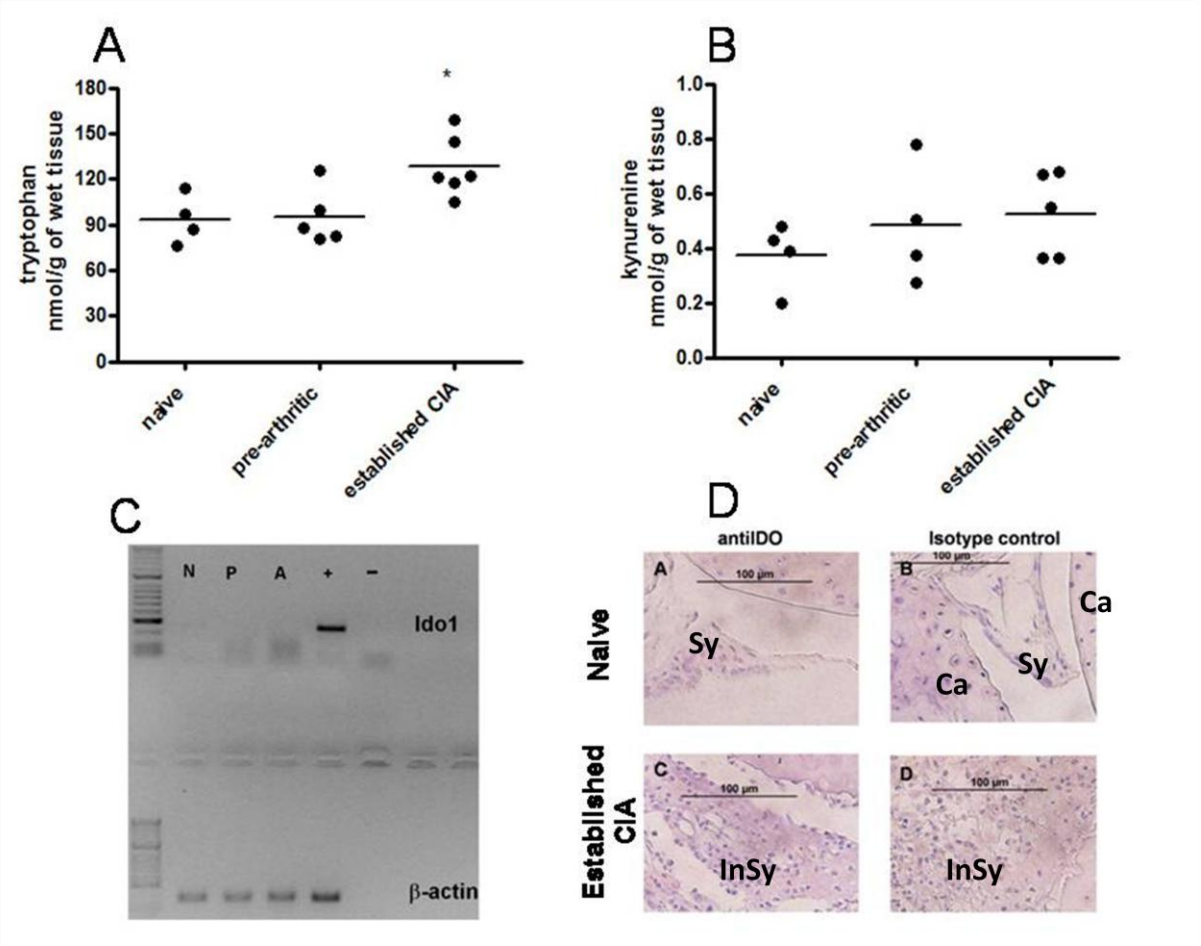


Figure 17 Tryptophan and kynurenine concentrations and IDO expression in paws of mice with CIA

CIA was induced in DBA/1 mice and hind paws were taken from mice (n=5) 14 days after immunisation (a pre-arthritic stage of CIA) and animals (n=6) with established CIA (10 days after first onset of disease become apparent). In fact, the same animals were used in the experiments described in the previous chapters. Results were compared with naive paws (n=4) **A)** Concentration of tryptophan. **B)** Concentration of kynurenine. **C)** Expression of mRNA for *Ido1* **D)** IDO expression by immunohistochemistry using an antibody that recognises both, IDO1 and IDO2, respectively * $p<0.05$. N stands for naive, P means pre-arthritic, A indicates on sample taken from mice with established CIA, - negative control, + positive control, Ca means cartilage, InSy stands for inflamed synovium, and Sy indicates on synovium.

Next, I determined whether the unchanged concentration of kynurenine in the paws with CIA could coincide with the sustained concentration of AA. However, the concentration

of AA was significantly decreased in the paws from mice with established CIA compared to naive mice (Figure 18A). As AA is generated by the activity of KYNU, I next assessed mRNA expression for *Kynu*. Unlike with *Ido1*, it was possible to measure *Kynu* mRNA expression by qRT-PCR. The results are presented in Figure 18B. Interestingly, mRNA expression for *Kynu* was not significantly changed between paws from naive mice, pre-arthritic mice, or mice with established CIA (Figure 18B). KYNU protein was also shown by immunohistochemistry to be expressed in paws from naive mice (Figure 18C). However, the intensity of staining was much stronger in the paws of mice with established CIA suggesting increased expression of KYNU in the arthritic paws (Figure 18D).

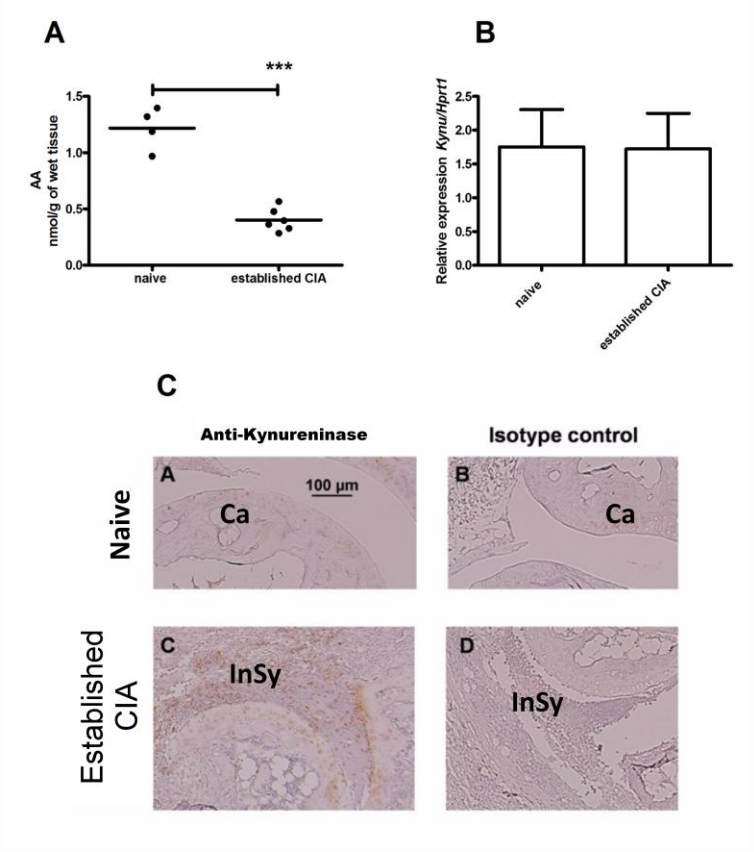


Figure 18 Concentration of AA and expression of kynureninase in paws of mice with CIA

CIA was induced in DBA/1 mice and hind paws were taken from mice with established CIA (n=6) and naive mice (n=4). However, the paws came from the same animals as used in other experiments described in this thesis. **A)** Concentration of AA. **B)** mRNA expression for *Kynu*. **C)** Immunohistochemical analysis of KYNU protein expression. *** $p<0.001$. Ca means cartilage, InSy stands for inflamed synovium, and Sy indicates on synovium.

To complete the study of kynurenine catabolism in the paws from mice with CIA it was of interest to measure the concentration of 3-HAA in these tissues. However, the levels of 3-HAA were below the quantification limit established for the HPLC method used in this project. Similarly, mRNA expression for HAAO was not detected by qRT-PCR. Consistent with these findings, HAAO protein was not detected by immunohistochemistry in the paws of naive mice, pre-arthritic mice or mice with established CIA (Figure 19).

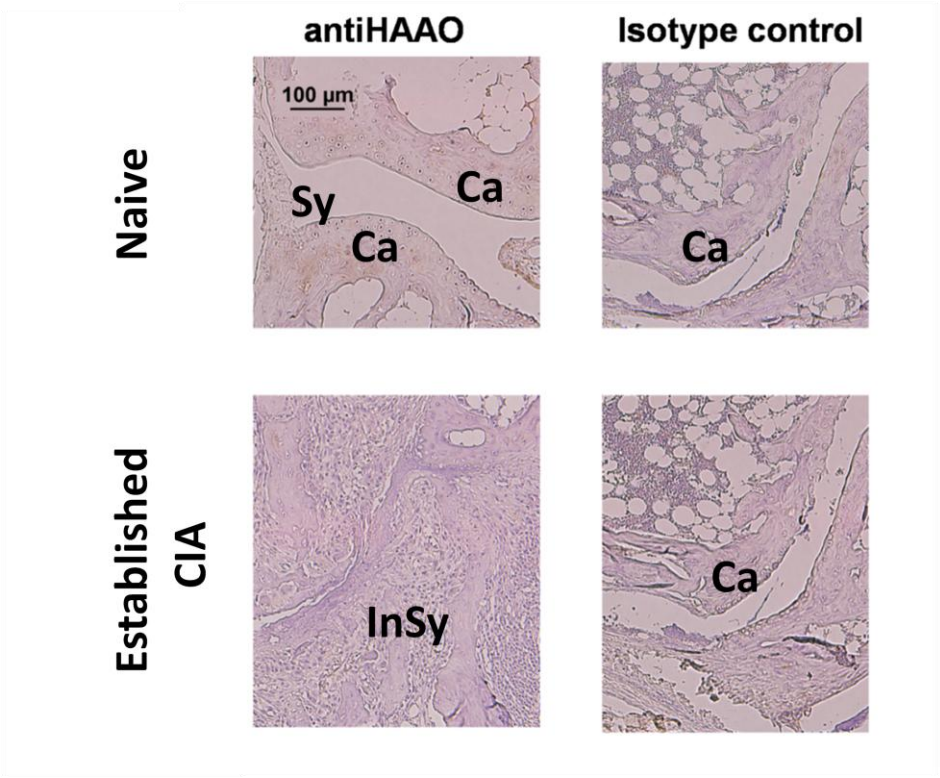


Figure 19 HAAO could not be detected in the paws of naive mice or mice with established CIA

CIA was induced in DBA/1 mice and hind paws were taken from mice with established CIA (n=6) and naive mice (n=4). The paws were sectioned and stained with anti-HAAO antibodies. However, HAAO enzyme was not detected. Nevertheless, when small intestine was subjected to the immunohistochemical reaction, strong staining was seen (chapter 2, section 2.6.5). Ca means cartilage, InSy stands for inflamed synovium, and Sy indicates on synovium.

4.3. DISCUSSION

Previous work by our group demonstrated the importance of IDO1 in CIA (Criado et al. 2009). Specifically, IDO1 expression has been shown to be up-regulated in the iLN during CIA, and the genetic deletion of IDO1 exacerbated arthritis. Conversely, systemic administration of kynurenine suppressed disease. Thus, the results presented in this chapter contribute to a better understanding of the metabolic regulation of the entire kynurenine pathway during experimental arthritis in the secondary lymphoid organs and inflamed paws. My data showed that in CIA, increased tryptophan catabolism via the kynurenine pathway was confined to draining iLN, whereas CIA did not significantly affect tryptophan catabolism in the spleen. This may be explained by the fact that spleen responds to blood borne antigens whereas lymph nodes are involved in processing antigens from other tissues like skin or joints (Junt et al. 2008). Wingender *et al*. have also shown that tryptophan metabolism can be activated in the spleen only when antigens were injected into the bloodstream (Wingender et al. 2006).

Interestingly, in the inflamed paws from mice with established CIA, tryptophan was found to be accumulated. This could partly be explained by accumulation of albumin in the inflamed paws, a phenomenon previously reported. Tryptophan is the only known amino acid which can reversely bind to albumin. Therefore, albumin could serve as a depot for tryptophan. However, the physiological consequence of its accumulation in the inflamed paws is not known. One possibility is that increased concentration of tryptophan helps to fuel the proliferation of pathological cells like e.g. Th17 and Th1 cells, thereby creating a permissive environment for the propagation of immune-mediated pathology. However, this hypothesis would need to be tested.

This study has shown for the first time that *Ido1/Ido2/Afm* mRNA expression is increased in iLN *in vivo* and this may be of physiological significance because catabolism

tryptophan was also depleted in iLN. In contrast, in the paws taken from either naive mice or animals with CIA the initial enzymes on the kynurenine pathway could not be detected. This may suggest that in the inflamed paws the kynurenine pathway is not active. However, the observation that it was possible to detect mRNA expression for the kynurenine pathway enzymes in the spleens suggests that in these organs this metabolic pathway is active. Moreover, as judged by the changes in mRNA expression for the genes on the kynurenine pathway and/or the concentration of the concentration of kynurenines, CIA did not apparently result in the increased activity of the kynurenine pathway.

This study has shown that the kynurenine concentration was significantly higher in iLN of mice with established CIA but not in iLN taken from pre-arthritic mice. This was despite the fact that the concentration of tryptophan was decreased and mRNA expression for the initial enzymes on the kynurenine pathway was increased in iLN of both pre-arthritic and arthritic mice. Thus, increased tryptophan metabolism may not necessarily result in kynurenine accumulation. Instead, the concentration of kynurenine may be regulated by its rate of catabolism (Salter et al. 1986). Hence, I addressed whether mRNA expression for the downstream genes on the pathway (*Kmo, Kynu,* and *Haao*) changed in iLN during CIA. I found that mRNA expression for all three genes: *Kmo, Kynu,* and *Haao,* was up regulated during the pre-arthritic phase of arthritis and returned to near normal levels in the iLN of mice with established CIA. This was consistent with the observations that the concentration of AA and 3-HAA was increased at this time. However, in CIA, catabolism of kynurenine was not significantly affected in the spleen. In contrast, in the inflamed paws of mice with established CIA the concentration of AA was significantly decreased. This suggests that in the spleen KYNU could catalyse conversion of kynurenine to AA less efficiently. However, the concentration of kynurenine was not changed in the paws of mice with established CIA. Hence, one may speculate that either AA is quickly removed from the inflamed paws or

enzymatic activity of KYNU undergoes metabolic regulation. Nonetheless, *Kynu* mRNA expression was unchanged in CIA, whereas its protein expression might be increased. Thus, it may be that mRNA expression could not correlate with protein expression. Nevertheless, in summary, it is difficult to draw a firm conclusion from these observations.

The changes in tryptophan and kynurenine concentration detected during CIA in iLN may have physiological consequences because lymph nodes are the main sites of T cell proliferation. Unlike RA, CIA in DBA/1 mice is a relatively acute disease that spontaneously begins to remit around 7-10 days after onset (Inglis et al. 2008). Therefore, the decreased tryptophan concentration and accumulation of kynurenines coincided with the resolution of inflammation. However, increased tryptophan metabolism on its own, as observed in pre-arthritic samples, did not protect from development of autoimmune arthritis as disease progressed. Instead, the resolution of inflammation coincided with increased tryptophan catabolism and the accumulation of the kynurenine-based metabolites in draining LN. Hence, this raises the intriguing possibility that the full anti-inflammatory potential of increased tryptophan metabolism via the kynurenine pathway can be achieved only when the tryptophan catabolites (kynurenines) accumulate. The immunomodulatory properties of kynurenines have been well-documented and it is noteworthy that tranilast, a derivative of 3-HAA, had a marked therapeutic effect in experimental autoimmune encephalomyelitis (EAE), an animal model of multiple sclerosis (Platten et al. 2005), and in CIA (Inglis et al. 2007).

Decreased tryptophan concentration and the accumulation of kynurenines can also modify the cellular composition of lymph nodes (Fallarino et al. 2002; Terness et al. 2002). In line with these findings, Desvignes and Ernst have demonstrated that an equimolar mixture of kynurenines (kynurenine, 3-HK, AA, and 3-HAA) could inhibit IL-17 production in a dose dependent manner with an IC_{50} value of 11.7 μM (Desvignes and Ernst 2009). When tested

separately, 3-HAA was the most potent tryptophan metabolite with an IC_{50} value of 27.7 μM. In addition, it has been shown that kynurenines were able to abrogate the Th17- promoting capacity of IL-23 in Th17 cells (Desvignes and Ernst 2009). Nonetheless, the mechanisms responsible for this effect remain unknown (Desvignes and Ernst 2009). However, my data shows that the concentration of 3-HAA in iLN from mice with established CIA was in the nanomolar range; whereas the concentration of AA reached the low micromolar range. Fallarino *et al*. showed that in long term cell culture (7 days), a combination of low tryptophan concentration (35 μM) and an equimolar (10 μM) mixture of kynurenine, AA, 3-HK, 3-HAA and QA promotes conversion of naive $CD4^+$ T cells into $CD25^+$ $Foxp3^+$ regulatory T cells (Treg) (Fallarino et al. 2006). In this project, I showed that the mean concentration of tryptophan and kynurenine in iLN from mice with established CIA was in a similar micro molar (μM) range to that used by Fallarino *et al*. (Fallarino et al. 2006). Thus, the levels of tryptophan and kynurenine found in this study were very likely to be physiologically relevant.

Taken together, the data presented in this chapter suggest that in the lymph nodes from mice with CIA the entire kynurenine pathway is functional. However, the full, anti-inflammatory, potential of this metabolic pathway may depend on a combination of increased tryptophan catabolism and reduced kynurenine degradation leading to accumulation of kynurenines. Hence, my findings are consistent with the hypothesis that the regulation of kynurenine catabolism plays a pivotal role in termination of pathological immune responses.

Chapter 5

Evaluation of the therapeutic potential of kynurenine catabolites in collagen induced arthritis

5.1. INTRODUCTION

In the fourth chapter, I have shown that the concentration of tryptophan was significantly decreased and kynurenines were accumulated in iLN from mice with established CIA. This stage of the disease precedes the resolution phase of CIA. Thus, I hypothesised that the synergistic effect of decreased tryptophan concentration and accumulation of kynurenines could contribute to the resolution of inflammation in CIA. This hypothesis is supported by previous work from our laboratory showing that *Ido1* KO mice exhibit exacerbated clinical and histological scores in CIA. This finding was also confirmed independently in another study which showed that inhibition of IDO1 can indeed exacerbate the disease (Szanto et al. 2007). In addition, in the third chapter, I have shown that the concentration of kynurenine was significantly decreased in the sera of arthritic *Ido1*-/- mice compared to aged-matched arthritic WT mice. In line with this observation, (Criado et al. 2009) have showed that intraperitoneal administration of kynurenine to DBA/1 mice reduced the severity of CIA and normalised kynurenine levels in sera from arthritic mice. Such observation is in the agreement with previously published reports and may suggest that the downstream catabolites of kynurenine (AA and 3-HAA) (Munn et al. 1999) could also exert an anti-arthritic effect. In line with this hypothesis, it was previously shown that exogenous administration of kynurenine and its downstream metabolites: AA, 3-HAA, and QA, were effective in reducing the severity of inflammatory disease in animal models (e.g. allergy and organ transplantation) (see Table 3). However, the very first experiments which were designed to measure turnover of exogenously injected 3-HAA have demonstrated very fast metabolism of 3-HAA (Hankes and Henderson 1957). Hence, pharmacological action of 3-HAA could be hampered by its high rate of catabolism. Nevertheless, recently, the beneficial role of 3-HAA has been shown in multiple studies (see section 1.1.3.6). In contrast to 3-HAA, pharmacological potential of AA is less known. However, AA and 3-HAA share

similar chemistry and exhibit minor differences in molecular mass (137.14 g/mol and 153.14 g/mol, respectively). Hence, AA and 3-HAA would be predicted to share similar routes of **A**bsorption, **D**istribution, **M**etabolism, and **E**xcretion (**ADME**) in DBA/1 mice with CIA. An additional reason for testing AA in CIA was that a chemical derivate of AA, *N*-(3', 4'-dimethoxycinnamonyl) anthranilic acid (tranilast®) is used in Asia for the treatment of bronchial asthma (Konneh 1998), keloid (Shigeki et al. 1997), and atopic dermatitis (Gondo, Saeki et al. 1985) and has been shown to be effective in CIA (Inglis et al. 2007). Another chemical derivate of AA, N-(3-Trifluoromethylphenyl)anthranilic acid, is an NSAID (Barnardo et al. 1966). In addition, there is also one publication in which the immunostimulatory action of AA has been demonstrated in adjuvant arthritis (Kunitomo et al. 1989). Therefore, taken together, it was of interest to assess anti-arthritic properties of AA and its hydroxylated derivate, 3-HAA in CIA.

Bone erosions, osteopenia, and cartilage damage are a frequent consequence of inflammatory arthritis and a common cause of disability in RA (Jansen et al. 2001). Classically, in animal models of inflammatory arthritis, the visualisation of these pathological features relies on histology (Inglis et al. 2008). However, histological sections do not reflect the 3D structure of diarthrodial joints. In contrast, imaging of bone pathology by μCT enables quantitative measurements of bone parameters (e.g. the mean cortical thickness) and qualitative analysis of joint integrity to be made without destruction of the sample (Bagi et al. 2006; Augat and Eckstein 2008; Muller 2009). In addition, it has recently been shown in patients with RA that bone pathology is not only restricted to bone erosions. Thus, changes in the surface of the bones have been reported, including increased roughness (Silva et al. 2006) and increased size of the bone channels (Marinova-Mutafchieva et al. 2002). It was, therefore, of interest to establish whether these pathological changes can also be detected in

CIA and whether they can be prevented by treatment with AA, 3-HAA or etanercept, an inhibitor of TNF.

5.2. RESULTS

5.2.1 Multiple bone deformities can be observed in CIA and their severity can be assessed semi-quantitatively

To test the utility of μCT for assessing bone lesions, micro-radiograms and movies showing the rotating skeleton of the hind paw were analysed. These analyses revealed that bone erosions coexisted in CIA with other pathological changes like newly formed bone/osteophytes, rough bone texture; increased number of visible bone channels, and expanded crack-like structures. These lesions were observed on the dorsal (Figure 20A) as well as on the plantar side (Figure 20B) of hind paws. No obvious pathology could be seen on the dorsal (Figure 20C) or plantar (20D) side of hind paws from naive mice.

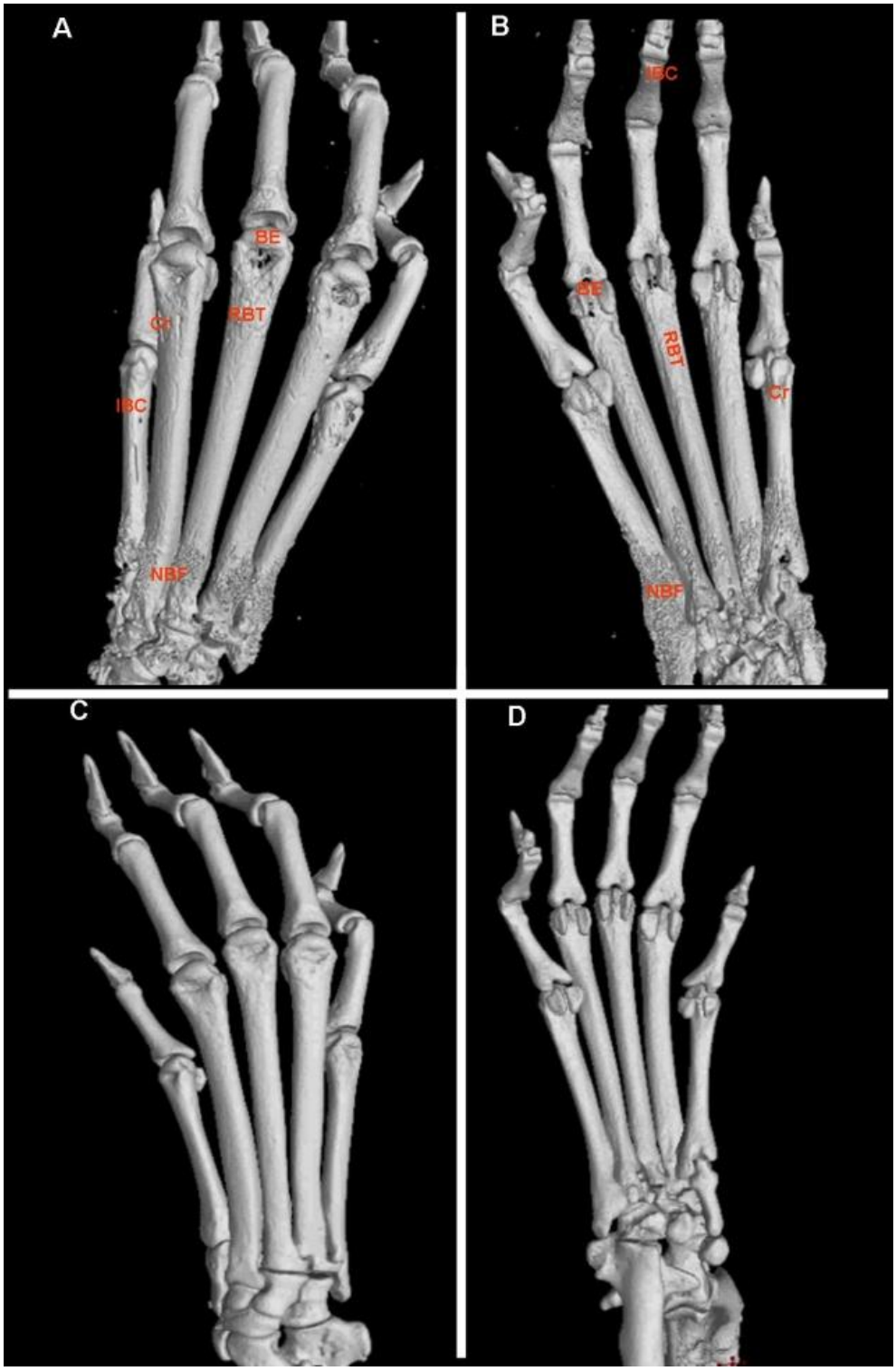


Figure 20 Multiple lesions are observed in the bones in CIA as visualised by μCT

CIA was induced in DBA/1 mice and micro-computed tomography with volumetric reconstructions was performed on the hind paws (n=44) at various stages of the disease. For comparison, hind paws (n=10) from naive mice were scanned and reconstructed. The following pathological changes were observed: bone erosions (**BE**), new bone formation (**NBF**), crack-like structures (**Cr**), increased number of visible bone channels (**IBC**), and rough texture of the bone surface (**RBT**). **A)** A representative micro-radiogram showing the dorsal view of a hind paw of a mouse with CIA. **B)** A representative micro-radiogram showing the plantar view of a hind paw of a mouse with CIA. **C)** A representative micro-radiogram showing the dorsal view of a hind paw of a naive mouse. **D)** A representative micro-radiogram showing the plantar view of a hind paw from a naive mouse.

The severity of arthritis was variable between inflamed paws and it was possible to assign a bone pathology score, ranging from 0 to 4, to each paw (Figure 21). A detailed description of the scoring system is presented in Table 17.

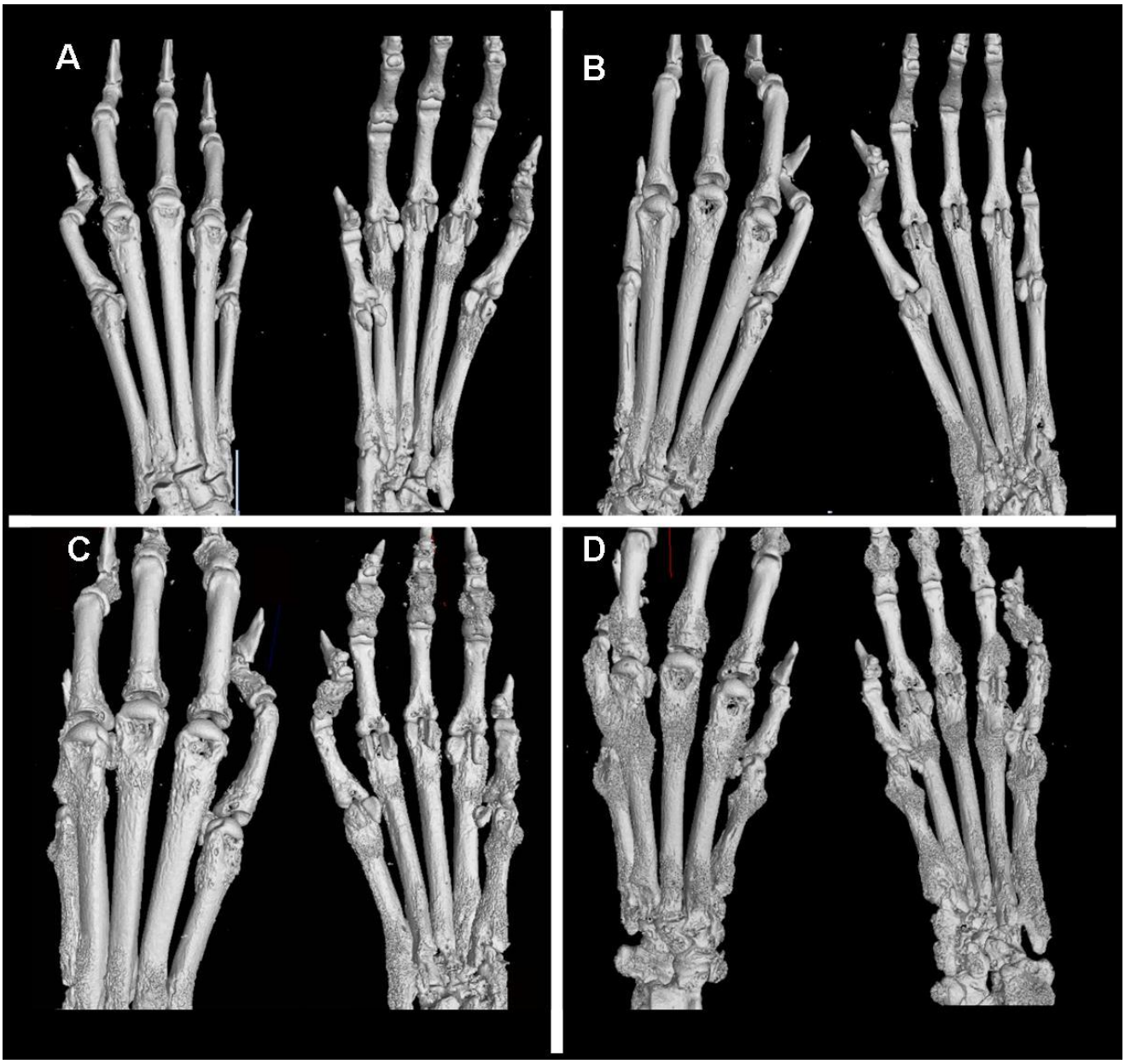


Figure 21 Scoring of bone and joint pathology in CIA by μCT

CIA was induced in DBA/1 mice and micro-computed tomography with volumetric reconstructions was performed on the hind paws (n=44) at various stages of the disease. **A)** A representative micro-radiogram of the skeleton of a hind paw with mild pathology scored with an arbitrary unit of 1. **B)** A representative micro-radiogram of the skeleton of a hind paw with mild pathology scored with an arbitrary unit of 2. **C)** A representative micro-radiogram of the skeleton of a hind paw with bone and joint damage scored with an arbitrary unit of 3. Pathology is widespread and almost all bones and joints are affected. **D)** A representative micro-radiogram of the skeleton of a hind paw scored with an arbitrary unit of 4.

Table 17 Semi-quantitative scoring system for assessment of bone pathology in the hind paws of mice with CIA

CIA was induced in DBA/1 mice and micro-computed tomography with volumetric reconstructions was performed on the hind paws (n=44) of mice at various stages of the disease. Based on the 3D reconstructions it was possible to assign bone pathology with scores ranging from 0 to 4.

Grade	0	1	2	3	4
Description	• no obvious pathology	• presence or absence of bone erosions • increased number of bone channels • increased number of crack like structures on metatarsal bones • signs of osteophyte formation	• presence of bone erosions • rough texture of bone surface • increased number of bone channels on metatarsal bones • increased number of crack like structures • Signs of osteophyte formation	• presence of bone erosions • some bone erosions are filled with newly formed bone • increased number of visible bone channels • increased number of crack like structures on metatarsal bones and phalanges • osteophytes visible but localised to metatarsal bones and phalanges	>95 % bones in the hind paw have at least one pathological feature • Extensive formation of osteophytes
Representative micro-radiogram	Figure 20C and 20D	Figure 21A	Figure 21B	Figure 21C	Figure21D

Next, the reproducibility of the scoring system was tested by two independent observers. Analysis of the scores assigned by two observers with the Bland-Altman method showed that the semi-quantitative assessment of bone pathology in three dimensions did not differ significantly (R^2= 0.1151; p=0.3075) between observers. I also addressed the question

of whether the clinical scores correlated with bone pathology scores. When analyzed with the Pearson correlation method, a positive correlation was found between clinical scores and scores of bone pathology $r = 0.16$; $p<0.001$ for observer1 and $r = 0.597$; $p<0.01$ for a second observer.

5.2.2. Bone pathology is associated with a decrease in the mean cortical thickness of the metatarsal bone

Bone erosions in RA are usually associated with a decrease in bone mass and the mean cortical thickness. It was therefore of interest to determine if variation in the severity of bone pathology in the hind paws from mice with CIA could correlate with the decrease in the mean cortical thickness of the metatarsal bone. 3mm long region of the 3rd metatarsal bone was selected for analysis and the results are presented in Table 18.

Table 18 Decrease in the mean cortical thickness of the 3rd metatarsal bone is negatively correlated with increasing severity of bone and joint damage

CIA was induced in DBA/1 mice and hind paws were taken from mice at various stages of the disease and scanned by μCT. The mean cortical thickness was measured using boneJ software.

Score	Number of analysed 3rd metatarsal bones	Mean cortical thickness (± Standard deviation)	Statistical analysis (p value) in comparison with score of 0
0	(n=10)	0.182 ±0.0049	----------
1	(n=5)	0.171 ±0.0059	0.05
2	(n=6)	0.164 ±0.0038	0.001
3	(n=6)	0.156 ±0.011	0.001
4	(n=6)	0.158 ±0.081	0.001

Finally, I tested whether scores of bone pathology correlated with decreased mean cortical thickness in the third metatarsal bone. When analyzed by Pearson's correlation coefficient method, a negative correlation was found between severity of bone pathology and

mean cortical thickness of the 3rd metatarsal bone ($r = -0.61$; $p<0.001$).

5.2.3. The formation of novel pathological features of bone destruction are driven in a TNF- dependent manner

I next addressed the question whether the pathological features observed by µCT are driven by TNF. In addition, this experiment gave me the opportunity to assess if bone imaging with µCT, established for this project, is sensitive enough to detect changes in pathology using an anti-arthritic treatment known to be effective in CIA. Therefore, CIA was induced in DBA/1 mice. When the first symptoms of the disease became apparent animals were randomly divided into two experimental groups: untreated and those treated with etanercept for 10 days. As expected, the clinical severity and paw-swelling were significantly reduced ($p<0.001$) in the etanercept treated animals compared to the control group (Figures 22A and 22B). These clinical observations were confirmed *ex vivo* by imaging with µCT. Thus, in the non-treated control mice bone pathology was evident (Figure 22C), whereas in the etanercept treated mice bone pathology was almost completely suppressed (Figure 22D). Semi-quantitative assessment of bone pathology with the scoring system described above revealed a statistically significant ($p<0.01$) reduction in the severity of bone damage in mice treated with etanercept compared to vehicle treated controls (Figure 22E). Similar results were seen when the mean cortical thickness in the 3rd metatarsal bone was measured. Thus, in the paws taken from control mice the mean cortical thickness was 0.164 ±0.008 mm whereas in the etanercept injected mice the mean cortical thickness was 0.182 ±0.0044 mm (Figure 22F). The difference was found to be significant $p<0.01$ (Figure 22F).

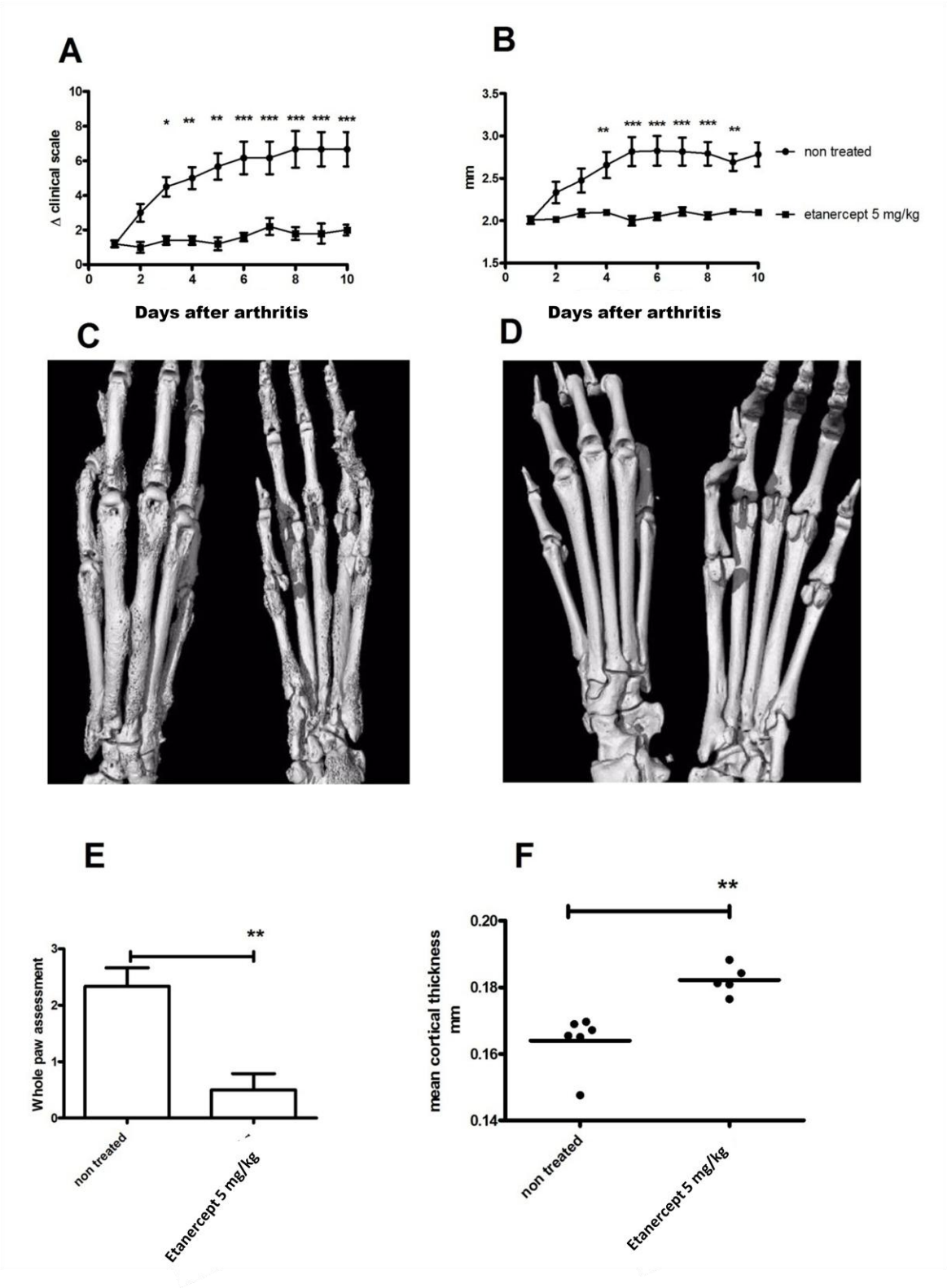


Figure 22 Treatment of CIA mice with etanercept reduced bone pathology

CIA was induced in DBA/1 mice. When the first symptoms of the disease were observed animals were randomly selected for treatment with 5 mg/kg of etanercept (n=5) or vehicle (n=6). After ten days animals were sacrificed and inflamed paws were removed and scanned by μCT. Movies of the rotating skeleton of the hind paws were assessed using a scale of 0-5. The mean cortical thickness of the 3rd metatarsal bones was measured with boneJ software. **A)** Clinical severity of CIA. **B)** Paw swelling. **C)** A representative plain micro-radiogram of the dorsal and plantar sites of the hind paw from a control arthritic mouse. **D)** A representative plain micro-radiogram of the dorsal and plantar sites of the hind paw of a mouse treated with etanercept. **E)** Bone pathology scores of the hind paws of mice treated with etanercept versus non-treated mice. **F)** Mean cortical thickness of the 3rd metatarsal bones in etanercept treated mice versus control mice.*$p<0.05$, **$p<0.01$, ***$p<0.001$

5.2.4. Neither treatment with AA nor with 3-HAA could reduce severity of CIA

Since, *in vitro*, it has been shown that 3-HAA is the most potent anti-inflammatory metabolite of kynurenine it was of interest to test its effect in established CIA. Thus, CIA was induced in DBA/1mice. When the first symptoms of arthritis became apparent animals were randomly assigned to one of three experimental groups and injected intraperitoneally with vehicle (1% $NaHCO_3$), 50 mg/kg of 3-HAA or 200 mg/kg of 3-HAA for 10 subsequent days. The clinical severity of arthritis was monitored on a daily basis by assessment of clinical scores and measurements of paw thickness. However, neither of treatment was effective.

Mice treated either with a low or a high dose of 3-HAA had CIA of a similar clinical scores to the vehicle treated animals (Figure 23A). A similar degree of paw swelling has been also observed (Figure 23B). In order to further confirm these *in vivo* observations *ex vivo* imaging with μCT was applied. 3D reconstructions of hind paws taken from vehicle treated mice (Figure 23C) revealed similar pathology to the animals treated with 200 mg/kg of 3-HAA (Figure 23D). Semi-quantitative assessment of hind paws of mice with CIA also showed comparable levels of bone pathology between vehicle treated mice and animals injected with 200 mg/kg of 3-HAA (Figure 23E). In line with these results, the mean cortical thickness in the 3rd metatarsal bone was comparable between vehicle treated mice and animals injected with 200 mg/kg of 3-HAA (Figure 23F).

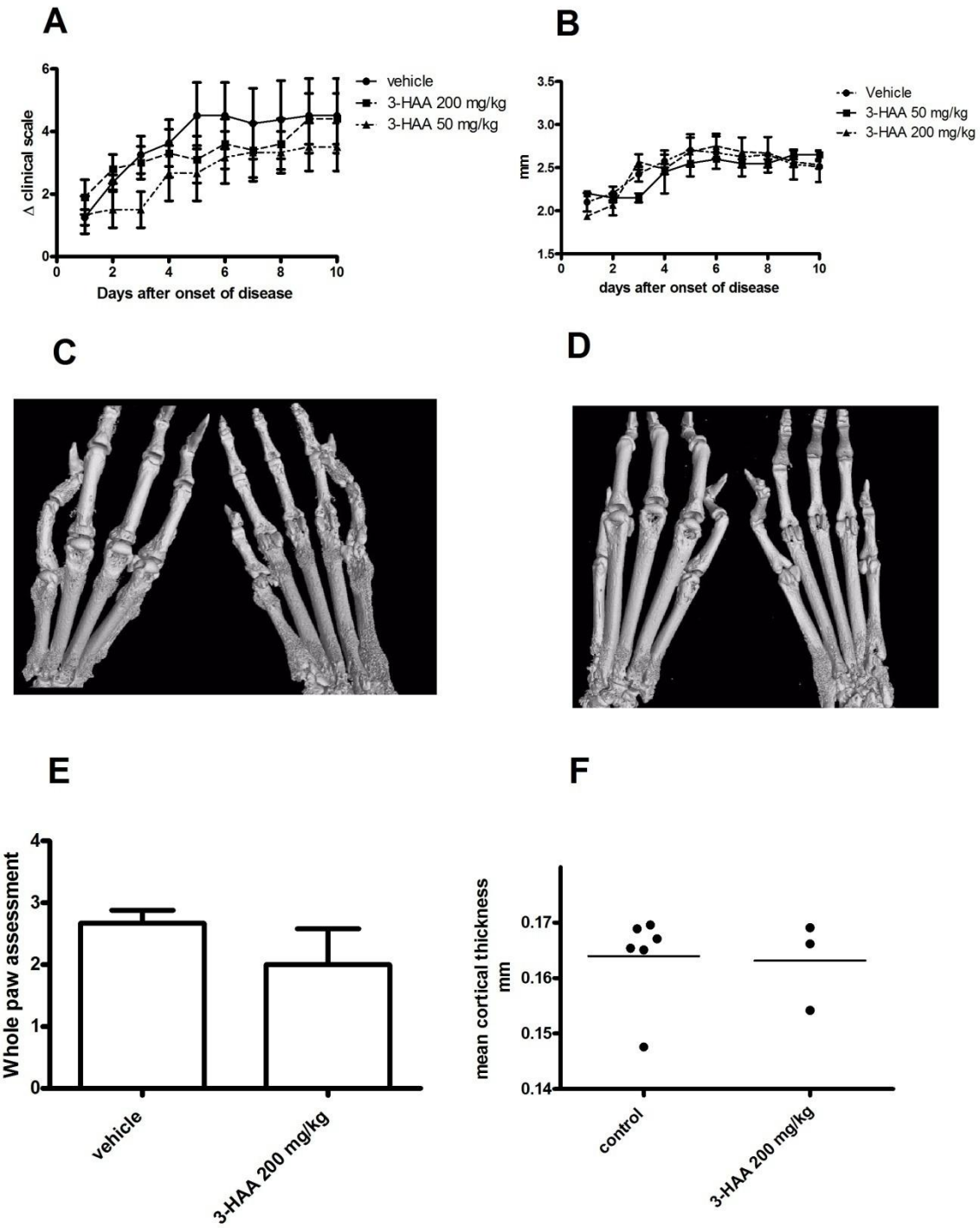


Figure 23 Treatment of mice with established CIA with 3-HAA was not effective

CIA was induced in DBA/1 mice and on the first day of arthritis animals were injected intraperitoneally with vehicle (n=5), 50 mg/kg of 3-HAA (n=5) or 200 mg/kg of 3-HAA (n=5). After 10 days animals were sacrificed and paws were taken for further analysis by μCT. **A)** Clinical scores. **B)** Paw swelling.

C) A representative micro-radiogram of the dorsal and plantar sites of the hind paw from a vehicle treated mouse. **D)** A representative plain micro-radiogram of the dorsal and plantar sites of the hind paw from a mouse treated with 200 mg/kg of 3-HAA. **E)** Bone pathology scores in the hind paws of mice treated with 3-HAA or vehicle alone. **F)** Mean cortical thickness in the 3rd metatarsal bone of 3-HAA treated and control mice.

Histological assessment was carried on the joints taken from the hind paws from mice treated with either with vehicle or 200 mg/kg of 3-HAA. Assessment of H&E stained sections revealed no significant differences between mice treated with 3-HAA or vehicle alone (Figure 24A). Similar results were observed when histological sections were stained with Safranin O and the severity of cartilage damage was assessed using the Mankin scale. Moreover, there were no statistically significant differences in cartilage damage in the joints from control mice and mice treated with 200 mg/kg at 3-HAA (Figure 24B). In order to confirm that the intraperitoneal injections of 3-HAA at a dose of 200 mg/kg for 10 subsequent days resulted in the increased concentrations of 3-HAA in serum, the concentration of 3-HAA was measured in the vehicle treated mice, those injected with 3-HAA, and in naive animals. The results revealed that treatment with 200 mg/kg of 3-HAA led to a trend towards an increased concentration of 3-HAA which however, did not reach the level of significance (Figure 24C).

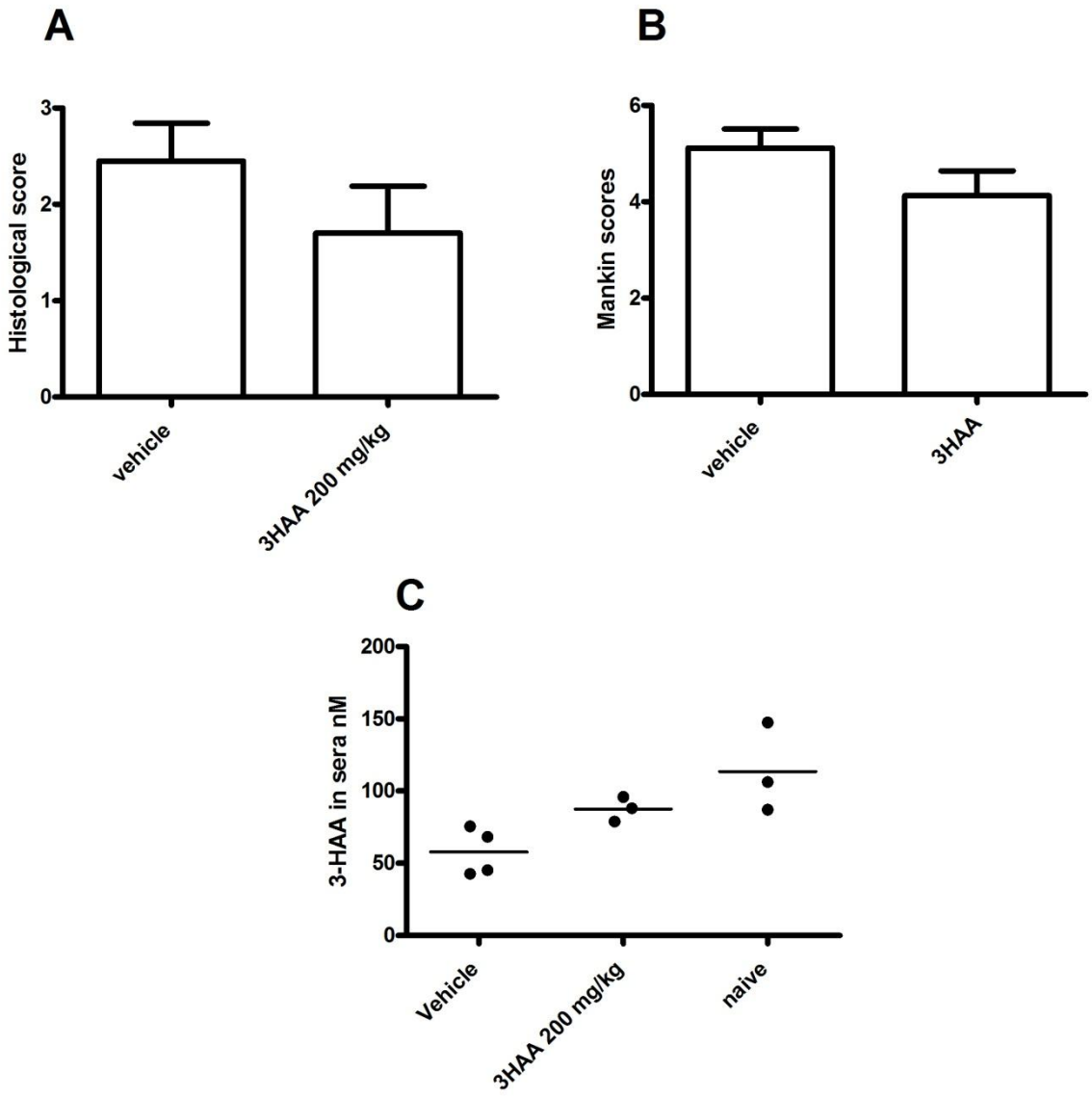


Figure 24 Treatment with 3-HAA did not reduce histological severity or prevent cartilage damage

CIA was induced in DBA/1 mice and treated with vehicle alone or 200 mg/kg of AA (n=5). After 10 days all animals were sacrificed and paws were taken for further analysis by histology. **A)** Histological severity. **B)** Assessment of cartilage according to the Mankin scale **C)** Serum levels of 3-HAA in treated and control mice and in naive mice.

In the next set of experiments, DBA/1 mice with CIA were injected intraperitoneally either with 50 mg/kg of AA or 200 mg/kg were injected for 10 days, starting on the first day of clinical arthritis. Progression of the disease was monitored by monitoring of clinical scores (Figure 25A) and the measurements of paw-swelling (Figure 25B). However, neither the treatment with AA reduced the severity of CIA. I have confirmed these findings by the assessment of the histological cross sections of inflamed joints taken from mice treated with 200 g/kg of AA. There was no significant difference in the histologicals score between AA treated and vehicle treated mice (Figure 25C). A similar result was obtained when histological sections were stained with Safranin O and the severity of cartilage damage was assessed using the Mankin scale (Figure 25D).

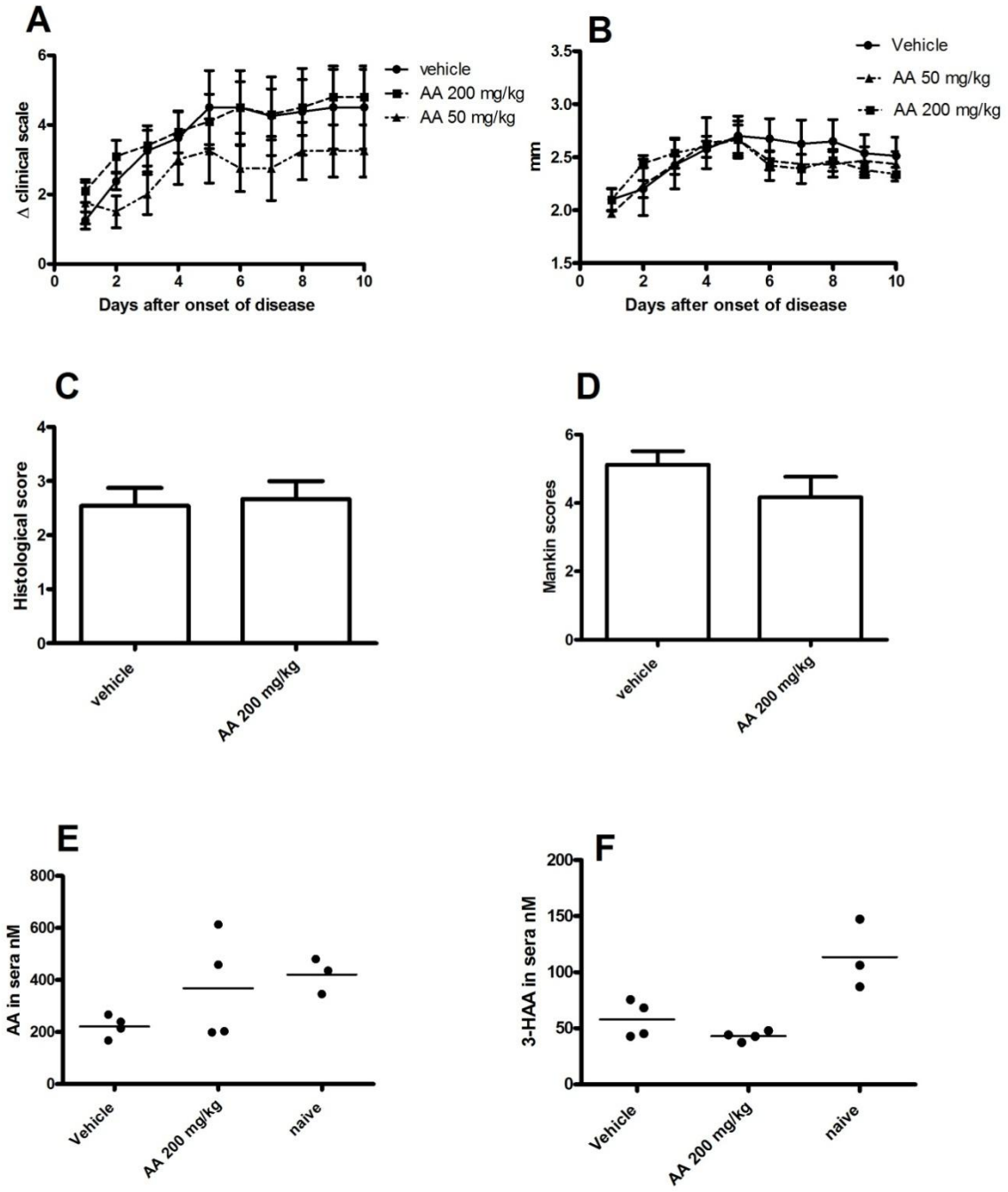


Figure 25 Treatment of established CIA with AA was not effective

CIA was induced in DBA/1 mice and treated from the first day of arthritis were treated with 200 mg/kg (n= 4) or 200 mg/kg of AA (n=4) or vehicle alone (n= 4). After 10 days all animals were sacrificed and paws were removed for further analysis by histology. Assessment of CIA using **A)** changes in the clinical scores. **B)** Paw swelling. **C)** Histological scores. **D)** Assessment of cartilage damage. **E)** Serum levels of AA in treated mice **F)** Serum levels of 3-HAA in mice treated with AA.

To confirm that intraperitoneal administration of AA at a dose of 200mg/kg resulted in the accumulation of AA in the sera from mice with CIA, the results were compared with previously presented data showing the concentration of AA in sera of naive mice and animals with established CIA. As it can be seen on the Figure 25C, treatment with 200 mg/kg of AA for 10 subsequent days did not significantly change the concentrations of AA in the sera. It is also known that AA may undergo spontaneous hydroxylation leading to the production of 3-HAA. Thus, it was of interest to measure the concentration of 3-HAA in mice treated with AA. However, the concentration of 3-HAA was not affected by the exogenous administration of AA (Figure 25D)

5.3. DISCUSSION

In RA, bone erosions are key pathological symptoms which develop early and progress with duration of the disease (Jansen et al. 2001; Visser et al. 2002). Recently, however, the use of μCT has revealed that small bone erosions can be also seen in the metacarpophalangeal (MCP) joints and wrists even in the healthy volunteers (Stach, Bauerle et al. 2010). Moreover, bone erosions bigger than 1.9 mm were found to be specific for RA (Stach et al. 2010). In addition, changes in bone surface like: osteophyte formation, cortical thickening, and fenestration were observed in patients with RA but not in the healthy volunteers (Stach et al. 2010). Therefore, bone pathology in RA can include a variety of defects. Using CIA as a model for RA and μCT, I have demonstrated a similar range bone defects in the hind paws from DBA/1 mice with arthritis. In these mice, bone erosions coexisted with new bone/osteophyte formation, rough bone texture, and propagation of crack-like structures. In fact, the formation of rough bone surface in CIA has been previously reported (Silva et al. 2006). However, it is not clear what drives this pathology and what are the consequences of the changes in the quality of the bone surface might be.

I also noticed an increased number of bone channels in the hind paws from mice with CIA. A similar observation was made previously when paws were analyzed by histology (Marinova-Mutafchieva et al. 2002). In this study, bone channels have been shown to be 2.5 times larger in mice with CIA than in naive animals. It has also been shown that in rats with CIA activated osteoclasts are localized in the bone channels even before onset of arthritis (Schett et al. 2005). Hence, osteoclast driven expansion of the bone channels may be responsible for bone fenestration observed in the patients with RA. However, it is difficult to precisely distinguish between bone erosions and bone channels. Thus, further studies are needed to clarify this issue. Nevertheless, the formation of new bone/osteophyte is a

pathological change shared between inflammatory arthritis, like RA, psoriatic arthritis, ankylosing spondylitis, and degenerative arthritis e.g. osteoarthritis (Finzel et al. 2011).

The treatment of CIA mice with etanercept, a TNF inhibitor, reduced the formation of bone erosions. The severity of the bone texture pathology was also reduced. This is in line with a previous observation showing that increased size of the bone channels was dependent on TNF-α (Marinova-Mutafchieva et al. 2002). I have also found that the treatment with etanercept reduced formation of the osteophytes. This is in contrast with a previous study showing that anti-TNF therapy did not prevent the formation of osteophytes in rats with CIA (Schett et al. 2009). However, it has been reported that DBA/1 mice can spontaneously develop osteophytes (Schuh et al. 2002) what may be due to chronic sub-clinical inflammation. Therefore, in this strain, inflammation may be a risk factor for new bone formation and anti-inflammatory treatment in the form of TNF blockade reduces the incidence of osteophyte formation.

In patients with RA, the formation of bone erosions was shown to correlate with disease duration. In contrast, changes in the bone surface have been shown to be related to the level of disease activity as measured by DAS28 score and the level of C-reactive protein (Stach et al. 2010). Thus, the standardized application of μCT in the monitoring of RA could improve our understanding of the bone pathology and help to monitor the effect of treatment. In fact, in the animal models of RA, application of μCT has been already well established (Barck et al. 2004; Bouxsein, et al. 2010).

In addition, I have shown that my novel scoring system of bone pathology in CIA was reproducible and positively correlated with the clinical severity of CIA. In fact, historically, similar approach was applied for scoring of the plain radiographs taken from patients with RA (Kellgren 1956; van der Heijde 1996). It has been also demonstrated that the pathology observed in histological sections of the paws of mice with CIA correlated with μCT results

(Silva et al. 2004; Silva et al. 2006; Seeuws et al. 2010).

In my experiments, the severity of bone pathology correlated negatively with the mean cortical thickness in the third metatarsal bone. In line with this observation, the reduction in bone pathology observed in animals treated with etanercept coexisted with the maintenance of the mean cortical thickness in the third metatarsal bone. This observation is in the agreement with previous findings showing decreased bone density (osteopenia) in the periarticular region of bones from patients with RA as well as mice with CIA (Barck et al. 2004). Hence, scoring of the movies showing skeleton of the inflamed hind paws supported by the measurement of the mean cortical thickness may provide useful parameters to assess the disease activity.

Observations showing the lack of therapeutic effect of 3-HAA in CIA could indicate that 3-HAA has no anti-arthritic properties. However, alternatively, it might have been that the dosing regimen (50 mg/kg/day or 200 mg/kg/day of 3-HAA) was insufficient to increase its concentration. This interpretation is strengthened by the observation that HAAO exhibits the highest enzymatic activity amongst enzymes on the kynurenine pathway. A similar explanation may also be true in the case of a lack of the therapeutic effect of the treatment with AA. As with 3-HAA, neither the 50 mg/kg nor the 200 mg/kg of AA was effective in CIA. Moreover, previous observations showing AA did not reduce proliferation of T cells or production of pro inflammatory cytokines *in vitro* (Terness et al. 2002; Bauer et al. 2005) indicate that AA is biologically inactive for immune cells at the doses tested so far. In this context, the therapeutic efficacy of the chemical derivative of AA which is tranilast, might be difficult to explain. The differences in the immunomodulatory properties of AA and tranilast *in vivo* could be due to differences in their half-life in the biological fluids e.g. serum. It has also been postulated that tranilast could exhibit its anti-inflammatory actions via the AhR receptor (Prud'homme et al. 2010) and/or reduce osteoclast differentiation in an Akt and

phospho-GSK3beta dependent manner (Sato et al. 2010). Alternatively, tranilast could serve as a source of potentially biologically active metabolites. For example, it has been shown that in humans tranilast is converted into a glucuronide and a phase I metabolite, 4-demethyltranilast (N-4) which can be further catabolised into the series of derivates e.g. N-2 [2-(4′-hydroxy-3′-methoxystyryl)-3,1-benzoxazin-4-one] and N-6 (1-benzoxazin-4-one) which are detected in urine (Katoh, Matsui et al. 2007). In line with this, it has been postulated that the formation of N-3 and N-4 derivates from tranilast is mediated by the enzyme, CYP2C9. In contrast, glucuronidation of tranilast is mainly mediated by UGT1A1 (Katoh et al. 2007). Interestingly, it has been shown the *Cyp2c9* gene exists in polymorphic alleles with *CYP2C9*2* and *CYP2C9*3* encoding the least enzymatically active form of CYP2C9 (Rokitta and Fuhr 2010). Thus, the pharmacokinetic and subsequent therapeutic effects of tranilast could depend on the genetic background of an individual patient.

In conclusion, in this chapter, I have shown that in DBA/1 mice with CIA bone pathology is manifested in various forms and can be scored in a semi-quantitative manner. I also showed that bone pathology scores correlated positively with the clinical severity and negatively with the mean cortical thickness of the 3rd metatarsal bone in the arthritic hind paw. In addition, I have demonstrated that bone pathology could be effectively prevented by the treatment with etanercept. In contrast, neither treatment with AA nor with 3-HAA was effective in reducing the severity of bone pathology. On this basis, I have concluded that these catabolites of kynurenine may have limited potential as anti-arthritic drugs although it would have been of interest, given further time and resources to investigate the pharmacologically active derivatives of these molecules.

Chapter 6

General discussion and future directions

Before I started this project, it was known that either genetic inactivation of *Ido1* or pharmacological inhibition of IDO1 and IDO2 resulted in the exacerbated symptoms of CIA (Criado et al. 2009). Conversely, administration of IDO-containing exosomes reduced severity of CIA (Bianco et al. 2009). In the line with these results, it has been also shown that mRNA expression for *Ido1* was specifically increased in the iLN but not in the spleens and inflamed paws taken from mice with CIA (Criado et al. 2009). In addition, the concentration of kynurenine was found to be reduced in sera from mice with CIA. In contrast, exogenous administration of kynurenine reduced severity of CIA (Criado et al. 2009). Thus, taken together, it was clear that catabolism of tryptophan and metabolism of kynurenine could modulate severity of CIA.

Therefore, I have studied tryptophan catabolism via the kynurenine pathway in two, well defined, stages of CIA: pre-arthritic stage of CIA and established phase of CIA. Results were compared with naive animals. Hence, such experimental regime did not only allow me to compare tryptophan catabolism between the diseased animals and naive mice but also tested if tryptophan catabolism could be different in the pre-arthritis stage of CIA from that one observed in the establish phase of the disease. It is well recognised that established phase of CIA is followed by self-induced resolution of inflammation (Williams 1995). Tryptophan catabolism via the kynurenine pathway is thought to exhibit an anti-inflammatory role. Hence, it was interesting and important to undertake the comparative study of tryptophan catabolism before inflammation results in the clinical symptoms and just before induction of self resolution.

Results showing changes in the mRNA expression in various organs during CIA are summerised in the table 19.

Table 19 Summary of results showing changes in the expression of mRNA for subsequent the genes on the kynurenine pathway in the several types of organs during CIA

Changes in the expression of mRNA was measured using qRT-PCR technology and ΔΔCt method. "+" indicates on the increased mRNA expression. In contrast, "-" implays dicreased mRNA expression. "=" means that mRNA expresion was not changed. Results were comapred with mRNA expression in the naive organs/tissues. ***** results were compared with pre-arthritic organs. In the paws mRNA expression was not detected.

Organs, tissue	mRNA	Pre-arthritic	Established CIA	Organs tissue	mRNA	Pre-arthritic	Established CIA
Liver	*Tdo2*	=	=	Kidneys	*Ido1*	=	=
	Ido2	-	-		*Ido2*	-	=
	Afm	-	-		*Afm*	=	=
	Kmo	=	=		*Kmo*	=	=
	Kynu	+	+		*Kynu*	-	=
	Haao	-	-		*Haao*	-	=
Spleen	*Ido1*	=	=	iLN	*Ido1*	+	+
	Ido2	=	=		*Ido2*	+	+
	Afm	=	=		*Afm*	+	+
	Kmo	=	=		*Kmo*	+	-*
	Kynu	=	=		*Kynu*	+	-*
	Haao	+	=		*Haao*	+	-*

The most important and interesting results coming from assessment of mRNA expression for the kynurenine pathway enzymes were found in iLN. I found that during the pre-arthritic stage of CIA, mRNA expression for the major genes on the kynurenine pathway: *Ido1*, *Ido2*, *Afm*, *Kmo*, *Kynu*, and *Haao* were increased in comparison with naive tissues. In contrast, in the established CIA, mRNA expression for genes involved only in catabolism of tryptophan and therefore, anabolism of kynurenine, (*Ido1*, *Ido2*, and *Afm*, respectively) was

increased. mRNA expression for other genes (*Kmo*, *Kynu*, and *Haao*) was normalised almost to the control level. Thus, based on these results and the theory of metabolic control analysis (see section 1.2.1), it could be predicted that the during pre-arthritic stage of CIA the flux through the kynurenine pathway might be shifted towards the final product of tryptophan catabolism via the kynurenine pathway, which is NAD. In contrast, during the establish CIA, the flux through this metabolic pathway could be abrogated resulting in the accumulation of kynurenine.

However, it is important to keep in mind that changes in mRNA expression for a gene, which encode an enzymes, do not necessarily directly translates into changes in the activity of the enzyme. Thus, to test if CIA could increase or decrease activity of enzymes on the kynurenine pathway the direct measurements of their activity would be needed.

Moreover, provided technical difficulties and time consuming procedures necessary to perform such analyses, I have decided to take more simplified approach. I have just measured the concentration of tryptophan and its catabolites, kynurenines, and interpreted results as a surrogate for the activity of enzymes on the kynurenine pathway. Findings are summerised on the figure 26.

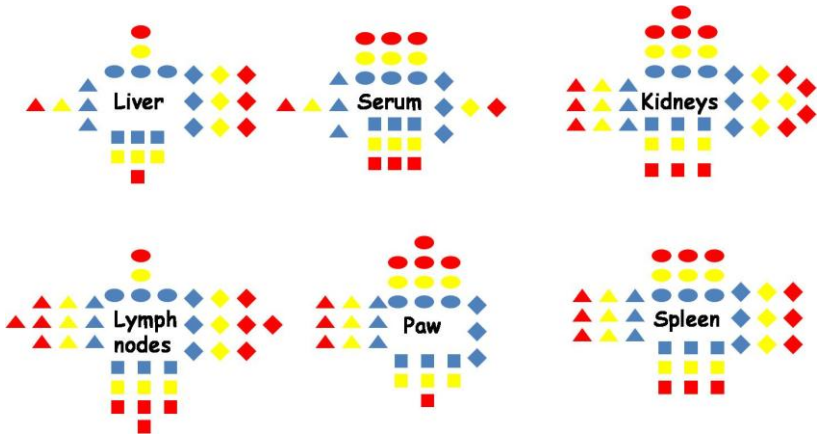


Figure 26 Summery of the experimental results showing changes in the concentration of tryptophan, kynurenine, and her metabolites in the various organs with CIA

The concentartion of tryptophan, AA, and 3-HAA was measured using HPLC whereas the concentartion of kynurenine was measured using a colorimetric method. In the blue colour the concentartion of a given molecule has been shown. The yellow colour has been used to show the concentartion of a given molecule in organs isolated from pre-arthrtitic mice. The red colour shows the concentartion of tryptophan and its catabolites via the kynurenine pathway in the organs taken from mice with established CIA. Ovals indicate on the concentartion of tryptophan. Triangles represents kynurenine. AA is shown as squares whereas diamonds stand for 3-HAA. The concentartion of a given molecule found in the inaive organs is shown as three and seperate figures (e.g. three ovals). The dicrease is shown as reduction in the number of elements (from three to one). In contrast, the increase is shown as an extra element on the figure (e.g. four ovals).

Interestingly, my original results showing increased expression of mRNA for the initial genes involved in the kynurenine pathway (*Ido1*, *Ido2*, and *Afm*, respectively) coincided with decreased concentration of tryptophan in pre-arthritic iLN and those isolated from mice with established CIA. Similarly, accumulation of kynurenine in iLN from mice with established CIA coincided with normalisation of mRNA expression for *Kynu* in comparison with pre-arthritic stage of CIA. In addition, I have also found that not only was kynurenine accumulated in iLN from mice with established CIA but also concentration of AA and 3-HAA was increased in iLN isolated from mice with this stage of the disease. This observation, similarly as expression for *Kynu* mRNA has also coincided with normalisation in mRNA expression for *Kmo* and *Haao* genes.

Results showing decreased concentration of tryptophan in iLN from pre-arthritic mice and those with established CIA suggest that tryptophan concentration on its own may not be an important factor involved in the resolution of inflammation. This is because, obviously, in the pre-arthritic mice, CIA progressed into the stage of established disease. However, in iLN from mice with established CIA, decreased concentration of tryptophan coincided with accumulation of kynurenines. Thus, my results supports a theory which states that anti-inflammatory action of the kynurenine pathway is fully manifested upon decreased tryptophan concentration and accumulation of kynurenines. However, to test if this theory is correct in the context of CIA inhibitors of KYNU should be injected into the pre-arthritic animals. If the establishment of CIA could be prevented by such treatment that would mean that both increased catabolism of tryptophan and decreased catabolism of kynurenine are involved in the resolution of inflammation. Similarly, administration of chemical activators of KYNU and HAAO into the mice with established CIA should result in the exacerbated disease. Nonetheless, these intellectual speculations need to be experimentally confirmed yet.

In this project, I have also confirmed previous results showing decreased concentration of kynurenine in sera taken from mice with CIA (Criado et.al. 2009) However, it was not know if CIA could induce changes in the concentration of tryptophan, AA, and 3-HAA. Thus, I have measured the concentration of tryptophan, AA, and 3-HAA in sera from the diseased mice. However, in the line with the existing literature, I found that tryptophan concentration was not changed in the sera from mice with CIA. However, I was able to demonstrated that during CIA 3-HAA was specifically accumulated in the kidneys. This observation coincided with the decreased concentration of 3-HAA in sera. Hence, it can be speculated that in CIA, 3-HAA might be extinguished in the kidneys more readily than in the naive animals. In fact, it has been previously shown that the urine from patients with RA contained increased concentration of 3-HAA (Spiera 1963; Labadarios, 1978).

The comparative measurements of tryptophan concentration together with kynurenines concentrations in the sera and other organs (e.g. liver, kidneys, and paws) taken from mice with CIA and those samples isolated from naive animals revealed that:

1) Serum may not be a good source of information about the concentration of tryptophan and kynurenines in the local tissue environment e.g. inflamed paws and lymph nodes.

2) In CIA, the concentartion of tryptophan and kynurenines in serum is likely to be regulated by the kidneys and the liver

3) In the naive and inflamed paws, catabolism of tryptophan via the kynurenine pathway might be of very limited physiological significance.

In addition to the biochemical and molecular investigation of the kynurenine pathway in the context of CIA, I have established a novel scoring system for the assessment of bone pathology in CIA using μCT and boneJ. Its novelty relies on the fact that I was able to

incorporate recently described additional pathological features of bone destruction (e.g. roughness of the bone surface and the increased size of the bone channels) together with bone erosions for the assessment of bone destruction in CIA. Therefore, I was able to fully test an anti-arthritic potential of 3-HAA and etanercept in the context of bone pathology.

In conclusion, experimental data presented in this thesis provide detailed picture of gene expression pattern for the kynurenine pathway enzymes in the several types of organs during CIA. In addition, I presented numerous of quantifiable data which may be useful if someone would like to use computational biology to draw an unifited theory of the kynurenine pathway action in CIA. In fact, I expect that in the future, projects like this one will be summarised with a research chapter dedicated to the computational model showing molecular and physiological interactions between organs and molecules *in vivo*.

Chapter 7

Bibliography

Adams, O., K. Besken, et al. (2004). "Role of indoleamine-2,3-dioxygenase in alpha/beta and gamma interferon-mediated antiviral effects against herpes simplex virus infections." J Virol **78** (5): 2632-2636.
Allegri, G., C. V. Costa, et al. (2003). "Enzyme activities of tryptophan metabolism along the kynurenine pathway in various species of animals." Farmaco **58** (9): 829-836.
Amori, L., P. Guidetti, et al. (2009). "On the relationship between the two branches of the kynurenine pathway in the rat brain in vivo." J Neurochem **109** (2): 316-325.
Andersson, S. E., A. Johansson, et al. (1998). "Physiological characterization of mBSA antigen induced arthritis in the rat. II. Joint blood flow, glucose metabolism, and cell proliferation." J Rheumatol **25** (9): 1778-1784.
Augat, P. and F. Eckstein (2008). "Quantitative imaging of musculoskeletal tissue." Annu Rev Biomed Eng **10**: 369-390.
Austin, C. J., B. M. Mailu, et al. (2010). "Biochemical characteristics and inhibitor selectivity of mouse indoleamine 2,3-dioxygenase-2." Amino Acids **39** (2): 565-578.
Aylward, M. (1975). "A review of possible mechanisms of action of the antirheumatic drug, alclofenac." Curr Med Res Opin **3** (5): 249-263.
Baban, B., P. Chandler, et al. (2004). "Indoleamine 2,3-dioxygenase expression is restricted to fetal trophoblast giant cells during murine gestation and is maternal genome specific." J Reprod Immunol **61** (2): 67-77.
Bagi, C. M., N. Hanson, et al. (2006). "The use of micro-CT to evaluate cortical bone geometry and strength in nude rats: correlation with mechanical testing, pQCT and DXA." Bone **38** (1): 136-144.
Ball, H. J., A. Sanchez-Perez, et al. (2007). "Characterization of an indoleamine 2,3-dioxygenase-like protein found in humans and mice." Gene **396** (1): 203-213.
Ball, H. J., H. J. Yuasa, et al. (2009). "Indoleamine 2,3-dioxygenase-2; a new enzyme in the kynurenine pathway." Int J Biochem Cell Biol **41** (3): 467-471.
Barck, K. H., W. P. Lee, et al. (2004). "Quantification of cortical bone loss and repair for therapeutic evaluation in collagen-induced arthritis, by micro-computed tomography and automated image analysis." Arthritis Rheum **50** (10): 3377-3386.
Barnardo, D. E., H. L. Currey, et al. (1966). "Mefenamic acid and flufenamic acid compared with aspirin and phenylbutazone in rheumatoid arthritis." Br Med J **2**(5509): 342-343.
Barth, M. C., N. Ahluwalia, et al. (2009). "Kynurenic acid triggers firm arrest of leukocytes to vascular endothelium under flow conditions." J Biol Chem **284** (29): 19189-19195.
Bauer, T. M., L. P. Jiga, et al. (2005). "Studying the immunosuppressive role of indoleamine 2,3-dioxygenase: tryptophan metabolites suppress rat allogeneic T-cell responses in vitro and in vivo." Transpl Int **18** (1): 95-100.
Beadle, G. W., H. K. Mitchell, et al. (1947). "Kynurenine as an Intermediate in the Formation of Nicotinic Acid from Tryptophane by Neurospora." Proc Natl Acad Sci U S A **33** (6): 155-158.
Belladonna, M. L., U. Grohmann, et al. (2006). "Kynurenine pathway enzymes in dendritic cells initiate tolerogenesis in the absence of functional IDO." J Immunol **177** (1): 130-137.
Belladonna, M. L., C. Volpi, et al. (2008). "Cutting edge: Autocrine TGF-beta sustains default tolerogenesis by IDO-competent dendritic cells." J Immunol **181** (8): 5194-5198.
Berry, L. J. and D. S. Smythe (1964). "Effects of Bacterial Endotoxins on Metabolism. Vii. Enzyme Induction and Cortisone Protection." J Exp Med **120**: 721-732.

Bianco, N. R., S. H. Kim, et al. (2009). "Therapeutic effect of exosomes from indoleamine 2,3-dioxygenase-positive dendritic cells in collagen-induced arthritis and delayed-type hypersensitivity disease models." Arthritis Rheum **60** (2): 380-389.

Bolon, B., M. Stolina, et al. (2011). "Rodent preclinical models for developing novel antiarthritic molecules: comparative biology and preferred methods for evaluating efficacy." J Biomed Biotechnol **2011**: 569068.

Bouxsein, M. L., S. K. Boyd, et al. (2010). "Guidelines for assessment of bone microstructure in rodents using micro-computed tomography." J Bone Miner Res **25** (7): 1468-1486.

Capece, L., M. Arrar, et al. (2010). "Substrate stereo-specificity in tryptophan dioxygenase and indoleamine 2,3-dioxygenase." Proteins **78** (14): 2961-2972.

Caulfield, J. P., A. Hein, et al. (1982). "Morphologic demonstration of two stages in the development of type II collagen-induced arthritis." Lab Invest **46** (3): 321-343.

Comai, S., C. V. Costa, et al. (2005). "The effect of age on the enzyme activities of tryptophan metabolism along the kynurenine pathway in rats." Clin Chim Acta **360** (1-2): 67-80.

Connor, T. J., N. Starr, et al. (2008). "Induction of indolamine 2,3-dioxygenase and kynurenine 3-monooxygenase in rat brain following a systemic inflammatory challenge: a role for IFN-gamma?" Neurosci Lett **441** (1): 29-34.

Criado, G., E. Simelyte, et al. (2009). "Indoleamine 2,3 dioxygenase-mediated tryptophan catabolism regulates accumulation of Th1/Th17 cells in the joint in collagen-induced arthritis." Arthritis Rheum **60** (5): 1342-1351.

Cunningham, V. J., L. Hay, et al. (1975). "The binding of L-tryptophan to serum albumins in the presence of non-esterified fatty acids." Biochem J **146** (3): 653-658.

de Jong, R. A., H. W. Nijman, et al. (2011). "Serum Tryptophan and Kynurenine Concentrations as Parameters for Indoleamine 2,3-Dioxygenase Activity in Patients With Endometrial, Ovarian, and Vulvar Cancer." Int J Gynecol Cancer.

del Amo, E. M., A. Urtti, et al. (2008). "Pharmacokinetic role of L-type amino acid transporters LAT1 and LAT2." Eur J Pharm Sci **35** (3): 161-174.

Desvignes, L. and J. D. Ernst (2009). "Interferon-gamma-responsive nonhematopoietic cells regulate the immune response to Mycobacterium tuberculosis." Immunity **31**(6): 974-985.

Dick, R., B. P. Murray, et al. (2001). "Structure--function relationships of rat hepatic tryptophan 2,3-dioxygenase: identification of the putative heme-ligating histidine residues." Arch Biochem Biophys **392** (1): 71-78.

Dobrovolsky, V. N., J. F. Bowyer, et al. (2005). "Effect of arylformamidase (kynurenine formamidase) gene inactivation in mice on enzymatic activity, kynurenine pathway metabolites and phenotype." Biochim Biophys Acta **1724** (1-2): 163-172.

Dobrovolsky, V. N., T. Bucci, et al. (2003). "Mice deficient for cytosolic thymidine kinase gene develop fatal kidney disease." Mol Genet Metab **78** (1): 1-10.

Doube, M., M. M. Klosowski, et al. (2010). "BoneJ: Free and extensible bone image analysis in ImageJ." Bone **47** (6): 1076-1079.

Dumonde, D. C. and L. E. Glynn (1962). "The production of arthritis in rabbits by an immunological reaction to fibrin." Br J Exp Pathol **43**: 373-383.

Durie, F. H., R. A. Fava, et al. (1993). "Prevention of collagen-induced arthritis with an antibody to gp39, the ligand for CD40." Science **261** (5126): 1328-1330.

Durie, F. H., R. A. Fava, et al. (1994). "Collagen-induced arthritis as a model of rheumatoid arthritis." Clin Immunol Immunopathol **73** (1): 11-18.

Emmons, J., W. H. Townley-Tilson, et al. (2008). "Identification of TTP mRNA targets in human dendritic cells reveals TTP as a critical regulator of dendritic cell maturation." RNA **14** (5): 888-902.

Espey, M. G., J. R. Moffett, et al. (1995). "Temporal and spatial changes of quinolinic acid immunoreactivity in the immune system of lipopolysaccharide-stimulated mice." J Leukoc Biol **57** (2): 199-206.
Fallarino, F., U. Grohmann, et al. (2002). "T cell apoptosis by tryptophan catabolism." Cell Death Differ **9** (10): 1069-1077.
Fallarino, F., U. Grohmann, et al. (2006). "The combined effects of tryptophan starvation and tryptophan catabolites down-regulate T cell receptor zeta-chain and induce a regulatory phenotype in naive T cells." J Immunol **176** (11): 6752-6761.
Fallarino, F., C. Volpi, et al. (2009). "IDO mediates TLR9-driven protection from experimental autoimmune diabetes." J Immunol **183** (10): 6303-6312.
Finzel, S., M. Englbrecht, et al. (2011). "A comparative study of periarticular bone lesions in rheumatoid arthritis and psoriatic arthritis." Ann Rheum Dis **70** (1): 122-127.
Finzel, S., S. Ohrndorf, et al. (2011). "A detailed comparative study of high-resolution ultrasound and micro-computed tomography for detection of arthritic bone erosions." Arthritis Rheum **63** (5): 1231-1236.
Finzel, S., J. Rech, et al. (2011). "Repair of bone erosions in rheumatoid arthritis treated with tumour necrosis factor inhibitors is based on bone apposition at the base of the erosion." Ann Rheum Dis **70** (9): 1587-1593.
Forrest, C. M., G. M. Mackay, et al. (2010). "Blood levels of kynurenines, interleukin-23 and soluble human leucocyte antigen-G at different stages of Huntington's disease." J Neurochem **112** (1): 112-122.
Fouque-Aubert, A., R. Chapurlat, et al. (2010). "A comparative review of the different techniques to assess hand bone damage in rheumatoid arthritis." Joint Bone Spine **77** (3): 212-217.
Frumento, G., R. Rotondo, et al. (2002). "Tryptophan-derived catabolites are responsible for inhibition of T and natural killer cell proliferation induced by indoleamine 2,3-dioxygenase." J Exp Med **196** (4): 459-468.
Fuchs, D., A. A. Moller, et al. (1991). "Increased endogenous interferon-gamma and neopterin correlate with increased degradation of tryptophan in human immunodeficiency virus type 1 infection." Immunol Lett **28** (3): 207-211.
Furset, G., Y. Floisand, et al. (2008). "Impaired expression of indoleamine 2, 3-dioxygenase in monocyte-derived dendritic cells in response to Toll-like receptor-7/8 ligands." Immunology **123** (2): 263-271.
Garrod, A. E. (1888). "A Contribution to the Theory of the Nervous Origin of Rheumatoid Arthritis." Med Chir Trans **71**: 89-105.
Gondo, A., N. Saeki, et al. (1985). "[Efficacy of tranilast administration and specific hyposensitization therapy of atopic dermatitis]." Arerugi **34** (5): 310-319.
Greene, E. R., S. Huang, et al. (2011). "Regulation of inflammation in cancer by eicosanoids." Prostaglandins Other Lipid Mediat.
Grohmann, U. and V. Bronte (2010). "Control of immune response by amino acid metabolism." Immunol Rev **236**: 243-264.
Gupta, N. K., A. I. Thaker, et al. (2011). "Serum analysis of tryptophan catabolism pathway: Correlation with Crohn's disease activity." Inflamm Bowel Dis.
Hankes, L. V. and L. M. Henderson (1957). "The metabolism of carboxyl-labeled 3-hydroxyanthranilic acid in the rat." J Biol Chem **225** (1): 349-354.
Hara, T., F. Yamakura, et al. (2008). "Diazotization of kynurenine by acidified nitrite secreted from indoleamine 2,3-dioxygenase-expressing myeloid dendritic cells." J Immunol Methods **332** (1-2): 162-169.
Harrington, L., C. V. Srikanth, et al. (2008). "Deficiency of indoleamine 2,3-dioxygenase enhances commensal-induced antibody responses and protects against Citrobacter rodentium-induced colitis." Infect Immun **76** (7): 3045-3053.

Hayaishi, O., F. Hirata, et al. (1975). "Indoleamine 2,3-dioxygenase. Note II. Biological function." Acta Vitaminol Enzymol **29** (1-6): 291-293.
Hayashi, T., J. H. Mo, et al. (2007). "3-Hydroxyanthranilic acid inhibits PDK1 activation and suppresses experimental asthma by inducing T cell apoptosis." Proc Natl Acad Sci U S A **104** (47): 18619-18624.
Henderson, B., T. Hardingham, et al. (1993). "Experimental arthritis models in the study of the mechanisms of articular cartilage loss in rheumatoid arthritis." Agents Actions Suppl **39**: 15-26.
Heyes, M. P., C. Y. Chen, et al. (1997). "Different kynurenine pathway enzymes limit quinolinic acid formation by various human cell types." Biochem J **326 (Pt 2)**: 351-356.
Heyliger, S. O., E. A. Mazzio, et al. (1999). "The anti-inflammatory effects of quinolinic acid in the rat." Life Sci **64** (14): 1177-1187.
Holmdahl, R., M. E. Andersson, et al. (1989). "Collagen induced arthritis as an experimental model for rheumatoid arthritis. Immunogenetics, pathogenesis and autoimmunity." APMIS **97** (7): 575-584.
Holmdahl, R., L. Jansson, et al. (1988). "Immunogenetics of type II collagen autoimmunity and susceptibility to collagen arthritis." Immunology **65** (2): 305-310.
Holmdahl, R., R. Jonsson, et al. (1988). "Early appearance of activated CD4+ T lymphocytes and class II antigen-expressing cells in joints of DBA/1 mice immunized with type II collagen." Lab Invest **58** (1): 53-60.
Holmdahl, R., J. C. Lorentzen, et al. (2001). "Arthritis induced in rats with nonimmunogenic adjuvants as models for rheumatoid arthritis." Immunol Rev **184**: 184-202.
Holmdahl, R., J. Mo, et al. (1989). "Collagen induced arthritis: an experimental model for rheumatoid arthritis with involvement of both DTH and immune complex mediated mechanisms." Clin Exp Rheumatol **7 Suppl 3**: S51-55.
Huang, Y. W., R. A. Jansen, et al. (2009). "Identification of candidate epigenetic biomarkers for ovarian cancer detection." Oncol Rep **22** (4): 853-861.
Huang, Y. W., J. Luo, et al. (2010). "Promoter hypermethylation of CIDEA, HAAO and RXFP3 associated with microsatellite instability in endometrial carcinomas." Gynecol Oncol **117** (2): 239-247.
Iagnocco, A., F. Ceccarelli, et al. (2011). "The role of ultrasound in rheumatology." Semin Ultrasound CT MR **32** (2): 66-73.
Inglis, J. J., G. Criado, et al. (2007). "The anti-allergic drug, N-(3',4'-dimethoxycinnamonyl) anthranilic acid, exhibits potent anti-inflammatory and analgesic properties in arthritis." Rheumatology (Oxford) **46** (9): 1428-1432.
Inglis, J. J., G. Criado, et al. (2007). "Collagen-induced arthritis in C57BL/6 mice is associated with a robust and sustained T-cell response to type II collagen." Arthritis Res Ther **9**(5): R113.
Inglis, J. J., E. Simelyte, et al. (2008). "Protocol for the induction of arthritis in C57BL/6 mice." Nat Protoc **3** (4): 612-618.
Ishiguro, I., J. Naito, et al. (1993). "Skin L-tryptophan-2,3-dioxygenase and rat hair growth." FEBS Lett **329** (1-2): 178-182.
Iwagaki, H., A. Hizuta, et al. (1995). "Decreased serum tryptophan in patients with cancer cachexia correlates with increased serum neopterin." Immunol Invest **24** (3): 467-478.
Jakoby, W. B. (1954). "Kynurenine formamidase from Neurospora." J Biol Chem **207** (2): 657-663.
Janossy, G., G. Panayi, et al. (1981). "Rheumatoid arthritis: a disease of T-lymphocyte/macrophage immunoregulation." Lancet **2** (8251): 839-842.

Jansen, L. M., I. E. van der Horst-Bruinsma, et al. (2001). "Predictors of radiographic joint damage in patients with early rheumatoid arthritis." Ann Rheum Dis **60** (10): 924-927.
Jiang, G. M., Y. W. He, et al. (2010). "Sodium butyrate down-regulation of indoleamine 2, 3-dioxygenase at the transcriptional and post-transcriptional levels." Int J Biochem Cell Biol **42** (11): 1840-1846.
Junt, T., E. Scandella, et al. (2008). "Form follows function: lymphoid tissue microarchitecture in antimicrobial immune defence." Nat Rev Immunol **8**(10): 764-775.
Kaklamanis, P. M. (1992). "Experimental animal models resembling rheumatoid arthritis." Clin Rheumatol **11** (1): 41-47.
Kanai, M., H. Funakoshi, et al. (2009). "Tryptophan 2,3-dioxygenase is a key modulator of physiological neurogenesis and anxiety-related behavior in mice." Mol Brain **2** (1): 8.
Kaper, T., L. L. Looger, et al. (2007). "Nanosensor detection of an immunoregulatory tryptophan influx/kynurenine efflux cycle." PLoS Biol **5** (10): e257.
Katoh, M., T. Matsui, et al. (2007). "Glucuronidation of antiallergic drug, Tranilast: identification of human UDP-glucuronosyltransferase isoforms and effect of its phase I metabolite." Drug Metab Dispos **35** (4): 583-589.
Kellgren, J. H. (1956). "Radiological signs of rheumatoid arthritis; a study of observer differences in the reading of hand films." Ann Rheum Dis **15** (1): 55-60.
Kincses, Z. T., J. Toldi, et al. (2010). "Kynurenines, neurodegeneration and Alzheimer's disease." J Cell Mol Med **14** (8): 2045-2054.
Knox, W. E. and A. H. Mehler (1950). "The conversion of tryptophan to kynurenine in liver. I. The coupled tryptophan peroxidase-oxidase system forming formylkynurenine." J Biol Chem **187** (1): 419-430.
Kolodziej, L. R., E. M. Paleolog, et al. (2010). "Kynurenine metabolism in health and disease." Amino Acids.
Konneh, M. (1998). "Tranilast Kissei Pharmaceutical." IDrugs **1** (1): 141-146.
Kunitomo, M., Y. Tanaka, et al. (1989). "Enhancing activity of anthranilic acid on adjuvant arthritis in rats and antibody formation in mice." Jpn J Pharmacol **50** (4): 507-510.
Kurz, K., M. Herold, et al. (2011). "Effects of adalimumab therapy on disease activity and interferon-gamma-mediated biochemical pathways in patients with rheumatoid arthritis." Autoimmunity **44** (3): 235-242.
Landre-Beauvais, A. J. (2001). "The first description of rheumatoid arthritis. Unabridged text of the doctoral dissertation presented in 1800." Joint Bone Spine **68**(2): 130-143.
Laperre, K., M. Depypere, et al. (2011). "Development of micro-CT protocols for in vivo follow-up of mouse bone architecture without major radiation side effects." Bone.
Leblhuber, F., J. Walli, et al. (1998). "Activated immune system in patients with Huntington's disease." Clin Chem Lab Med **36** (10): 747-750.
Lee, S. M., Y. S. Lee, et al. (2010). "Tryptophan metabolite 3-hydroxyanthranilic acid selectively induces activated T cell death via intracellular GSH depletion." Immunol Lett **132** (1-2): 53-60.
Liu, L. and E. F. Morgan (2007). "Accuracy and precision of digital volume correlation in quantifying displacements and strains in trabecular bone." J Biomech **40** (15): 3516-3520.
Liu, X. S., X. H. Zhang, et al. (2010). "High-resolution peripheral quantitative computed tomography can assess microstructural and mechanical properties of human distal tibial bone." J Bone Miner Res **25** (4): 746-756.

Luthman, J. (2000). "Anticonvulsant effects of the 3-hydroxyanthranilic acid dioxygenase inhibitor NCR-631." Amino Acids **19** (1): 325-334.
Luthman, J., A. C. Radesater, et al. (1998). "Effects of the 3-hydroxyanthranilic acid analogue NCR-631 on anoxia-, IL-1 beta- and LPS-induced hippocampal pyramidal cell loss in vitro." Amino Acids **14** (1-3): 263-269.
M, D. (2010). BoneJ.
MacNeil, J. A. and S. K. Boyd (2007). "Accuracy of high-resolution peripheral quantitative computed tomography for measurement of bone quality." Med Eng Phys **29** (10): 1096-1105.
Mankin, H. J., H. Dorfman, et al. (1971). "Biochemical and metabolic abnormalities in articular cartilage from osteo-arthritic human hips. II. Correlation of morphology with biochemical and metabolic data." J Bone Joint Surg Am **53** (3): 523-537.
Marechal, M., F. Luyten, et al. (2005). "Histomorphometry and micro-computed tomography of bone augmentation under a titanium membrane." Clin Oral Implants Res **16** (6): 708-714.
Marinova-Mutafchieva, L., R. O. Williams, et al. (2002). "Inflammation is preceded by tumor necrosis factor-dependent infiltration of mesenchymal cells in experimental arthritis." Arthritis Rheum **46** (2): 507-513.
Mc, M. R. and J. L. Oncley (1958). "The specific binding of L-tryptophan to serum albumin." J Biol Chem **233** (6): 1436-1447.
McIlroy, D., S. Tanguy-Royer, et al. (2005). "Profiling dendritic cell maturation with dedicated microarrays." J Leukoc Biol **78** (3): 794-803.
McMenamy, R. H. (1965). "Binding of indole analogues to human serum albumin. Effects of fatty acids." J Biol Chem **240** (11): 4235-4243.
Metz, R., J. B. Duhadaway, et al. (2007). "Novel tryptophan catabolic enzyme IDO2 is the preferred biochemical target of the antitumor indoleamine 2,3-dioxygenase inhibitory compound D-1-methyl-tryptophan." Cancer Res **67** (15): 7082-7087.
Mikecz, K., T. T. Glant, et al. (1987). "Immunity to cartilage proteoglycans in BALB/c mice with progressive polyarthritis and ankylosing spondylitis induced by injection of human cartilage proteoglycan." Arthritis Rheum **30** (3): 306-318.
Moffett, J. R., K. L. Blinder, et al. (1998). "Differential effects of kynurenine and tryptophan treatment on quinolinate immunoreactivity in rat lymphoid and non-lymphoid organs." Cell Tissue Res **293** (3): 525-534.
Moffett, J. R. and M. A. Namboodiri (2003). "Tryptophan and the immune response." Immunol Cell Biol **81** (4): 247-265.
Morgan, K., R. B. Clague, et al. (1987). "Incidence of antibodies to native and denatured cartilage collagens (types II, IX, and XI) and to type I collagen in rheumatoid arthritis." Ann Rheum Dis **46** (12): 902-907.
Morita, T., K. Saito, et al. (2001). "3-Hydroxyanthranilic acid, an L-tryptophan metabolite, induces apoptosis in monocyte-derived cells stimulated by interferon-gamma." Ann Clin Biochem **38** (Pt 3): 242-251.
Muller, A., K. Heseler, et al. (2009). "The missing link between indoleamine 2,3-dioxygenase mediated antibacterial and immunoregulatory effects." J Cell Mol Med **13** (6): 1125-1135.
Muller, R. (2009). "Hierarchical microimaging of bone structure and function." Nat Rev Rheumatol **5** (7): 373-381.
Munn, D. H., E. Shafizadeh, et al. (1999). "Inhibition of T cell proliferation by macrophage tryptophan catabolism." J Exp Med **189** (9): 1363-1372.
Munn, D. H., M. D. Sharma, et al. (2005). "GCN2 kinase in T cells mediates proliferative arrest and anergy induction in response to indoleamine 2,3-dioxygenase." Immunity **22** (5): 633-642.

Myint, A. M., Y. K. Kim, et al. (2007). "Kynurenine pathway in major depression: evidence of impaired neuroprotection." J Affect Disord **98** (1-2): 143-151.
Nakamura, T., S. Niimi, et al. (1987). "Multihormonal regulation of transcription of the tryptophan 2,3-dioxygenase gene in primary cultures of adult rat hepatocytes with special reference to the presence of a transcriptional protein mediating the action of glucocorticoids." J Biol Chem **262** (2): 727-733.
Nakamura, T., H. Shinno, et al. (1980). "Insulin and glucagon as a new regulator system for tryptophan oxygenase activity demonstrated in primary cultured rat hepatocytes." J Biol Chem **255** (16): 7533-7535.
Nelson, D. L. (2008). Lehninger Principles of Biochemistry: Chapter 15 (pages 569 - 582).
Nelson, D. L. (2008). Lehninger Principles of Biochemistry New York, W.H. Freeman and company Chapter 5 (pages 163-165).
Nelson, D. L. (2008). Lehninger principles of biochemistry: Chapter 28 (pages 1137-1146).
Nemeth, H., J. Toldi, et al. (2005). "Role of kynurenines in the central and peripheral nervous systems." Curr Neurovasc Res **2** (3): 249-260.
Nishimoto, Y., F. Takeuchi, et al. (1979). "Purification of L-kynurenine 3-hydroxylase by affinity chromatography." J Chromatogr **169**: 357-364.
O'Connor, J. C., M. A. Lawson, et al. (2009). "Induction of IDO by bacille Calmette-Guerin is responsible for development of murine depressive-like behavior." J Immunol **182**(5): 3202-3212.
Ohira, K., H. Hagihara, et al. (2010). "Expression of tryptophan 2,3-dioxygenase in mature granule cells of the adult mouse dentate gyrus." Mol Brain **3**(1): 26.
Okuda, S., N. Nishiyama, et al. (1996). "Hydrogen peroxide-mediated neuronal cell death induced by an endogenous neurotoxin, 3-hydroxykynurenine." Proc Natl Acad Sci U S A **93**(22): 12553-12558.
Okuda, S., N. Nishiyama, et al. (1998). "3-Hydroxykynurenine, an endogenous oxidative stress generator, causes neuronal cell death with apoptotic features and region selectivity." J Neurochem **70**(1): 299-307.
Onodera, T., M. H. Jang, et al. (2009). "Constitutive expression of IDO by dendritic cells of mesenteric lymph nodes: functional involvement of the CTLA-4/B7 and CCL22/CCR4 interactions." J Immunol **183** (9): 5608-5614.
Orabona, C., M. T. Pallotta, et al. (2008). "SOCS3 drives proteasomal degradation of indoleamine 2,3-dioxygenase (IDO) and antagonizes IDO-dependent tolerogenesis." Proc Natl Acad Sci U S A **105** (52): 20828-20833.
Orphanides, G. and D. Reinberg (2002). "A unified theory of gene expression." Cell **108** (4): 439-451.
Ostergaard, M., M. Stoltenberg, et al. (1997). "Magnetic resonance imaging-determined synovial membrane and joint effusion volumes in rheumatoid arthritis and osteoarthritis: comparison with the macroscopic and microscopic appearance of the synovium." Arthritis Rheum **40** (10): 1856-1867.
Pallotta, M. T., C. Orabona, et al. (2011). "Indoleamine 2,3-dioxygenase is a signaling protein in long-term tolerance by dendritic cells." Nat Immunol **12**(9): 870-878.
Pellegrin, K., G. Neurauter, et al. (2005). "Enhanced enzymatic degradation of tryptophan by indoleamine 2,3-dioxygenase contributes to the tryptophan-deficient state seen after major trauma." Shock **23** (3): 209-215.
Perkins, M. N. and T. W. Stone (1982). "An iontophoretic investigation of the actions of convulsant kynurenines and their interaction with the endogenous excitant quinolinic acid." Brain Res **247** (1): 184-187.
Platten, M., P. P. Ho, et al. (2005). "Treatment of autoimmune neuroinflammation with a synthetic tryptophan metabolite." Science **310** (5749): 850-855.

Prendergast, G. C. (2008). "Immune escape as a fundamental trait of cancer: focus on IDO." Oncogene **27** (28): 3889-3900.
Pritzker, K. P., S. Gay, et al. (2006). "Osteoarthritis cartilage histopathology: grading and staging." Osteoarthritis Cartilage **14** (1): 13-29.
Prud'homme, G. J., Y. Glinka, et al. (2010). "Breast cancer stem-like cells are inhibited by a non-toxic aryl hydrocarbon receptor agonist." PLoS One **5** (11): e13831.
Qiu, H., M. T. Garcia-Barrio, et al. (1998). "Dimerization by translation initiation factor 2 kinase GCN2 is mediated by interactions in the C-terminal ribosome-binding region and the protein kinase domain." Mol Cell Biol **18** (5): 2697-2711.
Ritman, E. L. (2011). "Current status of developments and applications of micro-CT." Annu Rev Biomed Eng **13**: 531-552.
Robinson, C. M., P. T. Hale, et al. (2005). "The role of IFN-gamma and TNF-alpha-responsive regulatory elements in the synergistic induction of indoleamine dioxygenase." J Interferon Cytokine Res **25** (1): 20-30.
Roivainen, A., R. Parkkola, et al. (2003). "Use of positron emission tomography with methyl-11C-choline and 2-18F-fluoro-2-deoxy-D-glucose in comparison with magnetic resonance imaging for the assessment of inflammatory proliferation of synovium." Arthritis Rheum **48** (11): 3077-3084.
Rokitta, D. and U. Fuhr (2010). "Comparison of enzyme kinetic parameters obtained in vitro for reactions mediated by human CYP2C enzymes including major CYP2C9 variants." Curr Drug Metab **11** (2): 153-161.
Russo, S., I. P. Kema, et al. (2003). "Tryptophan as a link between psychopathology and somatic states." Psychosom Med **65** (4): 665-671.
Sadler, E. M., M. Weiner, et al. (1984). "Activation of liver tryptophan oxygenase by hydrocortisone, hematin and tryptophan in streptozotocin-diabetic rats." Life Sci **34**(14): 1365-1370.
Sainio, E. L. and P. Sainio (1990). "Comparison of effects of nicotinic acid or tryptophan on tryptophan 2,3-dioxygenase in acute and chronic studies." Toxicol Appl Pharmacol **102** (2): 251-258.
Saito, K., J. S. Crowley, et al. (1993). "A mechanism for increased quinolinic acid formation following acute systemic immune stimulation." J Biol Chem **268** (21): 15496-15503.
Salter, M., R. G. Knowles, et al. (1986). "Quantification of the importance of individual steps in the control of aromatic amino acid metabolism." Biochem J **234** (3): 635-647.
Samelson-Jones, B. J. and S. R. Yeh (2006). "Interactions between nitric oxide and indoleamine 2,3-dioxygenase." Biochemistry **45** (28): 8527-8538.
Sato, S., S. Takahashi, et al. (2010). "Tranilast suppresses prostate cancer growth and osteoclast differentiation in vivo and in vitro." Prostate **70** (3): 229-238.
Schett, G., M. Stolina, et al. (2005). "Analysis of the kinetics of osteoclastogenesis in arthritic rats." Arthritis Rheum **52** (10): 3192-3201.
Schett, G., M. Stolina, et al. (2009). "Tumor necrosis factor alpha and RANKL blockade cannot halt bony spur formation in experimental inflammatory arthritis." Arthritis Rheum **60** (9): 2644-2654.
Schrocksnadel, K., B. Wirleitner, et al. (2006). "Monitoring tryptophan metabolism in chronic immune activation." Clin Chim Acta **364** (1-2): 82-90.
Schroecksnadel, K., S. Kaser, et al. (2003). "Increased degradation of tryptophan in blood of patients with rheumatoid arthritis." J Rheumatol **30** (9): 1935-1939.
Schuettengruber, B., A. Doetzlhofer, et al. (2003). "Alternate activation of two divergently transcribed mouse genes from a bidirectional promoter is linked to changes in histone modification." J Biol Chem **278** (3): 1784-1793.

Schuh, J. C., R. Hall, et al. (2002). "Periosteal hyperostosis (exostosis) in DBA/1 male mice." Toxicol Pathol **30** (3): 390-393.
Schutz, G., L. Killewich, et al. (1975). "Control of the mRNA for hepatic tryptophan oxygenase during hormonal and substrate induction." Proc Natl Acad Sci U S A **72** (3): 1017-1020.
Schwarcz, R. and R. Pellicciari (2002). "Manipulation of brain kynurenines: glial targets, neuronal effects, and clinical opportunities." J Pharmacol Exp Ther **303** (1): 1-10.
Seeuws, S., P. Jacques, et al. (2010). "A multiparameter approach to monitor disease activity in collagen-induced arthritis." Arthritis Res Ther **12**(4): R160.
Shigeki, S., T. Murakami, et al. (1997). "Treatment of keloid and hypertrophic scars by iontophoretic transdermal delivery of tranilast." Scand J Plast Reconstr Surg Hand Surg **31** (2): 151-158.
Shimizu, T., S. Nomiyama, et al. (1978). "Indoleamine 2,3-dioxygenase. Purification and some properties." J Biol Chem **253** (13): 4700-4706.
Silva, M. D., J. Ruan, et al. (2006). "Application of surface roughness analysis on micro-computed tomographic images of bone erosion: examples using a rodent model of rheumatoid arthritis." Mol Imaging **5** (4): 475-484.
Silva, M. D., A. Savinainen, et al. (2004). "Quantitative analysis of micro-CT imaging and histopathological signatures of experimental arthritis in rats." Mol Imaging **3** (4): 312-318.
Smith, S. A. and C. I. Pogson (1980). "The metabolism of L-tryptophan by isolated rat liver cells. Effect of albumin binding and amino acid competition on oxidatin of tryptophan by tryptophan 2,3-dioxygenase." Biochem J **186** (3): 977-986.
Smolen, J. S. and D. Aletaha (2011). "Monitoring rheumatoid arthritis." Curr Opin Rheumatol **23** (3): 252-258.
Smolen, J. S., R. Landewe, et al. (2010). "EULAR recommendations for the management of rheumatoid arthritis with synthetic and biological disease-modifying antirheumatic drugs." Ann Rheum Dis **69** (6): 964-975.
Smolen, J. S. and G. Steiner (2003). "Therapeutic strategies for rheumatoid arthritis." Nat Rev Drug Discov **2** (6): 473-488.
Speciale, C., K. Hares, et al. (1989). "High-affinity uptake of L-kynurenine by a Na+-independent transporter of neutral amino acids in astrocytes." J Neurosci **9** (6): 2066-2072.
Spiera, H. (1963). "Excretion of a Tryptophan Metabolite in Rheumatoid Arthritis." Arthritis Rheum **6**: 364-371.
Stach, C. M., M. Bauerle, et al. (2010). "Periarticular bone structure in rheumatoid arthritis patients and healthy individuals assessed by high-resolution computed tomography." Arthritis Rheum **62** (2): 330-339.
Staines, N. A. and P. H. Wooley (1994). "Collagen arthritis--what can it teach us?" Br J Rheumatol **33** (9): 798-807.
Stone, T. W. and L. G. Darlington (2002). "Endogenous kynurenines as targets for drug discovery and development." Nat Rev Drug Discov **1** (8): 609-620.
Stone, T. W. and M. N. Perkins (1981). "Quinolinic acid: a potent endogenous excitant at amino acid receptors in CNS." Eur J Pharmacol **72** (4): 411-412.
Stryer, L. (1995). Biochemistry: Chapter 14 (page 390).
Stryer, L. (1995). Biochemistry: Chapter 23 (pages 633-662).
Stryer, L. (1995). Biochemistry: Chapter 14 (pages 373-374).
Stuart, J. M., A. S. Townes, et al. (1982). "Nature and specificity of the immune response to collagen in type II collagen-induced arthritis in mice." J Clin Invest **69** (3): 673-683.

Sugimoto, H., S. Oda, et al. (2006). "Crystal structure of human indoleamine 2,3-dioxygenase: catalytic mechanism of O2 incorporation by a heme-containing dioxygenase." Proc Natl Acad Sci U S A **103** (8): 2611-2616.

Szanto, S., T. Koreny, et al. (2007). "Inhibition of indoleamine 2,3-dioxygenase-mediated tryptophan catabolism accelerates collagen-induced arthritis in mice." Arthritis Res Ther **9** (3): R50.

Taher, Y. A., B. J. Piavaux, et al. (2008). "Indoleamine 2,3-dioxygenase-dependent tryptophan metabolites contribute to tolerance induction during allergen immunotherapy in a mouse model." J Allergy Clin Immunol **121** (4): 983-991 e982.

Takeuchi, F. and Y. Shibata (1984). "Kynurenine metabolism in vitamin-B-6-deficient rat liver after tryptophan injection." Biochem J **220** (3): 693-699.

Takikawa, O., R. Yoshida, et al. (1986). "Tryptophan degradation in mice initiated by indoleamine 2,3-dioxygenase." J Biol Chem **261** (8): 3648-3653.

Tanizawa, K. and K. Soda (1979). "The mechanism of kynurenine hydrolysis catalyzed by kynureninase." J Biochem **86** (5): 1199-1209.

Taylor, P. C. Rheuamtoid arthritis in practice Chapter 1, page 6.

Taylor, P. C. (2007). Rheumatoid arthritis in practice: Chapter 6 (pages: 49 - 69).

Taylor, P. C. (2007). Rheumatoid arthritis in practice: Chapter 1 (pages: 3-17).

Taylor, P. C. (2007). Rheumatoid arthritis in practice, The Royal Society of Medicine Press Limited Chapter 2 (pages: 19 - 29).

Taylor, P. C. (2007). Rheumatoid arthritis in practice: Chapter 7 (pages:71 - 86).

Teo, J. C., K. M. Si-Hoe, et al. (2006). "Relationship between CT intensity, micro-architecture and mechanical properties of porcine vertebral cancellous bone." Clin Biomech (Bristol, Avon) **21** (3): 235-244.

Terness, P., T. M. Bauer, et al. (2002). "Inhibition of allogeneic T cell proliferation by indoleamine 2,3-dioxygenase-expressing dendritic cells: mediation of suppression by tryptophan metabolites." J Exp Med **196** (4): 447-457.

Ueno, A., S. Cho, et al. (2007). "Transient upregulation of indoleamine 2,3-dioxygenase in dendritic cells by human chorionic gonadotropin downregulates autoimmune diabetes." Diabetes **56** (6): 1686-1693.

van der Heijde, D. M. (1996). "Plain X-rays in rheumatoid arthritis: overview of scoring methods, their reliability and applicability." Baillieres Clin Rheumatol **10** (3): 435-453.

Visser, H., S. le Cessie, et al. (2002). "How to diagnose rheumatoid arthritis early: a prediction model for persistent (erosive) arthritis." Arthritis Rheum **46** (2): 357-365.

von Bubnoff, D., H. Matz, et al. (2002). "FcepsilonRI induces the tryptophan degradation pathway involved in regulating T cell responses." J Immunol **169** (4): 1810-1816.

Wagner, C. A., F. Lang, et al. (2001). "Function and structure of heterodimeric amino acid transporters." Am J Physiol Cell Physiol **281** (4): C1077-1093.

Walsh, J. L., W. P. Todd, et al. (1991). "4-halo-3-hydroxyanthranilic acids: potent competitive inhibitors of 3-hydroxy-anthranilic acid oxygenase in vitro." Biochem Pharmacol **42** (5): 985-990.

Wang, J., N. Simonavicius, et al. (2006). "Kynurenic acid as a ligand for orphan G protein-coupled receptor GPR35." J Biol Chem **281** (31): 22021-22028.

Wang, Y., H. Liu, et al. (2010). "Kynurenine is an endothelium-derived relaxing factor produced during inflammation." Nat Med **16** (3): 279-285.

Wek, R. C., H. Y. Jiang, et al. (2006). "Coping with stress: eIF2 kinases and translational control." Biochem Soc Trans **34** (Pt 1): 7-11.

Widner, B., A. Laich, et al. (2002). "Neopterin production, tryptophan degradation, and mental depression--what is the link?" Brain Behav Immun **16** (5): 590-595.

Widner, B., N. Sepp, et al. (2000). "Enhanced tryptophan degradation in systemic lupus erythematosus." Immunobiology **201** (5): 621-630.
Willcock, E. G. (1906). "The importance of individual amino-acids in metabolism: Observations on the effect of adding tryptophane to a dietary in which zein is the sole nitrogenous constituent." J Physiol **35** (1-2): 88-102.
Williams, R. O. (1995). Strategies for immune intervention in murine collagen-induced arthritis. PhD PhD thesis, University of London.
Wingender, G., N. Garbi, et al. (2006). "Systemic application of CpG-rich DNA suppresses adaptive T cell immunity via induction of IDO." Eur J Immunol **36**(1): 12-20.
Wirleitner, B., G. Neurauter, et al. (2003). "Interferon-gamma-induced conversion of tryptophan: immunologic and neuropsychiatric aspects." Curr Med Chem **10** (16): 1581-1591.
Wooley, P. H., J. R. Seibold, et al. (1989). "Pristane-induced arthritis. The immunologic and genetic features of an experimental murine model of autoimmune disease." Arthritis Rheum **32** (8): 1022-1030.
Yeh, J. K. and R. R. Brown (1977). "Effects of vitamin B-6 deficiency and tryptophan loading on urinary excretion of tryptophan metabolites in mammals." J Nutr **107** (2): 261-271.
Yeom, H., S. Blanchard, et al. (2008). "Correlation between micro-computed tomography and histomorphometry for assessment of new bone formation in a calvarial experimental model." J Craniofac Surg **19** (2): 446-452.
Yuasa, H. J., M. Takubo, et al. (2007). "Evolution of vertebrate indoleamine 2,3-dioxygenases." J Mol Evol **65** (6): 705-714.
Zaborske, J. M., J. Narasimhan, et al. (2009). "Genome-wide analysis of tRNA charging and activation of the eIF2 kinase Gcn2p." J Biol Chem **284** (37): 25254-25267.
Zhang, Y., S. A. Kang, et al. (2007). "Crystal structure and mechanism of tryptophan 2,3-dioxygenase, a heme enzyme involved in tryptophan catabolism and in quinolinate biosynthesis." Biochemistry **46** (1): 145-155.
Zhu, W. H., C. Z. Lu, et al. (2007). "A putative mechanism on remission of multiple sclerosis during pregnancy: estrogen-induced indoleamine 2,3-dioxygenase by dendritic cells." Mult Scler **13** (1): 33-40.
Zwerina, J., B. Tuerk, et al. (2006). "Imbalance of local bone metabolism in inflammatory arthritis and its reversal upon tumor necrosis factor blockade: direct analysis of bone turnover in murine arthritis." Arthritis Res Ther **8** (1): R22.
Zwilling, D., S. Y. Huang, et al. (2011). "Kynurenine 3-monooxygenase inhibition in blood ameliorates neurodegeneration." Cell **145** (6): 863-874.

Supplement 1 People who helped me to accomplish this thesis

Professor Ido Kema and his team independently have measured the concentration of tryptophan and its catabolites in the several types of tissues isolated from the animals with CIA. However, in this thesis only my original results have been presented.

Mr David Essex and his colleagues allowed me work to work in the Department of Histology in the Charing Cross Hospital were I could work on the results showing immunohistochemistry. In addition, Mr David Essex has sectioned and stained paws with H&E as well as with Safranin O. This allowed me to score joint damage using the scales described in the section 2.5.

Mr Leigh Madden provided me with results showing beneficial effect of anti-TNF treatment in mice with CIA (chapter 5, figure 22). Dr Ewa Paleolog conducted statistical analysis using the Bland-Altman method (chapter 5, section 5.2.1).